



Εθνικό και Καποδιστριακό  
ΠΑΝΕΠΙΣΤΗΜΙΟ ΑΘΗΝΩΝ

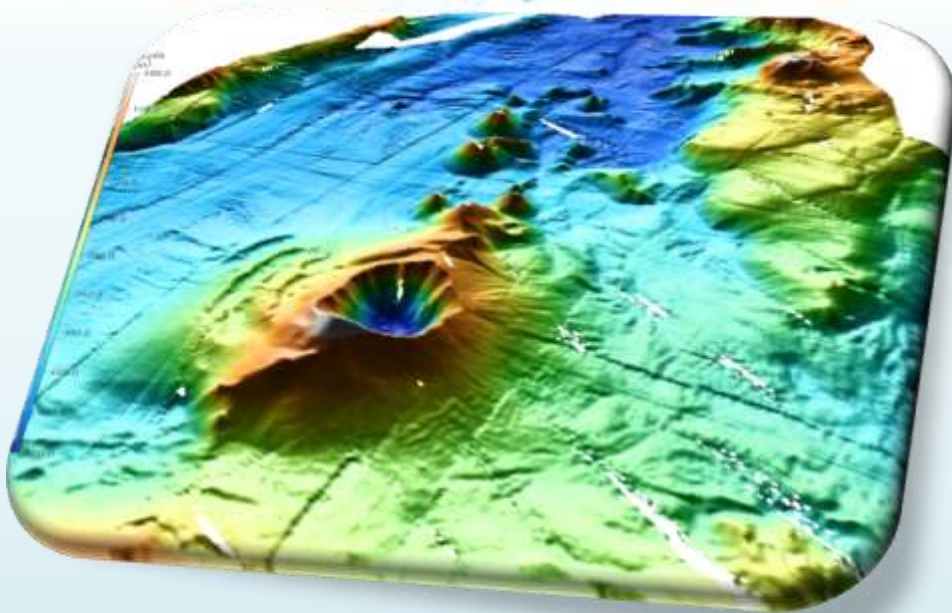
Τμήμα Γεωλογίας και  
Γεωπεριβάλλοντος



Τομέας Δυναμικής Τεκτονικής και  
Εφαρμοσμένης Γεωλογίας

Μεταπτυχιακό Πρόγραμμα Σπουδών  
ΔΥΝΑΜΙΚΗ ΤΕΚΤΟΝΙΚΗ & ΕΦΑΡΜΟΣΜΕΝΗ ΓΕΩΛΟΓΙΑ

Μεταπτυχιακή Διατριβή Ειδίκευσης  
**TECTONIC ANALYSIS OF THE VOLCANIC FIELD AROUND KOLUMBO  
VOLCANO**



Συντάκτης  
**ΜΠΕΤΖΕΛΟΥ ΚΩΝΣΤΑΝΤΙΝΑ**  
**Α.Μ. 2918**

Τριμελής επιτροπή  
ΕΠΙΒΛΕΠΩΝ ΚΑΘΗΓΗΤΗΣ: ΠΑΠΑΝΙΚΟΛΑΟΥ ΔΗΜΗΤΡΙΟΣ  
Β' ΜΕΛΟΣ: ΔΡ. ΣΑΚΚΕΛΑΡΙΟΥ ΔΗΜΗΤΡΙΟΣ  
Γ' ΜΕΛΟΣ: ΔΡ. ΛΕΚΚΑΣ ΕΥΘΥΜΙΟΣ

**ΑΘΗΝΑ 2013**

### **ΕΥΧΑΡΙΣΤΙΕΣ**

Ιδιαίτερα θα ήθελα να ευχαριστήσω τον καθηγητή μου κ. Δημήτριο Παπανικολάου, τόσο για την ανάθεση του θέματος, όσο και για την αμέριστη συμπαράστασή του κατά την εκπόνηση της παρούσας εργασίας. Επίσης, τις θερμές μου ευχαριστίες οφείλω να εκφράσω και στα υπόλοιπα μέλη της εξεταστικής επιτροπής, στον κ. Ευθύμιο Λέκκα καθώς και τον κ. Δημήτρη Σακελλαρίου για την πολύτιμη επιστημονική τους υποστήριξη κατά την σύνταξη της παρούσας διατριβής. Τέλος θα ήθελα να εκφράσω τις θερμές μου ευχαριστίες στην Δρ. Παρασκευή Νομικού για την μεγάλη εμπιστοσύνη που μου έδειξε, την ανεκτίμητη συμβολή της στην εκπόνηση της εργασίας καθώς και την αμέριστη στήριξή της κάθε στιγμή.

## Abstract

Anhydros basin, NE of Santorini, Greece, is a rift basin at the back arc area of the active Hellenic Orogenic Arc. A volcanic chain has been developed within the basinal area and its dominant feature, Kolumbo volcano, is the most spectacular submarine volcanic structure. Its distinct character is mainly based on the highly dynamic, unstable and affected by frequent earthquakes and volcanic activity hydrothermal vent field, situated chiefly on the northern part of the crater floor at an average depth of 500 meters.

A combined detailed analysis of bathymetric data obtained during "GEOWARN" project in 2001, ROV (Remotely Operated Vehicles) data collected in August 2010 in the frame of a collaborative project (New Frontiers in Ocean Exploration 2010) between the Graduate School of Oceanography at the University of Rhode Island (URI-USA), the Dept. of Geology & Geoenvironment of University of Athens (NKUA-GREECE), the Institute for Exploration (IFE-USA), and the Institute of Geology and Mineral Exploration (IGME-GREECE), and air-gun lithoseismic profiles recorded during "THERA" project in 2006 aboard the R/V Aegaeo, has led to the construction of a morphotectonic map of Anhydros basin. As revealed by the analysis of the data, KVC (Kolumbo Volcanic Chain) has been developed within the basinal area of Anhydros as a result of volcanotectonic processes. It forms an intra-graben tectonic horst and is line with Kolumbo fault at the onshore northern part of Santorini, points of hydrothermal activity at the northern part of Santorini caldera and dykes that occur at the northern Santorini caldera walls and the overall configuration of Santorini volcanic field. Thus, it is part of a wider volcanotectonic zone developed within a tectonic graben bordered by Ios Fault Zone to the NW and Anafi Fault Zone to the SE.

**Keywords:** Kolumbo volcano, Anhydros basin, seismic profiling, submarine volcanotectonics, swath bathymetry.

## Περίληψη

Η λεκάνη της Ανύδρου, ΒΑ της Σαντορίνης, είναι μια εφελκυστική λεκάνη στο χώρο όπισθεν του ενεργού Ελληνικού Ορογενετικού Τόξου. Μια ηφαιστειακή αλυσίδα έχει αναπτυχθεί εντός της επίπεδης περιοχής της λεκάνης και το κυρίαρχο χαρακτηριστικό της, το ηφαίστειο του Κολούμπο, αποτελεί την πιο θεαματική υποθαλάσσια ηφαιστειακή δομή. Ο ξεχωριστός χαρακτήρας του οφείλεται κυρίως στο υδροθερμικό πεδίο, το οποίο παρουσιάζει μια ιδιαίτερα δυναμική και ασταθή κατάσταση καθώς επηρεάζεται από αλληπάλληλους σεισμούς και ηφαιστειακή δραστηριότητα, που βρίσκεται κυρίως στο βόρειο τμήμα του πυθμένα του κρατήρα σε ένα μέσο βάθος 500 μέτρων .

Μια συνδυασμένη λεπτομερής ανάλυση βαθυμετρικών δεδομένων που ελήφθησαν κατά τη διάρκεια του προγράμματος " GEOWARN " το 2001, ROV (Υποβρύχια Τηλεκατευθυνόμενα Οχήματα) δεδομένων που συλλέχθηκαν τον Αύγουστο του 2010 στο πλαίσιο ενός προγράμματος συνεργασίας (New Frontiers in Ocean Exploration 2010) μεταξύ του Graduate School of Oceanography του Πανεπιστημίου του Rhode Island (URI - USA), του Τμήματος Γεωλογίας & Γεωπεριβάλλοντος του Πανεπιστημίου Αθηνών (ΕΚΠΑ - ΕΛΛΑΔΑ), το Ινστιτούτο για την Εξερεύνηση (IFE - ΗΠΑ), και το Ινστιτούτο Γεωλογικών και Μεταλλευτικών Ερευνών (IGME - ΕΛΛΑΔΑ), καθώς και λιθοσεισμικών προφίλ που καταγράφηκαν κατά τη διάρκεια του προγράμματος «THERA» το 2006, πάνω στο Ω/Κ

ΑΙΓΑΙΟ , οδήγησε στην κατασκευή ενός μορφοτεκτονικού χάρτη της λεκάνης της Ανύδρου. Όπως φάνηκε και από την ανάλυση των δεδομένων, η ηφαιστειακή αλυσίδα του Κολούμπο έχει αναπτυχθεί στο μέσο και κατά μήκος της λεκάνης ως αποτέλεσμα ηφαιστειο-τεκτονικών διαδικασιών. Αποτελεί τεκτονικό κέρας εντός της τάφρου και είναι σύμφωνη σε προσανατολισμό με το χερσαίο ρήγμα Κολούμπο στο βόρειο τμήμα της Σαντορίνης, τα σημεία υδροθερμικής δραστηριότητας στο βόρειο τμήμα της καλντέρας της Σαντορίνης και των φλεβών που συναντώνται στα βόρεια τείχη της καλντέρας της Σαντορίνης καθώς και την συνολική διαμόρφωση του ηφαιστειακού πεδίου της Σαντορίνης. Έτσι, αποτελεί μέρος μιας ευρύτερης ηφαιστειο-τεκτονικής ζώνης που αναπτύσσεται μέσα σε ένα τεκτονικό βύθισμα το οποίο οριοθετείται από το ρήγμα της Ίου προς τα ΒΔ και το ρήγμα της Ανάφης στα ΝΑ.

# ΠΕΡΙΕΧΟΜΕΝΑ

---

<b>1. INTRODUCTION</b>	<b>ΣΕΛ 1</b>
1.1. VOLCANISM	ΣΕΛ 1
1.2. SUBMARINE VOLCANISM	ΣΕΛ 6
1.2.1. KOLUMBO SUBMARINE VOLCANO	ΣΕΛ 8
1.2.2. HISTORICAL REFERENCES OF THE 1650 AD KOLUMBO ERUPTION	ΣΕΛ 9
<b>2. STUDY AREA</b>	<b>ΣΕΛ 10</b>
2.1. GEODYNAMIC SETTING AND EVOLUTION OF THE AEGEAN SEA	ΣΕΛ 10
2.2. GEODYNAMIC SECTORS OF THE AEGEAN SEA	ΣΕΛ 14
2.3. THE HELLENIC VOLCANIC ARC – GEODYNAMIC SETTING	ΣΕΛ 15
2.4. KOLUMBO VOLCANIC CHAIN – GEODYNAMIC SETTING	ΣΕΛ 18
2.5. GEOLOGIC SETTING OF SANTORINI VOLCANIC GROUP	ΣΕΛ 20
2.5.1. CHRISTIANNA	ΣΕΛ 20
2.5.2. SANTORINI, NEA AND PALEA KAMENI	ΣΕΛ 21
2.5.3. KOLUMBO FAULT LINE ON LAND OBSERVATIONS	ΣΕΛ 26
<b>3. METHODOLOGY</b>	<b>ΣΕΛ 28</b>
3.1. BATHYMETRIC DATA	ΣΕΛ 28
3.2. ROV DATA	ΣΕΛ 29
3.3. SEISMIC REFLECTION PROFILING	ΣΕΛ 30
<b>4. MORPHOLOGY</b>	<b>ΣΕΛ 32</b>
4.1. BATHYMETRY	ΣΕΛ 32
4.2. MORPHOLOGICAL SLOPE ANALYSIS	ΣΕΛ 38
<b>5. ROV EXPLORATION</b>	<b>ΣΕΛ 41</b>
<b>6. SEISMIC PROFILES</b>	<b>ΣΕΛ 50</b>
6.1. SEISMIC PROFILES THAT CROSS-CUT KOLUMBO SUBMARINE VOLCANO	ΣΕΛ 51
6.2. SEISMIC PROFILES THAT CROSSCUT THE EXTERNAL FLANKS OF KOLUMBO VOLCANO	ΣΕΛ 54
6.3. SEISMIC PROFILES THAT CROSSCUT THE ANHYDROS BASIN	ΣΕΛ 58
6.4. SEISMIC PROFILES PARALLEL TO THE LONG AXIS OF ANHYDROS BASIN	ΣΕΛ 70
<b>7. RESULTS</b>	<b>ΣΕΛ 73</b>

<b>7.1. TECTONIC ANALYSIS</b>	<b>ΣΕΛ 73</b>
<b>7.2. PALEOGEOGRAPHIC SYNTHESIS</b>	<b>ΣΕΛ 75</b>
<b>7.3. TSUNAMI GENERATION MECHANISMS</b>	<b>ΣΕΛ 77</b>
<b>8. CONCLUSIONS</b>	<b>ΣΕΛ 78</b>
<b>9. ACKNOWLEDGMENTS</b>	<b>ΣΕΛ 80</b>
<b>10. REFERENCES</b>	<b>ΣΕΛ 80</b>

## 1. Introduction

### 1.1 Volcanism

Volcanic activity has always been causing awe and horror to the human kind since they are included among the most devastating natural phenomena.

In the early stages of cultural evolution, man could only attribute the surface expression of volcanism to supernatural forces. The classical world of Greece and the early Roman Empire explained volcanoes as the work of the gods as science and alchemy had no explanation for their existence. Grecian myths and tales refer to the Atlantis, a fabled island that sank into the sea. Plato (428-348 BCE) described the disappearance of a vast island and its powerful civilization, the Atlanteans, in two of his dialogues, *Critias* and *Timaeus*.

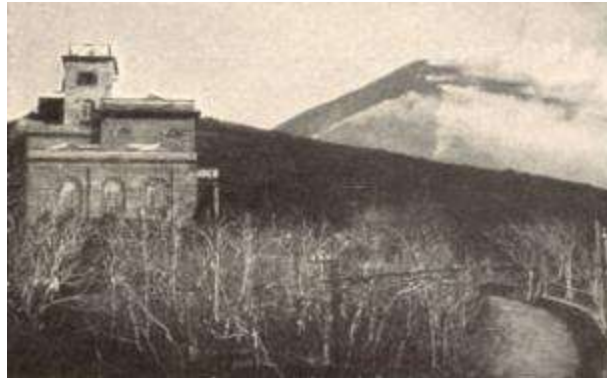
Greeks also considered that Hephaestus, the god of fire, sat below the volcano Etna, forging the weapons of Zeus. His minions, the cyclops with their single staring eye, may be an allegory to the round craters and cones of a volcano. Indeed, the Greek word used to describe volcanoes was Etna, or Hiera, after Heracles, the son of Zeus. The Roman poet Virgil, in interpreting the Greek myth, held that the hero Enceladus was buried beneath Etna by the goddess Athena as punishment for disobeying the gods; the mountain's rumblings were his tormented cries, the flames his breath and the tremors his railing against the bars of his prison. Enceladus' brother, Mimas, was buried beneath Vesuvius by Hephaestus, and the blood of other defeated giants welled up in the Phlegrean Fields surrounding Vesuvius.

The word volcano is derived from the name of Vulcano, a volcanic island in the Aeolian Islands of Italy whose name in turn originates from Vulcan, the name of a god of fire in Roman mythology. Volcanoes were considered to be the residence of Vulcan.



1. Painting by Peter Paul Rubens (1577–1640) *Vulcano forjando los rayos de Júpiter* (1636). Museo del Prado (Madrid). The god of fire forging Jupiter's thunderbolts.

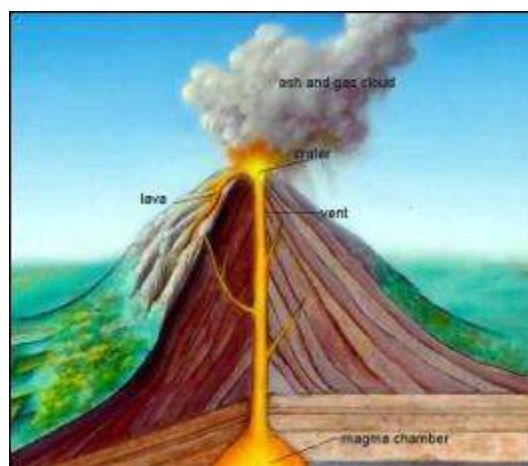
Through time, man has tried to find more rational explanations to ascribe to such phenomena. Since 1800 AD, scientists focused on a more systematic and organized investigation of volcanic activity based on observation and interpretation. In 1841, the first volcanological observatory, the Vesuvius Observatory (fig. 2), was founded in the Kingdom of the Two Sicilies.



2. Vintage photo of the Vesuvius Observatory ([http://www.vesuvioinrete.it/e\\_osservatorio.htm](http://www.vesuvioinrete.it/e_osservatorio.htm)).

The international scientific community has established commonly accepted theories concerning volcanoes, throughout years of research and observation. The term “volcano” refers to an opening or rupture on Earth’s surface, which allows hot magma to escape in the form of lava. On the other hand, “volcanology” is a much more complex term, since it does not only concern the volcanic activity on the surface, but also involves deep processes that are responsible for the presence of a volcano on a specific point of the Earth’s crust. At the points where lava is discharged volcanic cones appear that are built of successive layers of lava and ash, products of the explosive events that occurred at the area.

The basic component of a volcano is the central vent. It is an almost vertical, cylindrical conduit through which lava manages to reach the surface. A crater is commonly formed at the top of the vent of erupting volcanoes, where the lava is extruded. It usually has a funnel-like shape and is believed to be a collapse feature caused by molten lava subsiding as an eruption phase diminishes. Volcanic craters formed in these ways are relatively small, usually less than 1.6 km in diameter, and represent only a small fraction of the cone’s diameter at the base. The magmatic chamber, a reservoir of magma which supplies the volcano with material, is connected with the central vent at its deepest edge.



3. Schematic display of a typical volcanic cone (<http://pubs.usgs.gov/gip/volc/types.html>).

A caldera is a much larger crater, typically ranging from 5-30 km in diameter. A characteristic example lies in the Aegean Sea, the caldera of Santorini volcano, which was formed during the great historical eruption of 1760 BC. It is defined by the islands of Santorini, Therasia and Aspronisi (fig. 4). The maximum depth of the caldera is almost 400 m and its major axis is approximately 11km long. In a few instances, however, tremendous volcanic eruptions have left calderas 80 km or so, such as the case of Yellowstone National Park or the basin of Lake Toba, Sumatra, Indonesia (fig. 5). Most calderas are formed by the collapse of the central part of a cone during great eruptions.



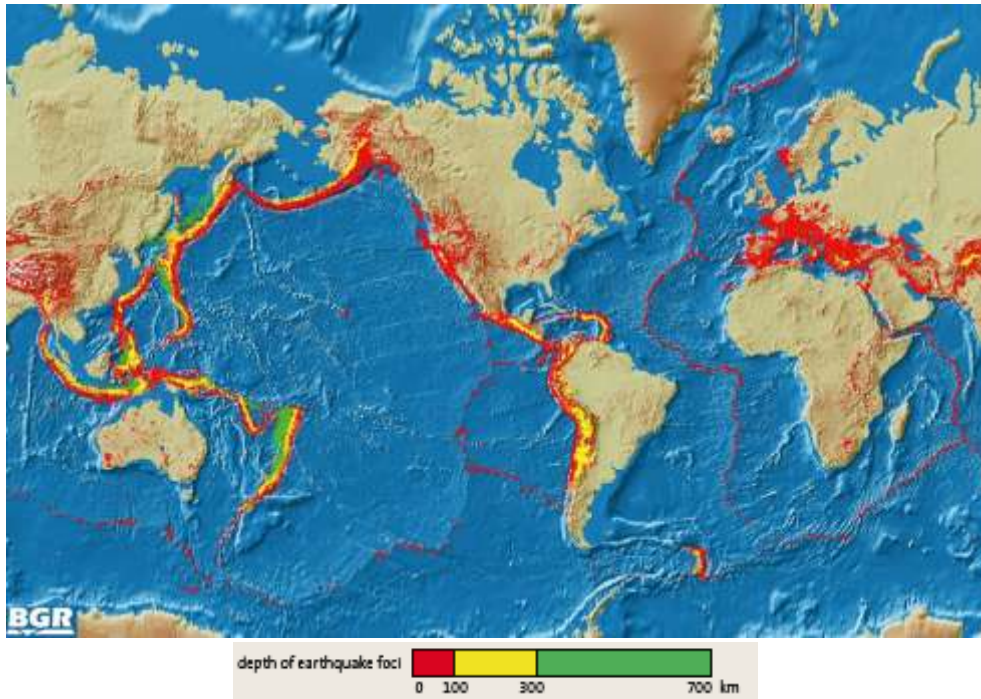
4. Santorini Island Group. The large, ring-shaped island of Thera encloses most of the caldera, with the smaller island, Therasia, in the foreground. The darker young volcanic islands of Palea and Nea Kameni in the center of the caldera. Courtesy of Birke Schreiber (copyright: Hankensbuettel, Germany - [www.kalliste.de](http://www.kalliste.de)).



5. Panoramic aspect of Lake Toba, Sumatra, Indonesia ([http://en.wikipedia.org/wiki/Lake\\_Toba](http://en.wikipedia.org/wiki/Lake_Toba)).

Volcanoes can be separated, according to their eruptive history, in active, dormant and extinct volcanoes. More specifically, the active volcanoes have at least erupted once during historical times and may be reactivated in the future. On the other hand the volcanoes, the eruptive activity of which has never been recorded, are characterized as dormant. An extinct volcano results after the fossilization of the underground network of magmatic circulation due to geodynamic processes. The remnants are then delivered to the functions of weathering and erosion.

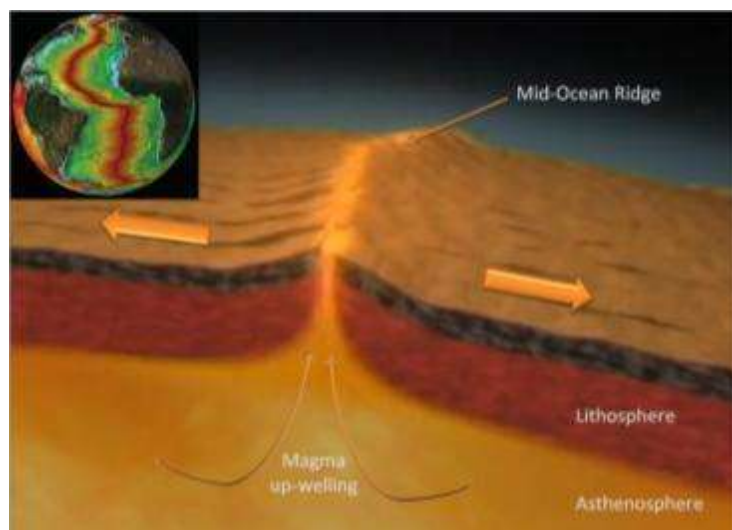
Approximately 700 known active volcanoes are located on land, while several thousand ones have been discovered underwater. The geographical distribution of the active volcanoes world-wide is not random. The actual volcanic activity is limited within certain zones that coincide the seismically active zones of the Earth (fig. ). These zones represent divergent, convergent or collision plate boundaries. Volcanism is not present along transform boundaries, whereas in specific cases volcanic activity occurs within a plate.



6. Global distribution of earthquake centers with epicenters mapped according to their depth. Note how the epicenters define plate boundaries and that most earthquakes occur within 100 km of the surface except along subduction zones where they deepen under the upper plate (produced with the kind support of Mrs. Agneta Schick, Federal Institute of Geosciences and Resources, BGR, Hannover, Germany).

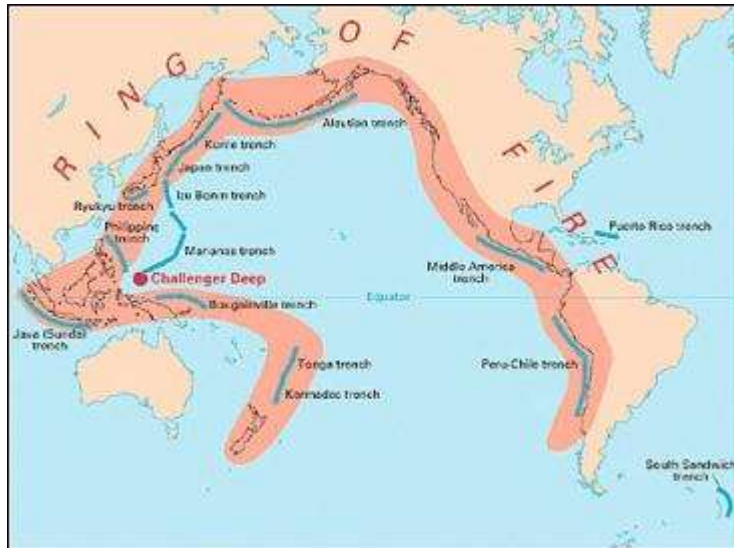
According to the above mentioned, three major zones of active volcanism can be distinguished:

- **Mid-Ocean Ridges (MOR).** Mid-Ocean ridges constitute a chain of volcanoes that stretches above 84.000 kilometers around the globe. Along these chains, two plates are pulling apart from each other as hot asthenosphere magma emerges from the mantle and oozes forth as lava to fill the crack continuously created by plate separation. The lava cools and attaches itself to the trailing edge of each plate, forming new ocean floor crust in a process commonly known as sea-floor spreading. So the plate boundaries are also called “constructive.



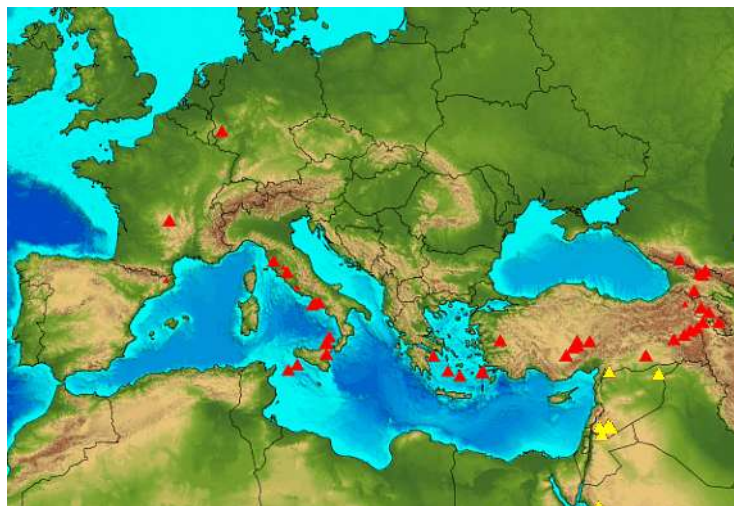
7. Schematic reconstruction of a divergent plate boundary (BBC Motion Gallery). In the left top image, the Mid-Atlantic Ocean Ridge is shown. Green color indicates the older crust components and red the newest ones.

- **The Ring of Fire.** It is a 40.000 kilometer long, horseshoe shaped zone that surrounds the Pacific Ocean (fig. 8). 452 volcanoes are included within this zone. It is the result of the ongoing subduction of the oceanic crust of the Pacific Ocean beneath all the surrounding lithospheric plates (North and South American plates. Eurasian plate and Australian plate).



8. More than 50% of the terrestrial volcanoes are located within the Ring of fire (archive USGS).

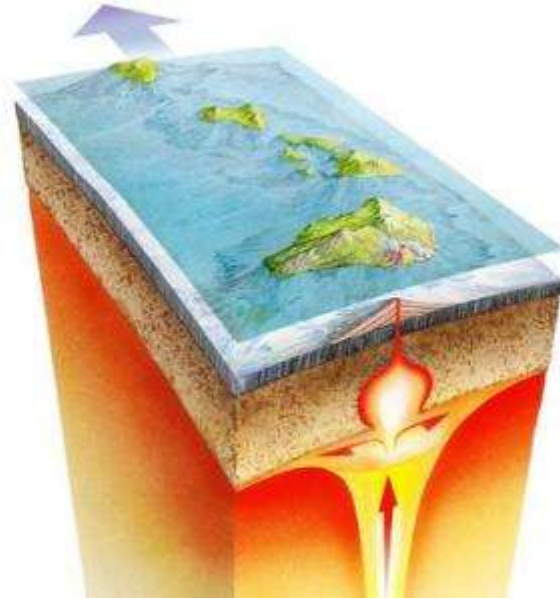
- **The Mediterranean-Asian belt.** It includes the Italian volcanoes (Lipari, Vesuvius, Etna, Stromboli etc), the Hellenic Volcanic Arc (Methana, Milos, Santorini, Nisyros etc) and the volcanoes of the Caucasus-Himalayan belt. It concerns volcanism that is related either to convergent plate boundaries, as in the case of the Mediterranean Sea where we have the ongoing subduction of oceanic lithosphere beneath the Eurasian plate,



9. Volcanoes of the Mediterranean and western Asia. Large red triangles show volcanoes with known or inferred Holocene eruptions; small red triangles mark volcanoes with possible, but uncertain Holocene eruptions or Pleistocene volcanoes with major thermal activity. Yellow triangles distinguish volcanoes of other regions (archive USGS).

- **Intra plate volcanism.** Volcanism far away from the margins of a plate has a linear arrangement. The most characteristic example is the one of the Hawaiian islands.

Volcanic activity is explained with the theory of the “hot spots”. A huge column of upwelling lava, known as a “plume,” lies at a fixed position under the Pacific Plate. As the ocean floor moves over this “hot spot” at about five inches a year, the upwelling lava creates a steady succession of new volcanoes that migrate along with the plate - a veritable conveyor belt of volcanic islands. Hot spots are of great importance because they provide science with information for the direction and velocity of the motion of a plate.



10. Artwork showing a hotspot forming an island in the Hawaiian-Emperor chain (credit: Gary Hincks/SPL).

### **1.2 Submarine volcanism**

About 75% of the annual magma output on the Earth’s surface is accounted to the activity of submarine volcanoes. The majority is also located near areas of relative motion between different tectonic plates and mostly at Mid-Ocean Ridges. Hence, most are located in the depths of oceans, but some also exist in shallow water and may eject material into the air during an eruption.

The water column above submarine volcanic features substantially affects the nature of each volcanic eruption. For instance, the increased thermal conductivity of water causes magma to cool and solidify much more quickly than in a terrestrial eruption, often turning it into a volcanic glass.

The lava formed by submarine volcanoes is quite different from terrestrial lava. Upon contact with water, a solid crust forms around the lava. Advancing lava flows into this crust, forming what is known as pillow lava.



11. The orange glow of superheated magma, about 1,204° C, is exposed as "pillow" lavas extrude from the eruption. These images represent an area about one meter across in an eruptive area roughly the length of a football field that runs along the summit (Image courtesy of NSF and NOAA).

Hydrothermal vents, sites of abundant biological activity, are commonly found near submarine volcanoes. In 1977, Woods Hole Oceanographic Institute expedition launched a deep sea submarine until 2,500 meters water depth to investigate hydrothermal activity on the ocean floor of the Galapagos rift, where they detected a dramatic change on the ocean's temperature. They discovered vents pouring hot, mineral-rich fluids from beneath the seafloor. This kind of activity is usually present on mid-ocean ridges. Water seeps through cracks and porous rocks in the seafloor and is heated by magma deep below the ocean crust to as high as 400°C. The heated fluids rise back to the surface through openings in the seafloor. Sulfur and other materials precipitate, or come out of solution, to form metal-rich towers and deposits of minerals on the seafloor. It is believed that hydrothermal vents accumulate vast amounts of potentially valuable minerals on the seafloor.

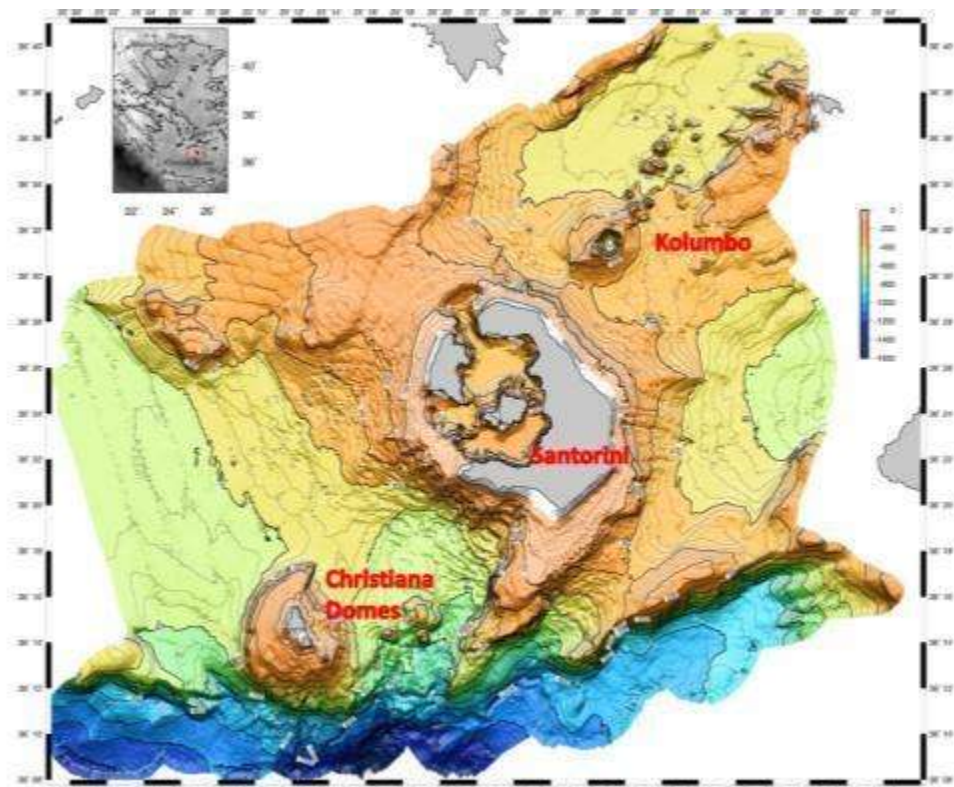
In addition, they also found the vents were inhabited by previously unknown organisms that thrived in the absence of sunlight. These discoveries forever changed our understanding of Earth and life on it.



12. The first hydrothermal vent also known as a “black smoker” discovered in 1977 by the scientists of the Galapagos Reef Expedition. It is surrounded by giant tube worms about eight feet tall (The strange ecosystem of hydrothermal vents, Isani Chan Ph.D).

### **1.2.1 Kolumbo Submarine Volcano**

Kolumbo submarine volcano is located in the south Aegean Sea and is part of the Hellenic Volcanic Arc. More specifically, it lies within a rift basin approximately 7 kilometers northeast of Cape Kolumbo, on Santorini island, Greece. Its shallowest point is at 18 meters below sea level. Within the volcanic cone of Kolumbo, there is a relatively flat-lying crater floor with an average depth of about 505 m (Nomikou, 2003). The crater may have been created by the partial collapse of a pre-existing volcanic cone or produced largely as a constructional feature associated with the growth of the edifice during an eruption.



13. A bathymetry map of the area around Santorini, which was produced using a 50 meter grid interval and plotted with a mercator projection at a scale of 1:100.000 - with 25 meter contours (Nomikou et al., 2012a).

Kolumbo’s existence has been known since 1650 AD when it burst from the sea and erupted, killing 70 people on the nearby island of Santorini according to historical references. Since then no other significant eruptive event has been recorded, but the last few years it has been causing the fear to the residents of Santorini and the surrounding islands due to the frequent seismic activity concentrated just below the volcano.

During ROV dives in 2006, a widespread hydrothermal vent field was discovered on the Northern edge of the Kolumbo crater floor (Sigurdsson et al., 2006). This hydrothermal vent field has evolved over a generally smooth crater floor at an average depth of 500 meters. More recent exploration on the Hydrothermal Vent Field of Kolumbo during 2010 and 2011 has been conducted. Geochemical and biomineralogical data based on recent these oceanographic missions show that Kolumbo is the first shallow sea floor observation of large

diffusely venting intermediate-temperature (70oC-220oC) sulfide-sulfate structures uniquely enriched in Tl+Sb(±Au, As Hg, Ag). Preliminary genetic analysis indicates for the first time in submarine hydrothermal vents, the predominance of Candidatus "Nitrosopumilus maritimus", a Crenarchaeota strain that is capable of chemoautotrophic growth on ammonia (nitrification) and CO<sub>2</sub> (Kiliyas et al., 2012 in review). In general, all the data analyzed show a number of geobiological characteristics which suggest that the uniqueness of this Hydrothermal field lies on its geodynamic setting.



14. Aspect of the Hydrothermal Vent Field (Nautilus 2010-2011, OET)



15. High-temperature venting occurs in the north central part of the crater, with vigorous gas emission and fluid temperatures up to 220°C. Hydrothermal vent nicknamed "Champagne" (Nautilus 2010-2011, OET).



16. Cluster of hydrothermal vents, nicknamed "Politeia" constructed of massive sulfides and sulfates and covered with bacteria. Some of these spires reach up to 4 m in height(Nautilus 2010-2011, OET).

### **1.2.2 Historical References of the 1650 AD Kolumbo eruption**

Much of the information about the 1650 event (Fouque, 1879) has come from historical accounts of individuals who were on Santorini and nearby islands at the time of the eruption. Fouqué's principle sources included an ancient Greek manuscript, a Greek poem, an anonymous account in Italian, and a report by a Jesuit priest of Santorini named Francois Richard that was published in Paris in 1656. Through these accounts we can define an evolution model of the eruption and its main impacts on the people of the area.

Since 1649 violent earthquakes- sign of a potential volcanic eruption- occurred at the area since 1949 for about a year. The seismic activity was becoming more and more frequent as the eruption approached.

Another phenomena that was observed was the discoloration of the sea surface which is often associated with submarine volcanic activity as magma interacts with seawater and causes hot turbid water to ascend to the surface.

On the evening of September 27th hot clouds of gas and volcanic particles rose into the atmosphere indicating that the first volcanic explosion above the sea surface was in progress. Small earthquakes continued, large quantities of floating pumice were produced, and plumes formed and dispersed on a roughly hourly cycle throughout the 28th. A small white island appeared from the sea where the smoke columns had come from, with periodic smoke plumes rising from the site.

On September 29th, 1650 the most violent eruptive activity occurred at Kolumbo. The activity continued until the 30<sup>th</sup> of the same month and after a few days of decreased activity the eruption diminished.



17. Ash and gas plume from submarine eruption in the Tonga Islands in 2009 as a simulation of the Kolumbo 1650 AD event.

Two of the main hazardous effects of this volcanic eruption on the local communities was the clouds of poisonous gases that were released. The gas caused eye pain, blindness, and cerebral congestion and many inhabitants temporarily lost consciousness for several hours. The second major impact from the eruption was the generation of tsunamis. At least one tsunami inundated Thera, carried away livestock, destroyed buildings, and eroded the roadways and 500 acres of the eastern coastline.

## **2. Study Area**

### **2.1 Geodynamic Setting and Evolution of the Aegean Sea**

The Aegean Sea at the Eastern Mediterranean occupies a submarine part of the Alpine mountain chain, which, until the recent geological history, joined the Hellenides to the west with Taurus to the east. This is a region with a very complex structure, as it is characterized by active extensional tectonics within the upper plate of a system of convergent plate boundaries (the African - Eurasian).



18. International Bathymetric Map of the Mediterranean (UNESCO 1981). The orange polygon indicates the area of the Aegean Sea.

The actual convergence rate is approximately 1cm/yr at the eastern part of the Mediterranean including the Hellenides. Since Early and Middle Miocene the collision of the two plates took place, in the regions of Western Mediterranean and Caucasus, respectively. Thus, the subduction of the last remnants of oceanic crust of the African plate occurs along the modern Hellenic Arc and Trench system, confined between Amvrakikos gulf to the northwest and Rhodes to the southeast, forming the Aegean micro-plate.



19. The main tectonic elements of the eastern Mediterranean from Moesia to Cyrenaica. NAF: North Anatolian Fault, NAB: North Aegean Basin. The arrows correspond to motion vectors obtained from GPS measurements (The Transmed Atlas, Papanikolaou D., 2004).

The moderation of the actual Hellenic Arc structures from previous thrust and fold belts, requires the separation of the Hellenides in North and South, on either side of Amvrakikos Gulf. The rate of convergence of the actual Hellenic Arc and Africa, is about 4cm/yr, which is several times higher than the rate of convergence between Europe and Africa. This difference resulted in the creation of an extensional field in the Aegean plate and the opening of the North Aegean basin. The lateral variation of the convergence rate on both

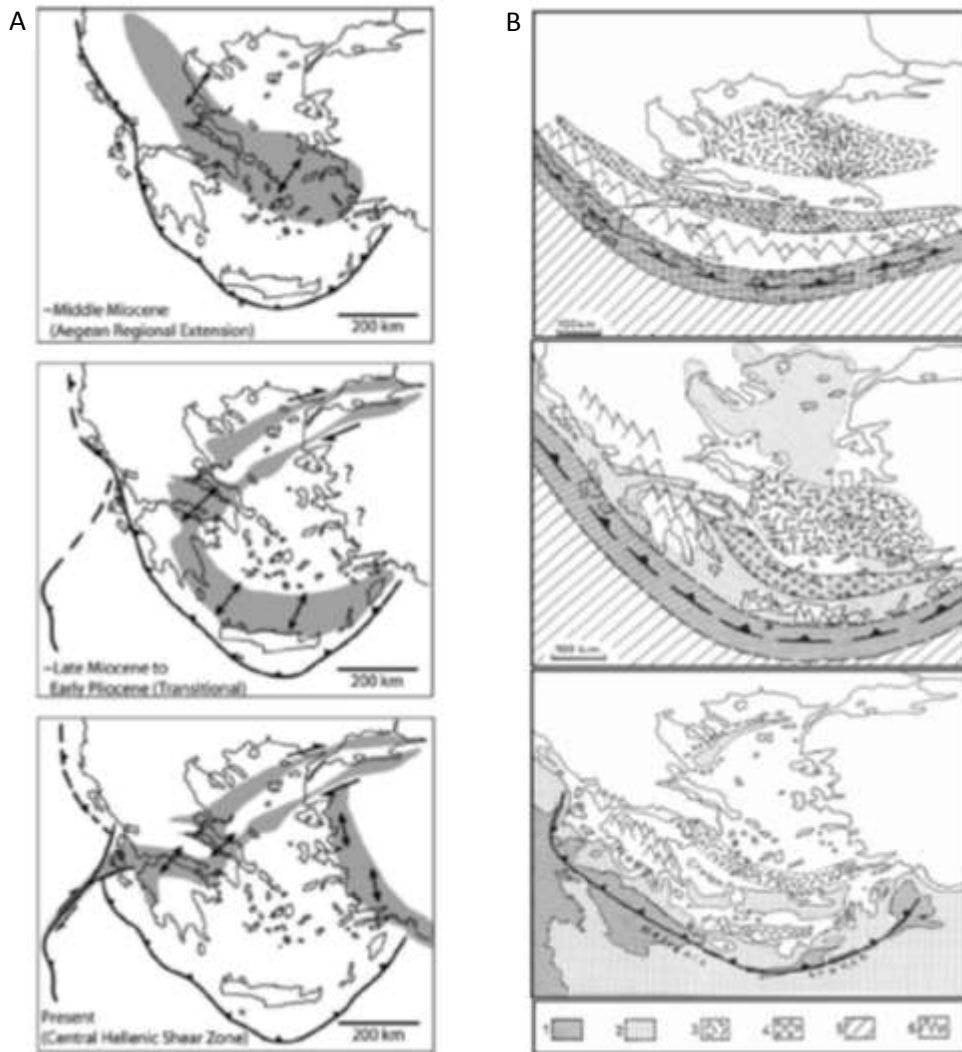
sides of Amvrakikos gulf is accommodated by transform faults. In the area of mainland Greece and the Aegean, the difference between the kinematics of the Aegean microplate to the south and the Eurasian plate to the north, has resulted in the creation of a vertical shear zone, Central Hellenic Shear Zone, which includes strike slip, oblique and normal faults. Another shear zone, West Anatolian Shear Zone, is developed on the eastern margin of the Aegean microplate, in the area of Asia Minor, due to the differential motion with respect to the Anatolian plate. The modification of the Hellenic Arc and its separation into North and South Hellenides took place during Late Miocene. The Tortonian is the last period of the earlier former Hellenic Arc, the Messinian is the period of reorganization and since Early Pliocene the new separation of the Hellenides and the geometry of the arc are consolidated. The Aegean area includes the following sections of the actual Hellenic Arc:

- The back-arc basin – Cretan Basin
- The Volcanic Arc (Methana, Milos, Santorini, Nisyros etc)
- The Northern Aegean Sea (N.A.S.), chiefly characterized by a series of aligned (trending between N50 and N70), relatively deep (up to 1600 m) depressions

The South Aegean and especially the Cretan basin is part of the active Hellenic Arc, while the Central and North Aegean, from Cyclades until Rodopi are not included in the active Hellenic Arc. The boundary between these two areas is the modern Hellenic Volcanic Arc.

Considering the evolution of Hellenic Arc during the Tertiary, the current inactive parts of the Aegean have been active in former geological periods, suggesting earlier “back-arc basin” structures and volcanic arcs. The area of the Aegean exists since the Early Tertiary, when the molassic basin of Rodopi - North Aegean was formed. After the migration of the Arc to the South, the molassic basin (Cretan basin) is currently found in south of Central and N. Aegean. The area of the North Aegean in the Cenozoic remained a marine environment with deep sea sedimentation:

- Molassic sedimentation during Eocene – Oligocene
- Post-orogenic sedimentation during Miocene



20. A. Progression of upper plate deformation within the Aegean region from approximately middle Miocene time until present, with cessation of regional-scale extension and progressive development of the Central Hellenic Shear Zone. Shaded areas show approximate locations of regions most affected by extension and/or strike-slip activity at each time period. Timing is approximate as the age of some events is not precisely determined. (Papanikolaou & Royden 2007).

B. Paleogeographic reconstruction of the Aegean during a) Miocene, b) Miocene - Pliocene, c) current structure of the Aegean (Papanikolaou 1993).

1. Fore-arc basin (flysch sedimentation)
2. Marine environment
3. Volcanic Arc
4. Back-arc basin (Molassic sedimentation)
5. Pre-orogenic areas
6. Island Arc

The figures above illustrate the gradual widening of the stabilized Eurasian lithosphere, which followed the migration of the Arc to the south. Thus, during Eocene, the stabilized sections of the Eurasian plate reached until Rhodopes, while during the Miocene they gradually reached Lemnos, Chios, Samos until their current location at S. Cyclades.

The extension of the paleo-back arc basins has been certified through outcrops of molassic sediments that occur in the Aegean Sea, either onshore or offshore. These outcrops can be grouped (Papanikolaou, 1993) and matched with previous back arc basins that existed in the Aegean starting from the oldest to the newest as follows:

- Early Tertiary – molassic sediments of the N. Aegean
- Lower Miocene – molasse of the Cyclades islands, which is the Seward prolongation of the Messohellenic Molassic Basin (Dermitzakis & Papanikolaou, 1980)
- Upper Miocene – Quaternary: molassic sediments of the Cretan Basin

Regarding the migration of the volcanic arc, it is certified by outcrops of tertiary volcanic rocks (Limnos, Lesvos) or their respective plutonium (Cyclades).

During the Cenozoic, there were periods in which the area of the Aegean was a unitary marine environment and periods when it was divided into a southern and a northern basin from an intermediate land area known as "Aegaeis." This differentiation occurred during Early Miocene when the Cycladic molassic basin was formed in the area of S. Cyclades, separated from the basin of the North Aegean. At that time, mainland Greece and Asia Minor were joined through Attica, Evia, B. Cyclades, Samos, Ikaria. The "Aegaeis" was maintained until Late Miocene when intense volcanic activity dominated.

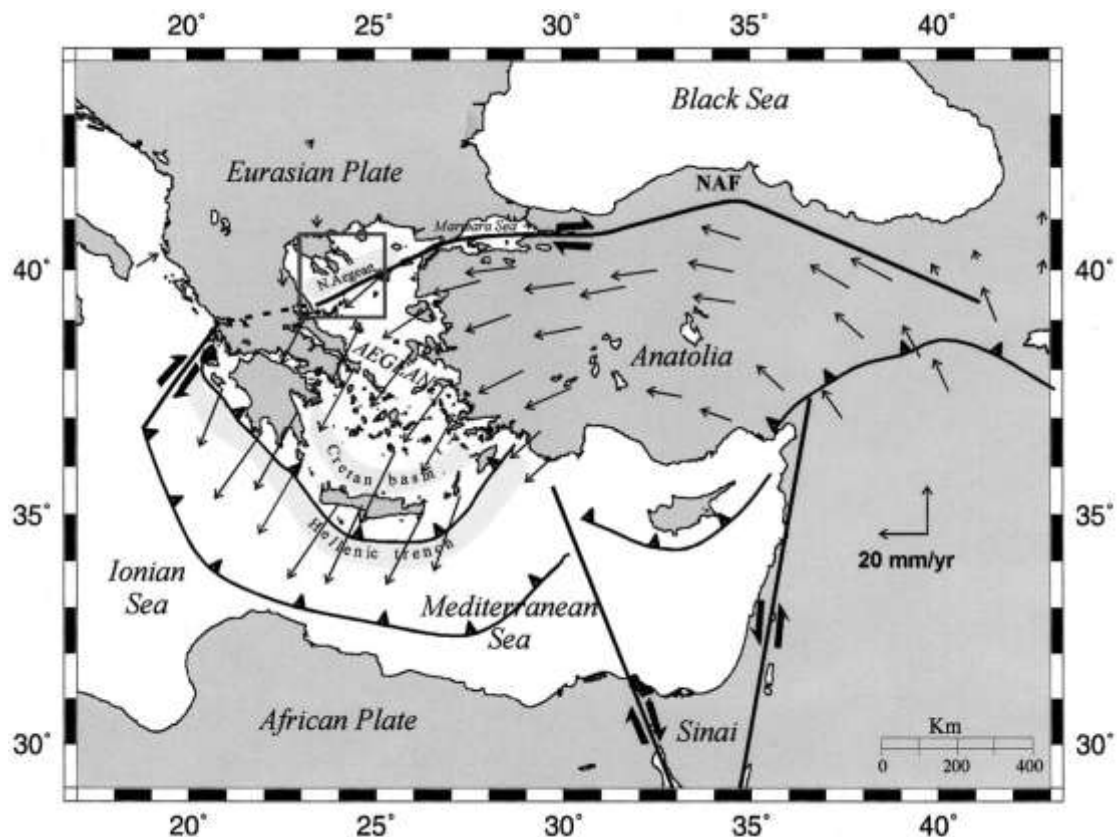
During late Miocene, the opening of the Cretan basin occurred between the "Aegaeis" and Crete, while the previous molassic basin of the Cyclades was uplifted and displaced to a parautochthonous position by gravitational movements. The reorganization of the arc is related to the lateral escape of Anatolia (Papanikolaou & Dermitzakis, 1979) and the westward prolongation of the Northern Anatolia fault zone, under the new tectonic regime established after the collision of the Arabian plate with the Eurasian plate in the area of Caucasus in Late Middle Miocene.

Present day Cyclades islands represent the peaks of the mountains of the preexistent land in this area, "Aegaeis". The subsidence took place during the Quaternary creating the submarine Cycladic platform unifying all the islands at depths ranging from 100-140m. The margins of this platform is the submerged paleocoast of the last glacial period, which subsided due to vertical eustatic movements, following the Quaternary climatic changes.

## **2.2 Geodynamic Sectors of the Aegean Sea**

The area of the Aegean Sea can be divided into 3 distinct geodynamic areas:

a) The North Aegean Basin is located between Thessaly, Macedonia and Thrace and the islands of Lemnos and Sporades. Initially, during late Eocene - Oligocene, the area of the Northern Aegean was a marine sedimentary molassic basin and stretched from the islands of Lemnos and Agios Efstratios to the south until the Rhodope Mountains to the north. During Miocene important parts of the preexistent basin were uplifted until Late Miocene - Pliocene. At that period a neotectonic activity begins due to the westward escape of Anatolia accommodated by dextral strike slip motion of the Northern Anatolia Fault Zone, which was created as a result of the collision between Arabia and Eurasia in the Caucasus. So today's active tectonic structures in the North Aegean Basin are the result of a neotectonic regime that overlapped an earlier below - Tertiary Alpine - molassic structure. Regarding the current position of this basin, it is located behind the main morphostructural elements of the active Hellenic Arc and has joined the stabilized Eurasian lithosphere.



21. Geotectonic position of the North Aegean Basin within the plate-tectonics framework of the Eastern Mediterranean. The arrows corresponding to the annual rate of the slip vector determined by GPS measurements (based on data by Reilinger et al., 2000) indicate the existence of a tectonic boundary along the North Aegean Basin (Papanikolaou et al., 2002).

b) The area of the central Aegean Sea stands out for its numerous islands (Cyclades, Ikaria, Samos etc.), consisting of Tertiary HP / LT metamorphic rocks that reached the surface during the period of Miocene - Pliocene. Tertiary sedimentary basins, similar to those of the North Aegean, are absent in this region. The molassic sediments of Early Oligocene – Late Miocene overly metamorphic rocks, is allochthon and their tectonic transport is placed in the Upper Miocene.

c) The southern part of the Aegean is a relatively geometric arcuate deep basin, which separates the Cycladic islands to the north from the island of Crete to the south. The Cretan basin, is the modern Hellenic back-arc basin formed during Late Miocene behind the island arc Peloponnese - Kythera - Crete - Dodecanese. Northwards it is bounded by the active Aegean volcanic arc (Methana, Milos, Santorini, Nisyros) which also forms the southern margin of the underwater platform of the Cyclades.

### **2.3 The Hellenic Volcanic Arc – Geodynamic Setting**

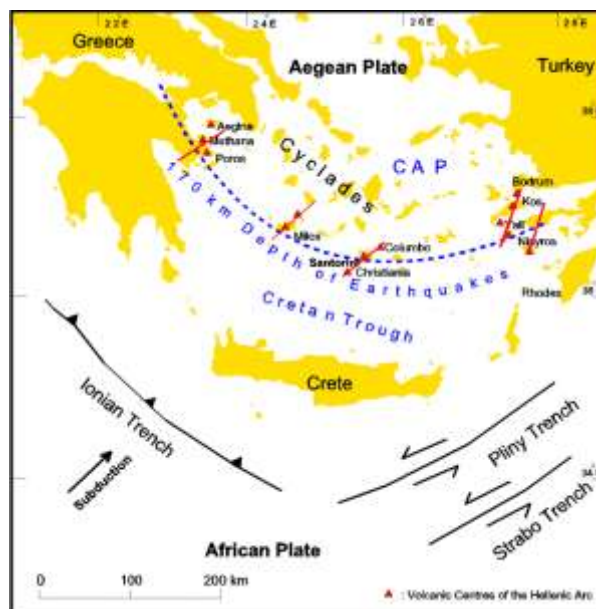
The Hellenic Volcanic Arc has been formed at the back arc region of a convergent plate boundary, where the oceanic crust of the African plate is subducting northwards underneath the active margin of the European plate (McKenzie, 1972; Ninkovich & Hays, 1972; Dewey et al, 1973; Angelier, 1979; LePichon & Angelier, 1979). According to geochronological data the actual Hellenic Volcanic Arc has been active during the early Pliocene with significant activity during the Quaternary (Pe-Piper & Piper, 2002).

The crust of the Aegean is continental with thicknesses in the range of 20-32 km; compared with average crustal thicknesses of the mainland of Greece and Turkey, 40-50 km, a stretching factor of about two due to tectonic extension is implied. The strongest extension seems to have been in the Cretan Trough whereas the Central Aseismic Plateau (CAP) on which the Cyclades are situated forms a relatively stable strongly faulted crust block. The volcanic centers of the Aegean Arc are placed along the southern rim of the CAP. They are aligned on five 60E NE-going seismic lineaments that are interpreted as deep lithosphere rupture zones which permit mantle-derived magma ascent.

The Cyclades are a metamorphic complex area, the Cycladic Massif, that formed in Triassic to Tertiary time and were folded and metamorphosed during the Alpine folding around 60 million years ago. The Cycladic Massif was a coherent landmass until tectonic movement of the plates and the beginning subduction caused its disintegration by subsidence and upheaval of single units following partial flooding in the late Miocene.

Volcanism in the Aegean Arc generally first occurred about 3-4 million years ago with the exception of the island of Kos where Keller and others report ignimbrites from Miocene age about 10-11 million years old.

As previously mentioned, the study of the Tertiary volcanic rocks on several islands of the Aegean, has shown a southward migration of the Volcanic Arc since Late Eocene which started from the North Aegean area until its present day configuration along the southern margin of the Cycladic platform and the northern of the Cretan Basin (Bellon et al., 1979, Fytikas et al., 1984, Papanikolaou, 1993). The migration rate has been estimated to 10 km/myears, since the total displacement is approximately 400 km within 40 myears (Ppanikolaou, 1993, Royden & Papanikolaou, 2011).



22. The South Aegean Volcanic Arc and the tectonic setting of Santorini. After Friedrich (1994).

Four groups of volcanic rocks comprise the volcanic arc, including both onshore and offshore outcrops. Methana group, including Paphsania submarine volcano, at the western edge of the volcanic arc in western Saronikos Gulf, Milos and Santorini group together with Kolumbo

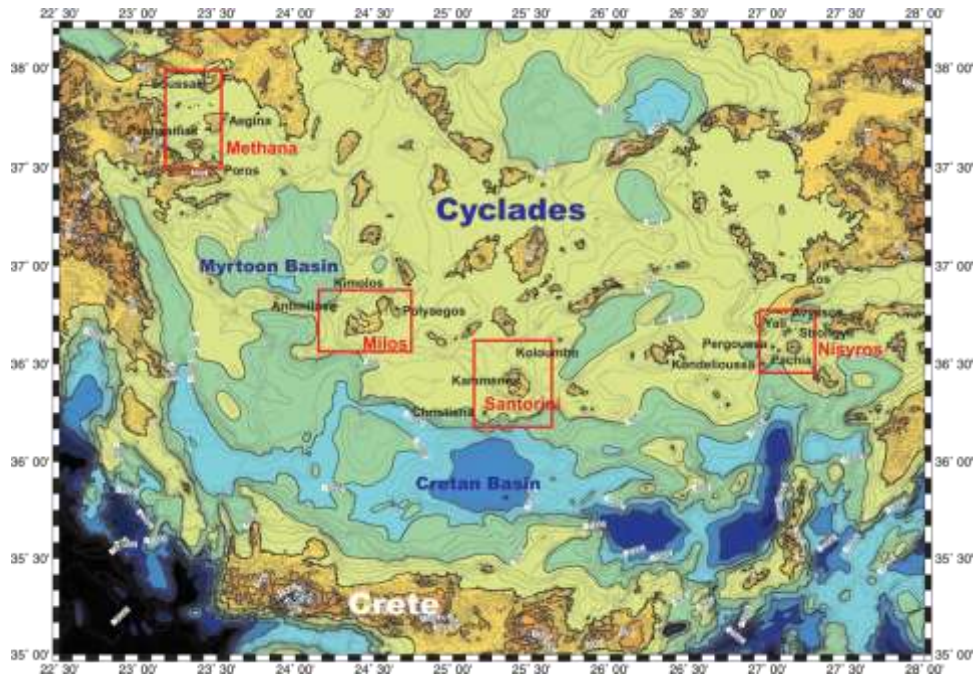
volcanic chain at the submarine area northeast of Santorini, and Nisyros group at the eastern edge including several submarine volcanic features.

The volcanic centers are usually located within neotectonic grabens formed by normal faulting, sometimes overprinted by subvertical strike-slip structures especially in the Santorini and Nisyros volcanic groups, which form the eastern part of the arc depth (Nomikou et al.2012b). This strike-slip component has been proposed to have a NE-SW direction in the Santorini – Kolumbo volcanic line based on the subvertical faults in the offshore Anhydros Basin and the associated system of volcanic dikes (Sakellariou et al, 2010). Thus, the overall tectonic regime in the central and eastern part of the arc is better described as transtensional with prevailing NE-SW direction.

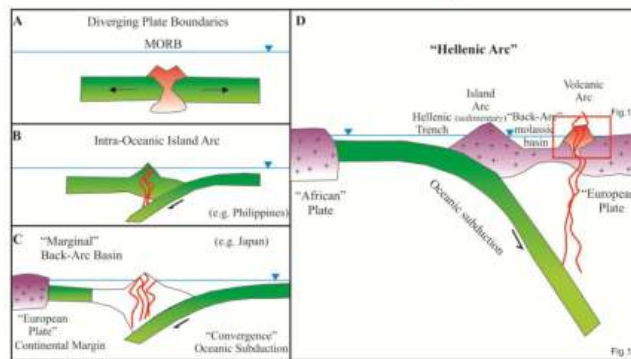
The prevailing tectonic trend in Milos and Methana group is in the NW-SE direction, following the general direction of the Hellenic arc. This tectonic trend has been overprinted by E-W normal faults after the disruption of the arc parallel structures of the Hellenic arc by younger structures creating the neotectonic horst and graben structure (Papanikolaou & Royden, 2007; Royden & Papanikolaou 2011).

Recent research within Kolumbo submarine volcano has revealed a rather unique site of volcanism, as it hosts an active hydrothermal field of intermediate.

Submarine hydrothermal systems associated to recent or active volcanic arcs show a number of geobiological characteristics depending on their geodynamic setting. Most cases reported in the literature concern primarily divergent plate boundaries along mid-ocean ridges and secondarily convergent plate boundaries along intraoceanic island arcs (e.g. Philippines) or along subduction systems beneath active continental margins with back-arc marginal basins (e.g. Japan). These convergent geodynamic environments are contrasted with the oceanic subduction beneath active continental margins, without back-arc basins where volcanic belts form mountain belts (e.g. Andes). A transitional situation exists in some convergent settings, where the active continental margin characterized by a back arc molassic basin built on thinned continental crust, without the existence of marginal basin as this is observed in the Hellenic arc and in the Taupo rift in New Zealand. The Kolumbo hydrothermal system is part of the submerged part of the Hellenic Volcanic arc developed on subducted East Mediterranean oceanic crust (northern edge of the African plate) beneath the Hellenic Active continental margin (southern edge of the European plate). Its geodynamic position is unique as it lies on Aegean continental crust behind the Hellenic Arc and Trench system.



23. Topographic map of the southern Aegean Sea combining onshore and offshore data from recent oceanographic surveys. The four modern volcanic groups are indicated within red boxes together with the names of the main terrestrial and submarine volcanic centers along the volcanic arc Nomiko;u et al, 2012b).



24. Schematic tectonic sketches of different geodynamic environments showing where sea floor hydrothermal vents occur.

A: Mid-Ocean Ridges along divergent plates.

B: Intra-Oceanic Arcs within convergent boundaries (e.g. Philippines).

C: Marginal back-arc basins and island arcs along active continental margins with oceanic subduction (e.g. Japan)

D: "Hellenic Volcanic Arc", within active continental margin, developed behind the molassic back-arc basin, hosted over thinned continental crust (Kiliyas et. al. 2012-in review).

## 2.4 Kolumbo Volcanic Chain – Geodynamic Setting

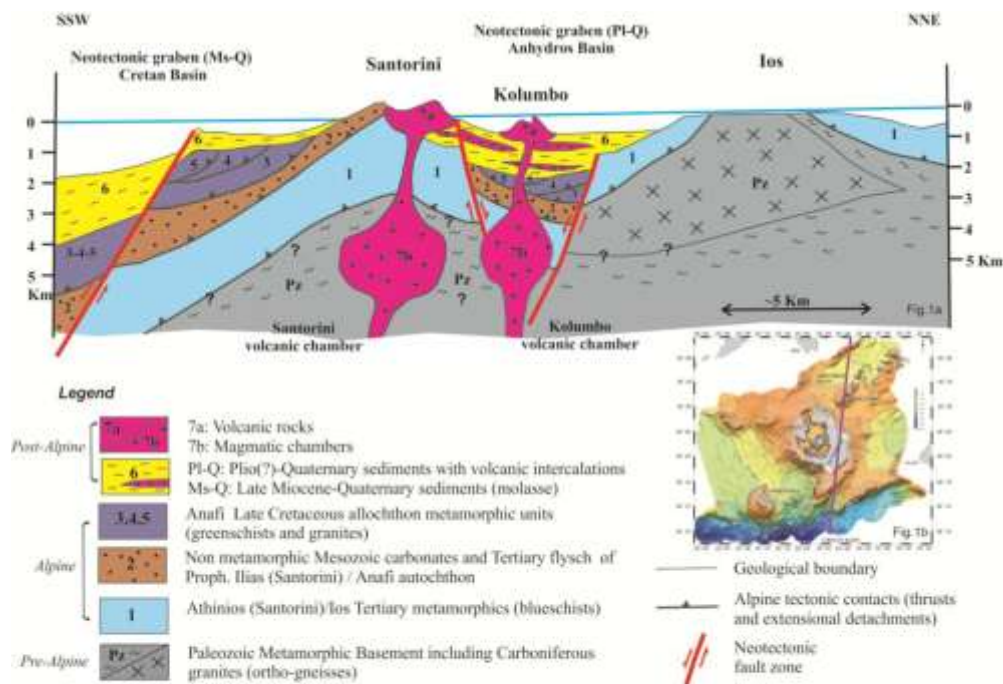
The Kolumbo volcanic chain extends 20 km to the northeast of the main island of Santorini, as a linear distribution of over 20 submarine cones of varying sizes. It has been developed within a local extensional tectonic regime, along with a significant strike – slip component, in the overall compressive geodynamic setting of the active Hellenic Orogenic Arc. It is located in a small, elongated, rifted basin, known as Anhydros Basin, and its southwestern edge, Kolumbo volcano, is approximately 6.5 km NE of Santorini island.

Kolumbo submarine volcano is the largest of the 20 submarine volcanic cones within the basin. The key for understanding the evolution of this volcanic center is hiding beneath the

seafloor, in the different layers of the continental crust. The composition of the crust beneath Kolumbo determines the type of volcanism on the surface.

As magma is created and rises through the Aegean lithosphere, which is rather thin due to the extensional regime, it crosses a pre-Alpine continental crust component, approximately 10-15 km thick. This includes a core of carboniferous granites (ortho-gneisses) and a mantle of garnet-mica schists (Van der Maar & Jansen 1983) corresponding to the Palaeozoic Metamorphic Basement occurring at the southern part of Ios island. Thereafter, it crosscuts alpine units, that have been exposed through a detachment fault system during middle Miocene, comprising Tertiary metamorphics (Athinos/ Ios blueschists), non metamorphic Mesozoic carbonates (Tertiary flysch of Proph. Ilias/ Anafi autochthon) and Late Cretaceous allochthon metamorphic units (Anafi greenschists and granites). During Late Pliocene – Early Pleistocene the transgression of the sea on the former land generated a sequence of marine sediments that overlaid the previously described basement. Finally, during Late Pleistocene extensional tectonic structures crosscutting the arc dominated at the Aegean area, leading to the formation of neotectonic grabens such as the Anydhros graben where Kolumbo is located. At the same time intensive volcanic activity successively led to the current configuration of the volcanic arc. Seismic reflectors observed on air-gun profiles support this since they most likely correspond to different volcanic eruptions that have occurred at the area.

The Mesozoic Carbonates exposed at the NE part of Santorini continue towards the south, at the underwater area and reach the northern marginal fault zone of the Cretan Basin, which is the back arc basin of the Hellenic Arc. Unlike the Anydhros Basin, where the Alpine units are disrupted by magma ascend, in the Cretan basin volcanism is absent. In addition, its development dates back to Late Miocene until recently in Quaternary, whereas the rift of Anydhros started in Pliocene times. The Alpine units in the Cretan basin are disrupted by the northern marginal fault zone which at the same time is the southern margin of volcanism.



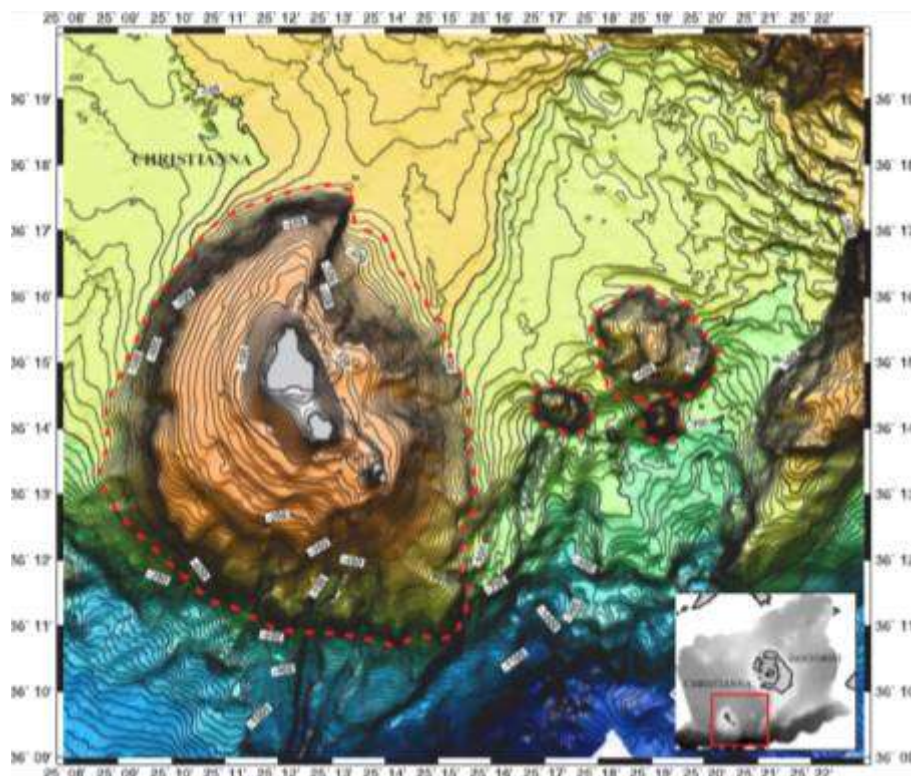
25. Schematic Geological section through the Hellenic Volcanic Arc, from the molassic back-arc Cretan Basin to the Cyclades island (Ios) in the back-arc area (Kiliyas et. al. 2012-in review).

## **2.5 Geologic Setting of Santorini Volcanic Group**

The volcanic complex of Santorini currently represents the most active volcanic field of the Hellenic Volcanic Arc. It lies on the faulted southern margin of the Central Aseismic Plateau, on which the Cyclades are situated, on a major NE-SW-trending lithospheric rupture zone (Papazachos K Panagiotopoulos 1993). The stress regime in this part of the Aegean is extensional. The crust beneath Santorini is about 30km thick and continental in nature. The sea floor to the northeast it split into alternating horsts and grabens by NE-SW-trending normal faults. Santorini has developed on the northern margin of a basement horst called the Santorini-Amorgos ridge. If extrapolated, the fault defining the northern margin of the horst passes through the Santorini caldera. It also passes near the submarine Kolumbo volcano, 6.5km northeast of Santorini, and the volcanic Christiana Islands to the southwest. Kolumbo, Saniorini, and Christiana lie on an extension of the same NE-SW fault.

### **2.5.1 Christianna**

Christiana islands are four small islets SE of Santorini. They belong to a volcanic cone that updomed the sea floor and, it produced various flows and pyroclastic deposits. The edifice was built at the junction of a pair of fault zones trending NNW-SSE and NNE-SSW with most prominent the later one, cutting sharply the volcanic cone and continuing along the western coast of the northern island.



26. Swath bathymetric Map of Christianna Volcanic Field using 10m isobaths. The submarine volcanic outcrops are shown by dashed red lines. (Nomikou et al., 2012b)

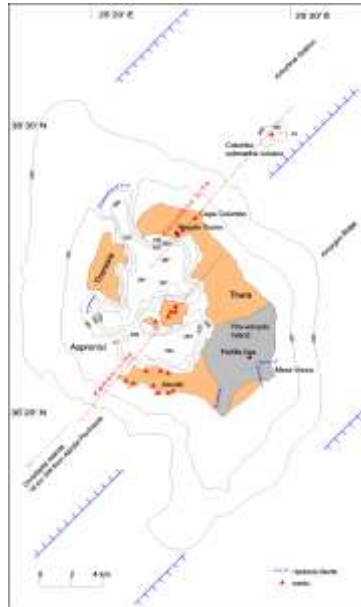
### **2.5.2 Santorini, Nea and Palea Kameni**

Santorini is one of the largest Quaternary volcanoes of the Aegean region. The incomparable beauty of the island is the result of several explosive eruptions that have occurred through time. The caldera cliffs expose several sequences of lavas and pyroclastic deposits, which record the evolution of the volcano in space and time. These include the products of 12 major explosive eruptions and the dissected remains of several ancient lava shields, stratovolcanoes, and lava-dome complexes (Druitt 1999). Santorini is best known for the Minoan eruption of the late Bronze Age (Bond & Sparks 1976, Heiken & McCoy 1984, Sparks & Wilson 1990), but some of the previous explosive eruptions may have been as large (Druitt et al. 1989).

Santorini is a complex of five islands. Thera, Therasia, and Aspronisi are arranged in a dissected ring around a flooded caldera, in which lie the islands of Palea and Nea Kameni. The steep caldera cliffs of Thera and Therasia reach more than 300 m above sea level at Cape Tourlos. Southeastern Thera is dominated by two basement massifs, Mount Profitis Ilias and Gavrillos Ridge, which are the protruding peaks of an island that existed prior to volcanism. The original west coast of this island is preserved at Athinios, where it has been exhumed by caldera collapse. Mount Profitis Ilias (552m) is the highest peak on Santorini. The rocks consist of metamorphosed limestone and schist from Triassic to Tertiary time folded during the Alpine folding. The observed metamorphose grade is a blue-schist facies resulting from tectonic deformation by the plate collision in the Oligocene to Miocene. At Athinios a 9.5 million year old Miocene granite intrusion has been found; it is part of the Cycladic Granitic Province and is the source of ore minerals including talcum, chalcopyrite, chrysocolla, magnetite and others. Other peaks include Mounts Loumaravi and Archangelos in southern Thera. Mounts Micros Profitis Ilias and Megalo Vouno in northern Thera, and Mount Viglos on Therasia, all of which are volcanic in origin.

Most of the tectonic lines seen both on Santorini and on seismic profiles follow the general southwest-northeast trend. The most important one is named Kameni Line. It intersects the caldera and defines most of the known eruption centers. It aligns the Christiania islands, the Akrotiri peninsula and Palea and Nea Kameni. A parallel one, the Columbo line, perhaps identical with the Kameni line, passes through the centers of Megalo Vouno, the maar at Cape Columbo beach and the Columbo volcano. It seems that the rising magma has exploited existing deep-reaching tectonic fault zones.

The earliest Quaternary volcanics occur on the Akrotiri Peninsula (Early centres of Akrotiri Peninsula). These and some younger cinder cones (Cinder cones of Akrotiri Peninsula) are covered by a sequence of pyroclastic deposits which in places exceeds 200 m in thickness. These deposits also drape over the basement massif and dominate the cliffs of southern Thera. They are composed of dacitic lavas that updomed the sea floor and produced various flows and pyroclastic deposits. They have been strongly altered by hydrothermal activity. The updomed areas still are well visible on the Akrotiri peninsula (Lumaravi and Archangelos hills). From marine fossils embedded in the tuffs, Seidenkrantz and Friedrich (1992) concluded a minimum age for the Akrotiri peninsula of 2 million years.



27. The caldera and structural setting of the Santorini volcanic field. After Heiken and McCoy (1984).

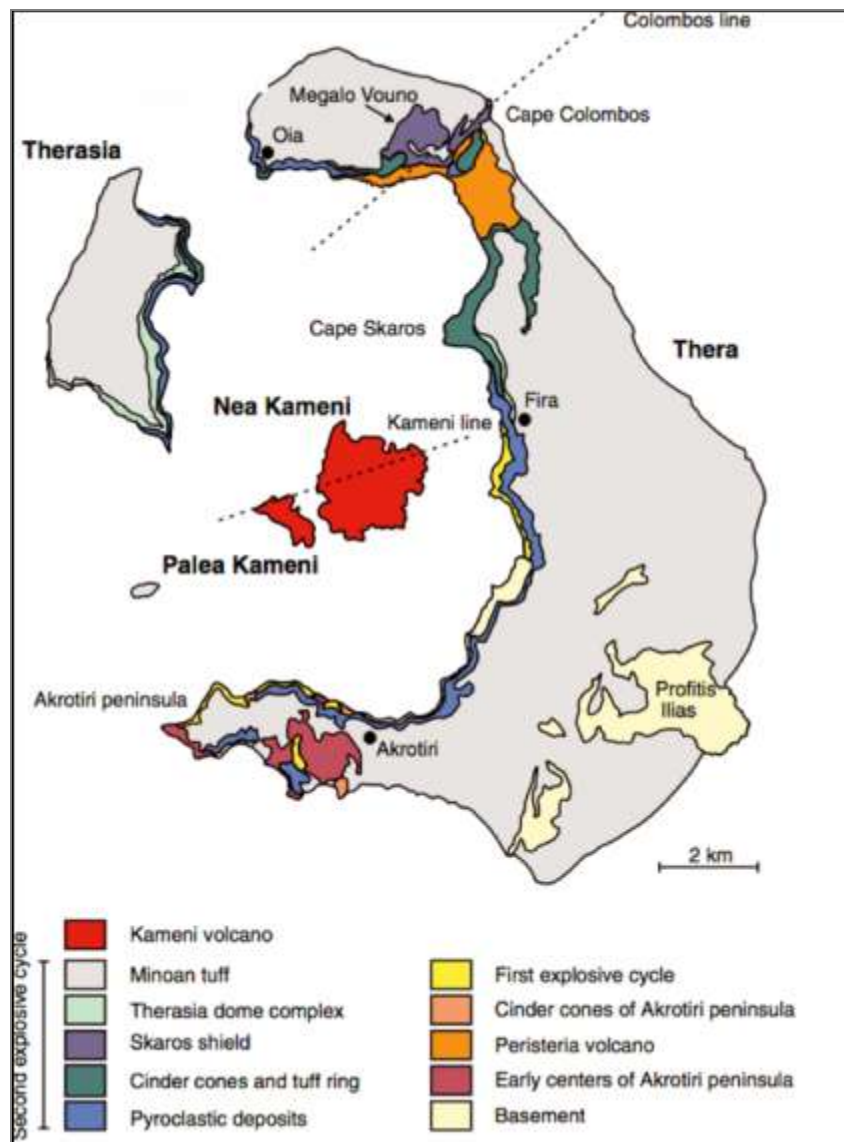
The earliest Quaternary volcanics occur on the Akrotiri Peninsula (Early centres of Akrotiri Peninsula). These and some younger cinder cones (Cinder cones of Akrotiri Peninsula) are covered by a sequence of pyroclastic deposits which in places exceeds 200 m in thickness. These deposits also drape over the basement massif and dominate the cliffs of southern Thera. They are composed of dacitic lavas that updomed the sea floor and produced various flows and pyroclastic deposits. They have been strongly altered by hydrothermal activity. The updomed areas still are well visible on the Akrotiri peninsula (Lumaravi and Archangelos hills). From marine fossils embedded in the tuffs, Seidenkrantz and Friedrich (1992) concluded a minimum age for the Akrotiri peninsula of 2 million years.

At the localities of Balos ("Red Beach"), Kokkinopetra, Mavropetra and Mavrocachidi, basaltic to andesitic strombolian scoria cones are exposed that flank the Akrotiri volcanoes. They might be related to the later volcanic centers of northern Thera (Megalo Vouno and Mikro Profitis Ilias). Druitt and Sparks (1996) recently dated them to 344 ± 25 thousand years. At this early stage the Akrotiri peninsula probably was a separate island and not yet connected to the non-volcanic island.

In contrast, the cliffs of Therasia and northern Thera are dominated by the remains of four effusive centres: the Peristeria Volcano, the Simandiri shield, the Skaros shield, and the Therasia dome complex. The contrast in caldera wall geology between the north (mainly lavas) and south (mainly pyroclastic deposits) is a striking feature of Santorini.

The pyroclastic succession is the product of 12 large explosive eruptions and numerous deposits related to more minor explosive eruptions. The Thera pyroclastics preserve evidence for two cycles of explosive activity, as recognized on the basis of long-term trends in magma composition (Druitt et al. 1989). Each explosive cycle commenced with eruptions of mafic to intermediate magmas and terminated with a pair of major silicic eruptions and caldera collapse.

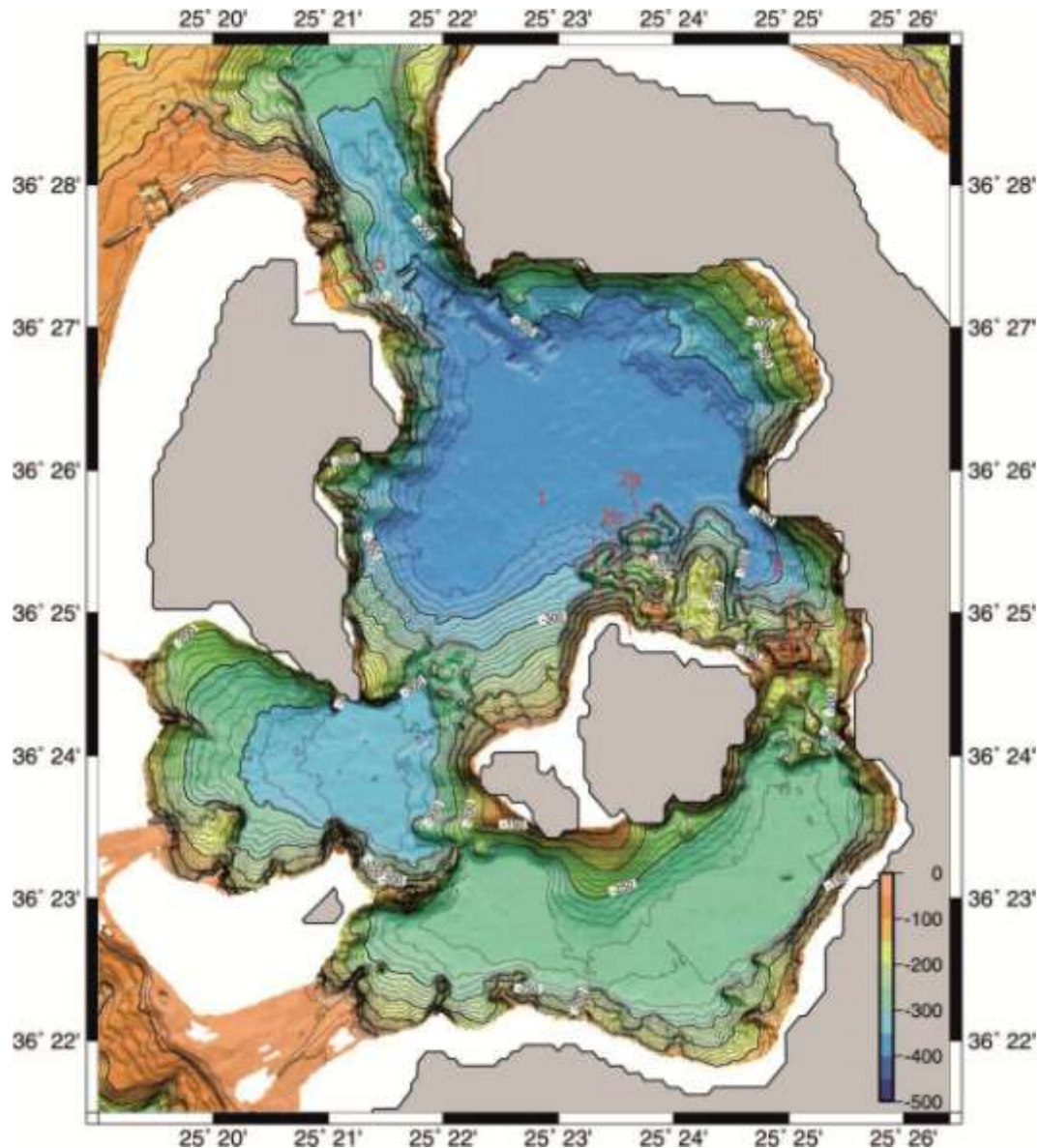
Thera, Therasia and Aspronisi are each capped by a continuous Layer of white tuff laid down by the Minoan eruption in the late Bronze Age. The broad, gently inclined coastal plains of Thera and Therasia are composed mainly of Minoan ignimbrite.



28. Simplified Geological Map of Santorini (Druitt et al. 1999).

The caldera is a composite structure resulting from at least four collapse events (Druitt & Francaviglia 1992). The present configuration of the caldera after the Minoan eruption consists of three distinct basins that form separate depositional environments, divided by the Kameni volcanic islands (Nomikou et al., 2012b) (Fig.1): i) The North Basin is the largest and deepest (389 m) developed between the Kamenes, Therasia and the northern part of the Santorini caldera. It is connected by a narrow channel with steep slopes at the depth of 300m with a semi-caldera formation outside Santorini Caldera, at the NW part of Oia Village. As shown by the shape of the circular isobaths, the rim of the caldera is at almost 100m depth with mild internal slopes and an opening between Oia Village and Thirasia island. The western and eastern slopes of the North basin are very steep, as it is revealed by the high density of isobaths. At the NE part of the basin, at the depth of 340 m, a vent field has been discovered in 2006 (Sigurdsson et al., 2006) with vent mounts up to 1m height with no hydrothermal activity (Nomikou et al., 2012c). ii) The West Basin is the smaller and lies alongside Aspronisi islet, Palaea Kameni and Southern Therasia with a medium depth (325 m). The flanks of the basin are more gentle in the western part and more abrupt close to Thirasia and Aspronisi iii) The South Basin is developed between the Kamenes and the

southern part of the Santorini caldera covering a medium area with the shallowest sea bottom (297 m). It is noticeable, that this basin has been separated from the other ones by the development of submarine volcanic domes in a NE-SW direction. The most known one is Pagos dome close to Fira Port, developed from 200m up to 40m depth, above which many cruise ships are moored during the high touristic season.



29. Swath bathymetric map of Santorini caldera using 10m isobaths, where the three post-Minoan caldera subbasins are indicated (the dotted borders show the basinal parts) (Nomikou et al, 2011) The red lines indicate the ROV transects of 2011.

The Minoan eruption occurred the 17<sup>th</sup> century BC, in the Late Bronze Age. It was one of the largest plinian eruptions in younger time. It produced 30-40 km<sup>3</sup> rhyodacitic magma and is ranked VEI=6 (Volcanic Explosivity Index after Simkin and others, 1981). The eruption was followed by collapse of the magma chamber that enlarged an existing caldera. The height of the plinian eruption column is estimated 36-39 km (Pyle, 1990). It dispersed tephra throughout the Eastern Mediterranean and might have led to global climatic impacts. Its deposits on Santorini consist of up to 50 m thick layers of white pumice and ash.



### **2.5.3 Kolumbo fault line on land observations**

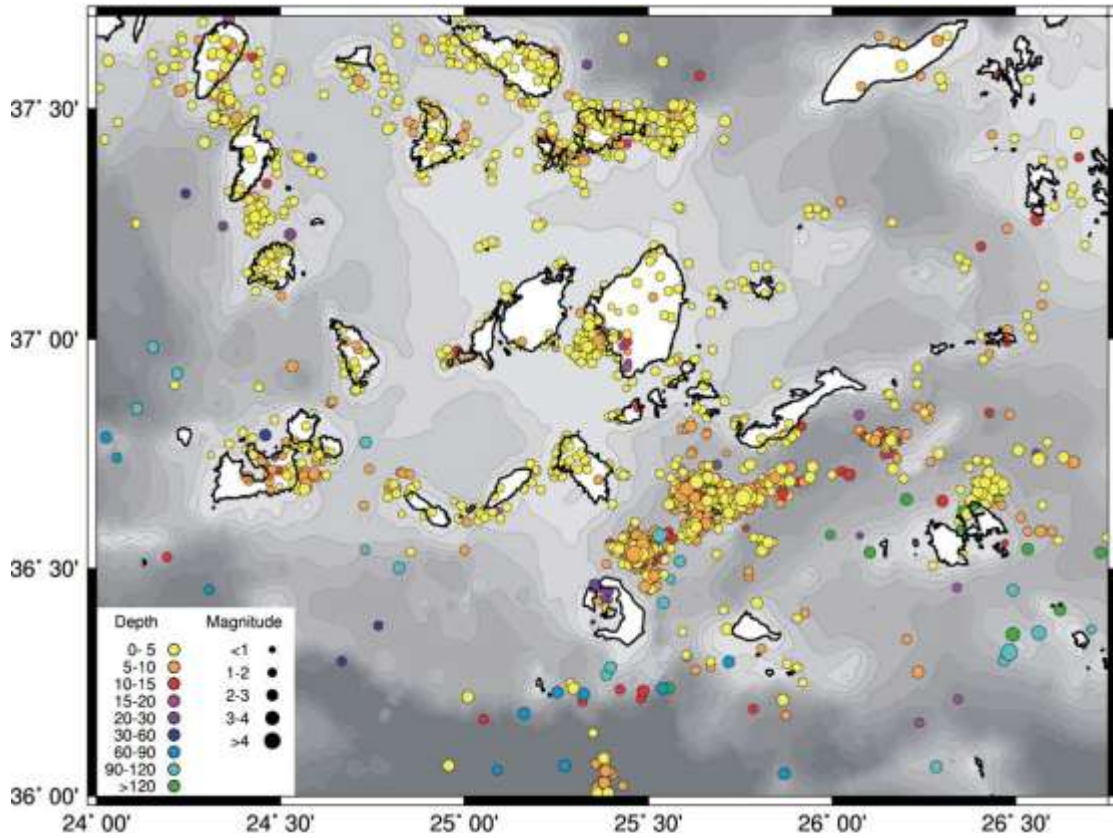
The Kolumbo line passes through the centers of Megalo Vouno, the Cape Kolumbo beach and the Kolumbo submarine volcano. It has served as path for magma ascend. Recent neotectonic studies have revealed the existence of NE-SW faults near Mikros Profitis Ilias of dextral strike-slip and normal character that belong to the Kolumbo line. The dykes observed at the north part of the caldera are related to these faulting. Their orientation coincides with the orientation of faulting at the area.



32. Lava dykes trending NE-SW at the northern part of the Santorini caldera walls (Nomikou et al. 2012a).

The lava succession near Mikros Profitis Ilias is cut by two faults (Druitt & Francaviglia 1991). Matching of rock types across the faults shows that the intervening block has moved down ( - 50 m) and into the caldera (200-400 m). This sector of northeast Thera is particularly narrow and probably weak structurally. According to Druitt & Francaviglia, 1991 the faulting probably relates to incipient slumping of the northeastern fault block due to subsidence on the caldera side. The northeastern fault block cannot relate to Minoan collapse because the Minoan deposits drape across the faults, the scarps of which were well eroded by Minoan time. The fault block was interpreted as a failed breach associated with either the Skaros or Cape Riva collapses.

The most recent seismicity is focused along a northeast trending fault system that includes Kolumbo submarine volcano (~7 km NE of Santorini) and the other smaller submarine cones in the Anhydros Basin (Bohnhoff et al., 2006).



33. Hypocenter catalogue for the central Hellenic Volcanic Arc determined by CYCNET during the time interval September 2002–July 2004. Hypocentral depth is color encoded and size of circles scales with magnitude. Gray shading indicates water depth in 100 m steps for the first 500 m; dark gray areas in the south reach water depth of more than 1000 m. (Bonhoff et al. 2006)



34. View of Kokkino Vouno, Megalo Vouno and the normal fault that ends at Cape Kolumbo.



35. View of Profitis Ilias and Megalo Vouno from an eastern point.

### **3. Methodology**

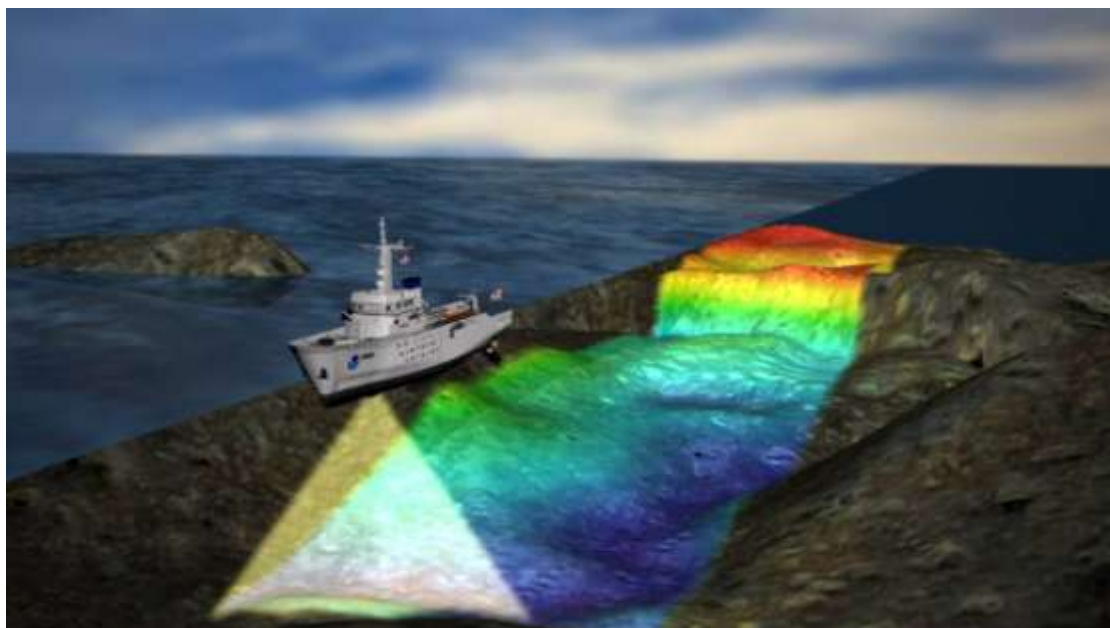
#### **3.1 Bathymetric Data**

The bathymetric data presented in this paper were collected during two oceanographic surveys. The first systematic swath bathymetry survey of the study area was conducted in 2001 using the 20 kHz SEABEAM 2120 swath system on R/V Aegaeo in the frame of “GEOWARN” project. The 19 volcanic cones NE of Kolumbo were discovered at that time. Supplementary swath bathymetry data were also collected in the frame of a collaborative project (NSF grant OCE-0452478) “THERA”, between the University of Rhode Island (URI-USA), the Hellenic Centre for Marine Research (HCMR-Greece), and the Institute of Geology and Mineral Exploration (IGME-Greece) in 2006, onboard R/V Aegaeo.

The SEABEAM 2120 is a hull-mounted swath system operating at 20 kHz in water depths not exceeding 6000 m. It has an angular coverage sector of 150° with 149 beams, covering a swath width from 7.5 to 11.5 times the water depth for depths from 20 m to 5 km. The maximum swath coverage can reach 9 km at maximum depth and gives satisfactory data quality at speeds up to 11 knots.



36. The exploration vessels “Aegaeo” and “Endeavor”.



37. Illustration of the operation of a multibeam echosounder.

### **3.2 ROV Data**

ROV Data presented in this paper was collected during a marine geological survey using the E/V Nautilus, conducted northeast of Santorini island in August 2010 as a collaborative project (New Frontiers in Ocean Exploration 2010) between the Graduate School of Oceanography at the University of Rhode Island (URI-USA), the Dept. of Geology & Geoenvironment of University of Athens (NKUA-GREECE), the Institute for Exploration (IFE-USA), and the Institute of Geology and Mineral Exploration (IGME-GREECE). ROV data have previously been collected in 2006 onboard R/V Aegaeo and R/V Endeavor. Additional ROV dives have been performed in late 2006 during R/V Aegaeo cruise “Nautilus 2006”.

E/V Nautilus is equipped with the ROVs Hercules and Argus, which make up a dual-body deepwater system (4,000 m depth rating). Hercules and Argus are state-of-the-art deep-sea robotic vehicle systems capable of exploring depths up to 4000 m. Each remotely operated vehicle (ROV) has its own suite of cameras and sensors that receive electrical power from the surface through a fiber-optic cable, which also transmits data and video. Engineers and scientists command the vehicles from a control room aboard Nautilus, with some dives lasting more than three days (Phillips et al., 2011).



38. The exploration Vessel “Nautilus” (OET).

A 20-hp electric/hydraulic pump powers the mechanical functions on Hercules. Two manipulator arms, one dexterous and the other strong, work together to sample and move equipment around on the seafloor. High-definition video cameras provide a clear, precise window to the world below and create dazzling images.



39, 40. ROV "Hercules" (OET).

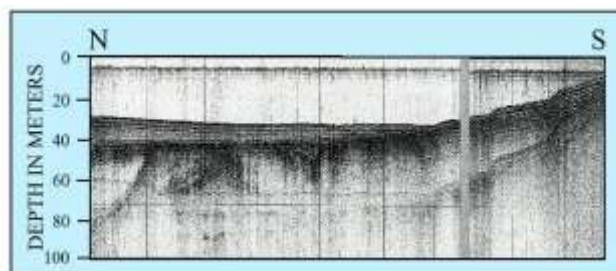
Capable of working as a stand-alone system, Argus becomes a towed-body instrument for large-scale deepwater survey missions. Side-scan sonar looks out on either side of the vehicle up to 400 m away, identifying features as small as a brick. Powerful 1200-watt lamps provide light miles below where sunlight is absorbed by seawater.



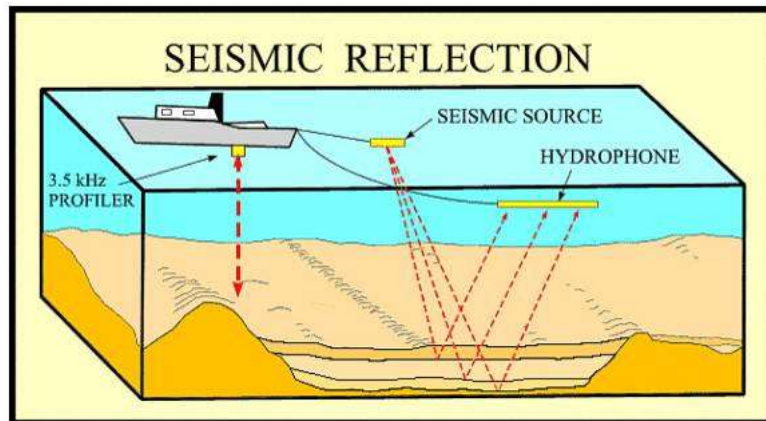
41, 42. ROV "Argus" (OET).

### **3.3 Seismic reflection profiling**

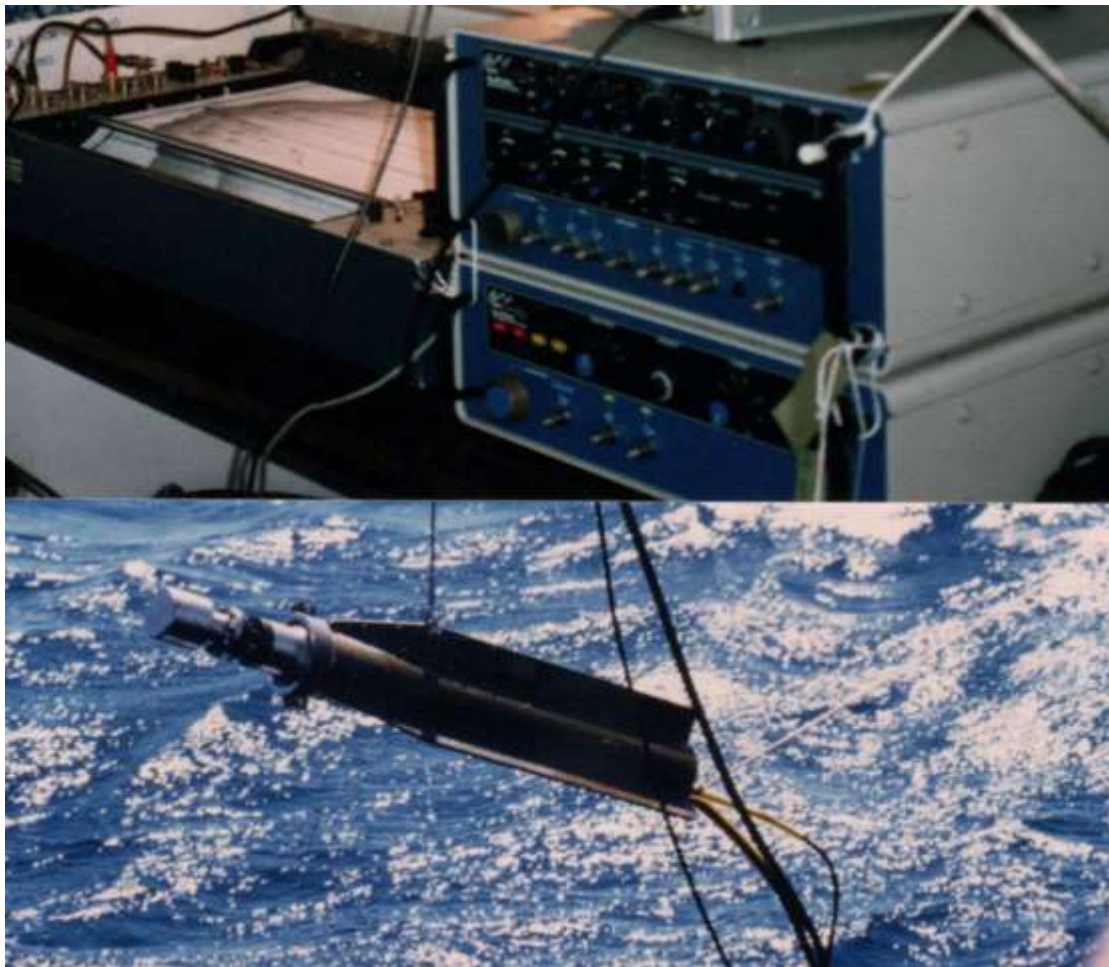
Air-gun profiles were obtained during the "THERA" oceanographic mission in 2006. Seismic reflection profiling was used to obtain two-dimensional cross-sections that would reveal the structure of the rocks and sediments below the seafloor. The technique utilizes a high powered sound source that is towed behind the ship. The sound waves reflect off different layers beneath the seafloor depending on the difference in sediment or rock properties. These reflections are then recorded by a hydrophone towed behind the sound source. Computer software is able to translate the reflections into a plot that shows the depths of different types of rock or sediment formations below the ocean floor (fig. 4, upper). These profiles are critical to understand how volcanic deposits on the seafloor have accumulated over time.



43. Seismic profile (<http://noc.ac.uk/science-technology/marine-resources/energy/hydrocarbons>).



44. Seismic reflection survey (<http://noc.ac.uk/science-technology/marine-resources/energy/hydrocarbons>).



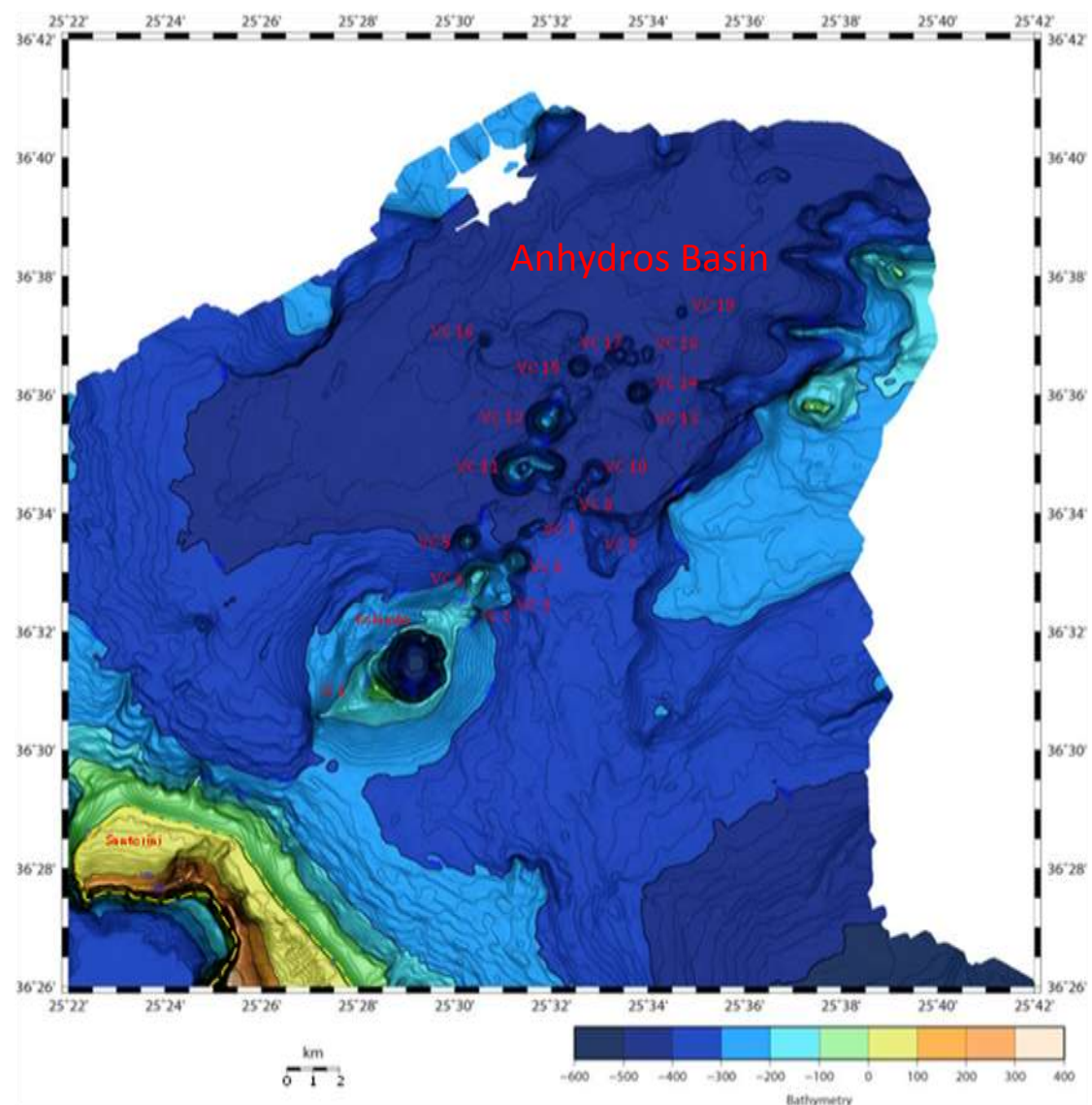
45, 46. Air-gun system. Units for the derivation, amplification and processing of the sound waves (upper photo) and the towable air-detonation unit (lower photo).

## 4. Morphology

### 4.1 Bathymetry

The multibeam bathymetric surveys were carried out by the R/V Aegaeo of the Hellenic Centre for Marine Research, using a SEABEAM 2120 swath system, which is a hull-mounted swath system operating at 20 kHz in water depths not exceeding 6000 m. It has an angular coverage sector of  $150^{\circ}$  with 149 beams, covering a swath width from 7.5 to 11.5 times the water depth for depths from 20 m to 5 km. The maximum swath coverage can reach 9 km at maximum depth and gives satisfactory data quality at speeds up to 11 knots. GPS navigation (Trimble 4000) provided the average position of the ship to within  $\pm 10$  m. The multibeam data have been extensively processed and provided a detailed swath bathymetric map.

The bathymetric map of Anhydros basin was combined with the on-land topographic data and the final map was designed with 10 different colors corresponding to 100 m topographic intervals and with additional contours of 10 m (Fig. 47).



47. Synthetic Topographic map of the NE part of Santorini Volcanic Field based on multibeam data (10m isobaths) and digitized onshore data.

This map permits a thorough description of the geometry of the submarine morphological structures within the Anhydros basin. However, the bathymetric data are not sufficient enough to distinguish the continental shelf.

The configuration of the continental slopes that border the basinal area differs from place to place. Towards the NW there is an abrupt transition from the slopes to the basin. The density of the bathymetric contours indicates that the depth at the northwestern slopes increases by 50m average within a horizontal distance of 1.5 km. At specific points the density is much higher and the depth increases by 100 m within a horizontal distance of 200 m. As for the geometry of the slopes, the bathymetry at this area clearly illustrates a linear part of the continental slope which trends NE-SW.

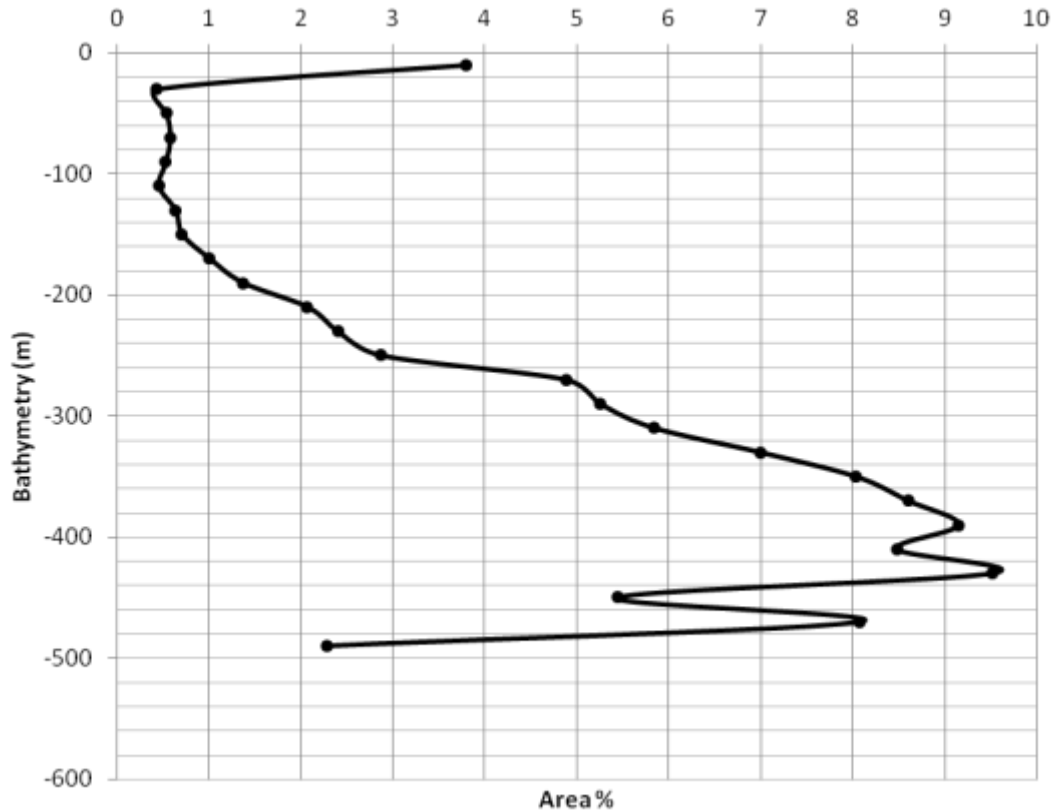
The western slopes display a more gradual transition to the basinal area and a preferred orientation N-S, in contrast to the southwestern margin of the basin. The latter is the submarine continuation of the external flanks of Santorini. Due to the lack of data until the bathymetric contour of 100 m, little can be described about this part. Until the contours of 200-250m the depth increases by 100 m within a horizontal distance of 1 km. Below this level, the transition towards the basinal area becomes more gradual. Small-scaled valleys and ridges can be distinguished along the slope, the orientation of which is NW-SE.

At the southeastern part the area seems to deepen. In fact, it is the transition towards a deeper basinal area in vicinity that extends until south of Amorgos island.

Towards the east, a ridge is formed that separates the two basins trending NE-SW. The slope that borders Anhydros basin at this area follows approximately the same trend with a few variations as we move to the north. To the south, the slope has a NNE-SSW trend and the depth increases by 50 m average within 800 m of horizontal distance. On the other hand, to the north it trends NE-SW and the depth increases by 50 m average within 500 m of horizontal distance. As a whole, the continental slope at this area is characterized by a linear morphology. However, the northern part displays a different configuration with several ridges and valleys trending E-W.

The basinal area appears to be elongated, with its long axis oriented NE-SW. The horizontal distance between the contours reaches at some points up to 6 km showing that it is a rather flat area. The continuity of the flat seafloor is interrupted by the occurrence of several cone shaped volcanic features which seem to be aligned along two different linear trends (N 29°E and N42°E). Their merging point is Kolumbo, which apparently is the largest volcanic cone within the basin.

The analysis of the submarine topography on the basis of 20-m isobaths (Fig. 48) shows the distribution of the bathymetry with a maximum between 400 and 500 m depth. This maxima corresponds to the basinal area lying at an average depth of 450 m.

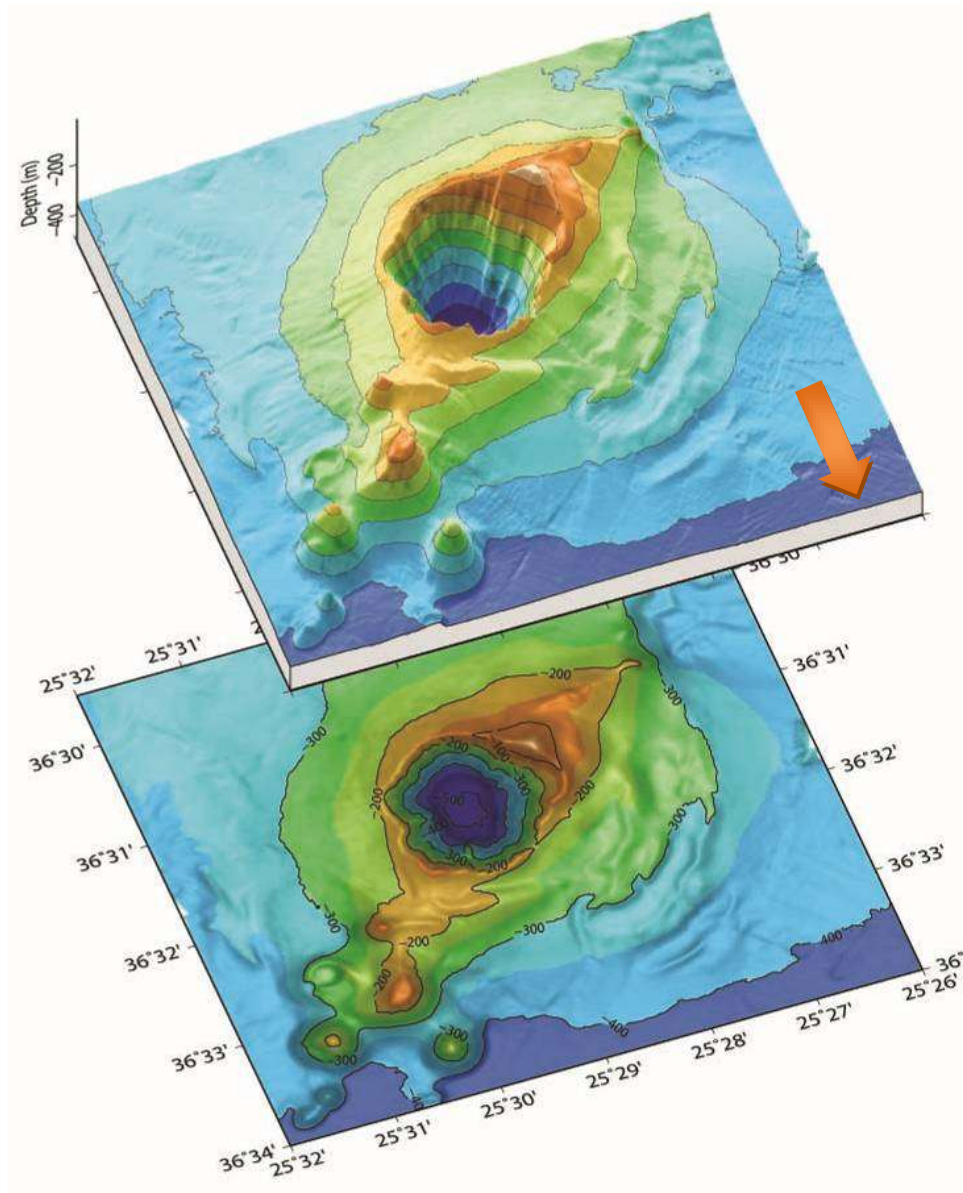


48. Statistical analysis of the submarine topography derived from the area distribution with depth based on analysis of 20-m isobaths.

Kolumbo is a 4 km diameter cone with a 1500 m wide crater. The crater rim lies at an average depth of 150 m, whereas its shallowest point to the south-west is just 18 m below sea level (Fig. 49).

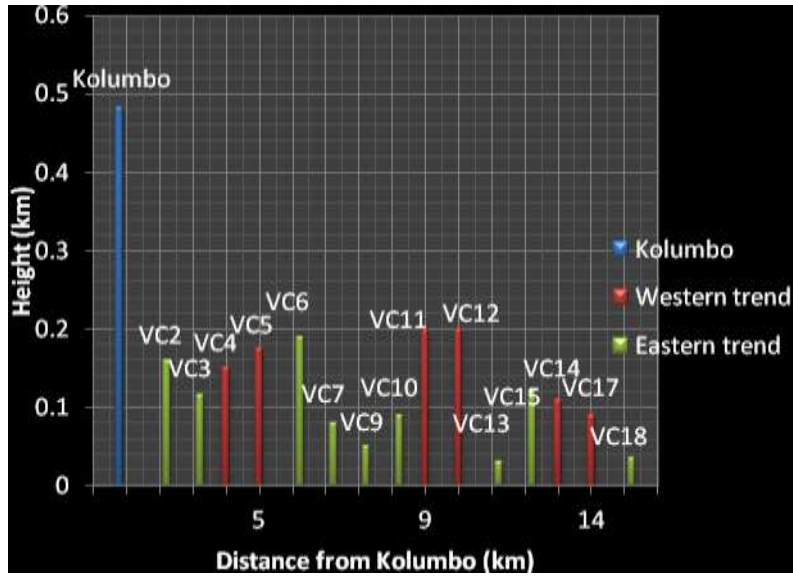
The surface of the external flanks of Kolumbo, and especially the northern ones, display a rippled morphology due to the presence of curvilinear scarps with inward dipping faces which may represent remnants of a pre-existent volcanic cone.

The flat crater floor lies at the depth of approximately 500 m, and the topographic difference formed between the seafloor of the crater and the rim forms a submarine circular cliff of 350 m height. In addition, the density of the bathymetric contours is extremely high within the crater, showing an almost vertical morphology of the walls, which is apparently created by the collapse of a relevant volcanic cone (Nomikou, 2003).

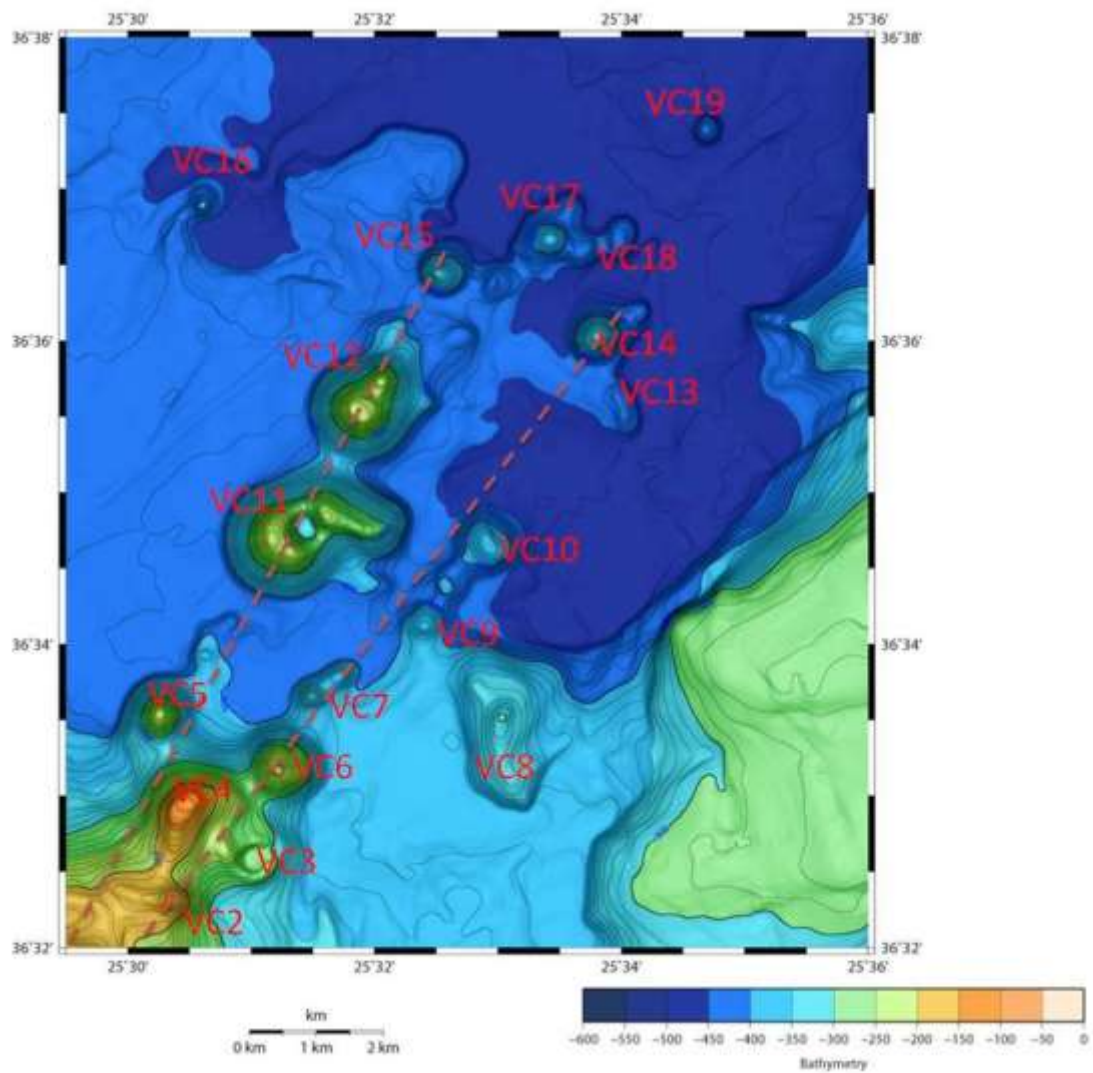


49. 3-D map of Kolumbo submarine volcano (Nomikou et al, 2013)

The rest of the volcanic cones lies within the basinal area which is rather flat. Most of these volcanic cones are circular or concave with abrupt, steep slopes. Some have well-defined craters, whereas others are dome-shaped. The summits of the cones lie between 130 and 370 meters deep with the majority in the depth range 200-350 m. They have been constructed on seafloor that ranges in depth from 300 to 450 meters (Fig 51). Cones in the more northerly trend are generally larger, whereas cones in the more easterly trend are smaller and more uniform in size. The histogram that follows (Fig. 50) describes the variations of the cones height as distance from Kolumbo is increased. What is indicated through this, is that the cones become smaller towards the NE edge of the two trends. Their linear distribution in space, is probably the result of tectonic structures that have facilitated magma ascend to surface of the seafloor.



50. Histogram showing the distribution of the Height of volcanic cones along the volcanic chain from Kolumbo to the eastern most volcanic cone No 19.



51. Bathymetric map of the area of the volcanic cones.

VC1 is located at the SW flanks of Kolumbo. It has no apparent crater and its summit lies at the depth of 130 m. It is not associated in space with the majority of the smaller volcanic cones NE of Kolumbo.

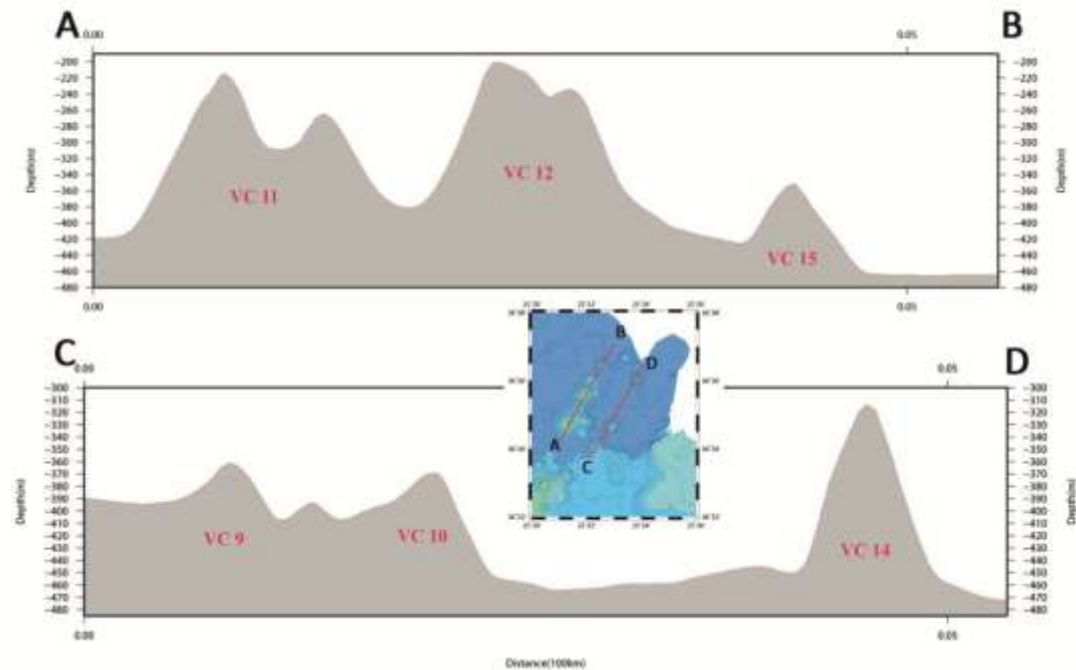


Fig. 52. Topographic profiles A-B and C-D across volcanic domes aligned in the two different trends, oriented in NE-SW direction

VC2 is dome shaped with abrupt slopes. Its distance from Kolumbo is 2.85 km. Its summit lies at the depth of approximately 130m as well.

VC3 is located 4.22km northeast of Kolumbo and consists of a symmetrical, well-defined crater. The smooth crater floor (290m depth) has a diameter of ~200m.

VC4 is a dome-shaped structure that is elongated to the northeast. It lacks the presence of a crater. It is also located almost 4 km northeast of Kolumbo. The top of the cone is a rather flat surface, with its shallowest part lying at a depth of 130m. The base of the cone is at depth ~300m on the northwest and ~230m on the southeast.

VC5 is also a dome shaped feature, 5.12 km NE of Kolumbo, with its base lying at 400m depth to the North side, 300m to the south and 350m to the east.

VC6 is located almost 5.4 km northeast of Kolumbo. It is also characterized by the absence of a crater and has a circular, dome-like symmetric shape. The base lies at a depth of 300m. A prominent valley is formed along the north slope with a slight NE-SW orientation. The summit is at the depth of 190 m.

VC7 is the next cone that lies along the more easterly trend, 6.44 km NE of Kolumbo. This cone has a circular, symmetrical shape with a smaller subsidiary cone slightly to the northeast that is separated by a narrow saddle.

VC8 lies east of the easterly trend and has got an unusual shape. It is elongated and oriented NW-SE. Its base lies at the depth of 380 m at its west side and 360m at its east. The summit is at about 300 m depth.

VC9 is also dome-like and circular and 8.5 km NE of Kolumbo.

VC10 is an ellipsoid structure with its major axis trending NW-SE. It is located 10km northeast of Kolumbo. There is no crater at the summit of this cone and its slopes are steep with the exception of the southwest part where the topography is more gentle and descends into the saddle area. The summit lies at a depth of 370m, whereas the base of cone is at depth of about 400m.

VC11 is elongated in the NE-SW direction with two peaks surrounding a crater at a depth of 300 m. Distance from Kolumbo is about 8.5 km.

VC12 is dome-like with no apparent crater and 10.3 km NE of Kolumbo.

VC13 is formed by two smaller centers. Distance from Kolumbo is approximately 12.6 km. These are elongated to a NNW-SSE direction. The base of the two smaller cones lies at a depth of 450m and the summits at 410m water depth.

VC14 lies at the far end of the easterly trend, 13 km NE of Kolumbo. It is dome-shaped and circular without a summit crater and rises at a depth of 340 meters.

VC15, 12.8 km NE of Kolumbo, is circular and dome-like with a summit at a water depth of 340 m.

VC 16 is does not belong to either of the two trends. It is an isolated feature within the basinal area. It is small in size and circular. Its base lies at a depth of 450 m and the summit at the depth of 400 m.

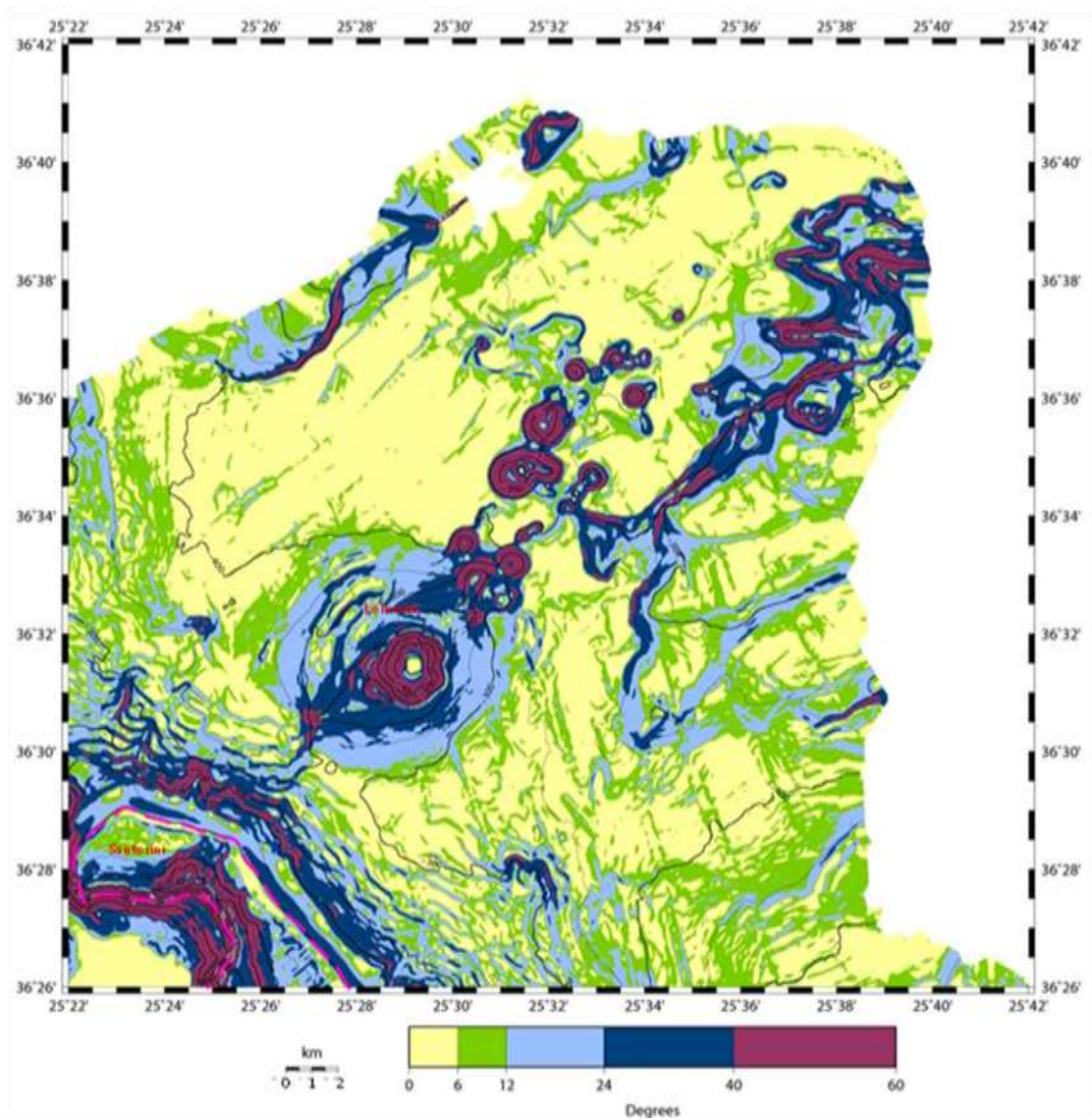
VC 17 is also circular and lacks a well-defined crater. Its summit depth is slightly deeper than the one of cone 15, at 370 meters. It is located 13.8 km NE of Kolumbo.

VC18 is a small sized dome and elongated in a N-S orientation, 14.5 km NE of Kolumbo. Its base lies at 450m water depth and the summit is at 425m depth.

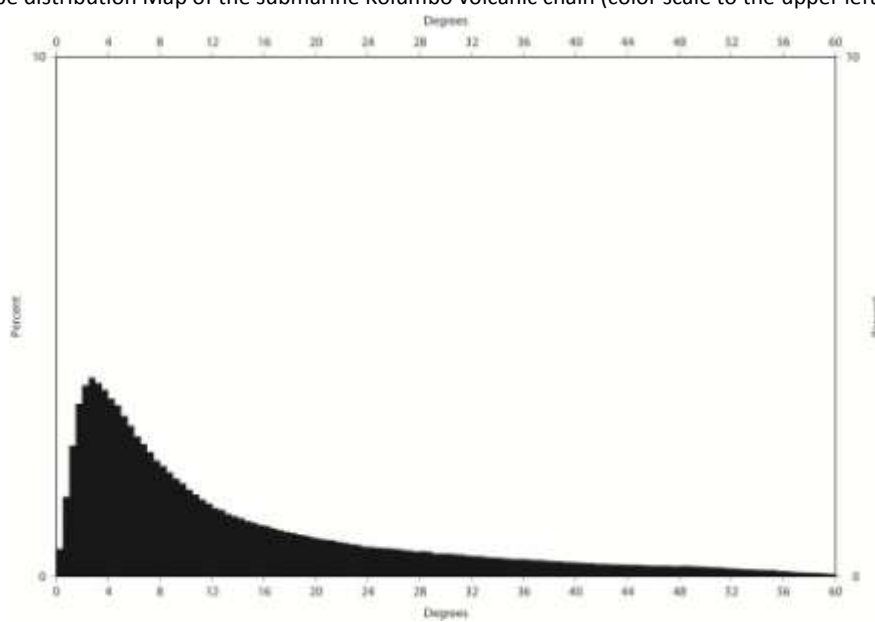
VC 19 lies at the far end of the westerly trend, 16.7 km NE of Kolumbo. It is a symmetrical cone of small size. Its basal contour is at the depth of 460m, whereas the summit is at the depth of 460 m.

#### **4.2 Morphological Slope Analysis**

The following map illustrates slope distribution within the study area. The slope values have been classified into five different groups: (1) areas of mean morphological slope 0-6%, (2) areas of 6-12%, (3) areas of 12-24%, (4) areas of 24-40% and (5) areas of 40-60%. This classification permits the distinction of areas of low morphological slope magnitudes – basinal areas – and high morphological slope magnitudes which mainly correspond to active tectonic features, inner crater walls of the volcanic cones or external flanks.



53. Slope distribution Map of the submarine Kolumbo volcanic chain (color scale to the upper left of map).

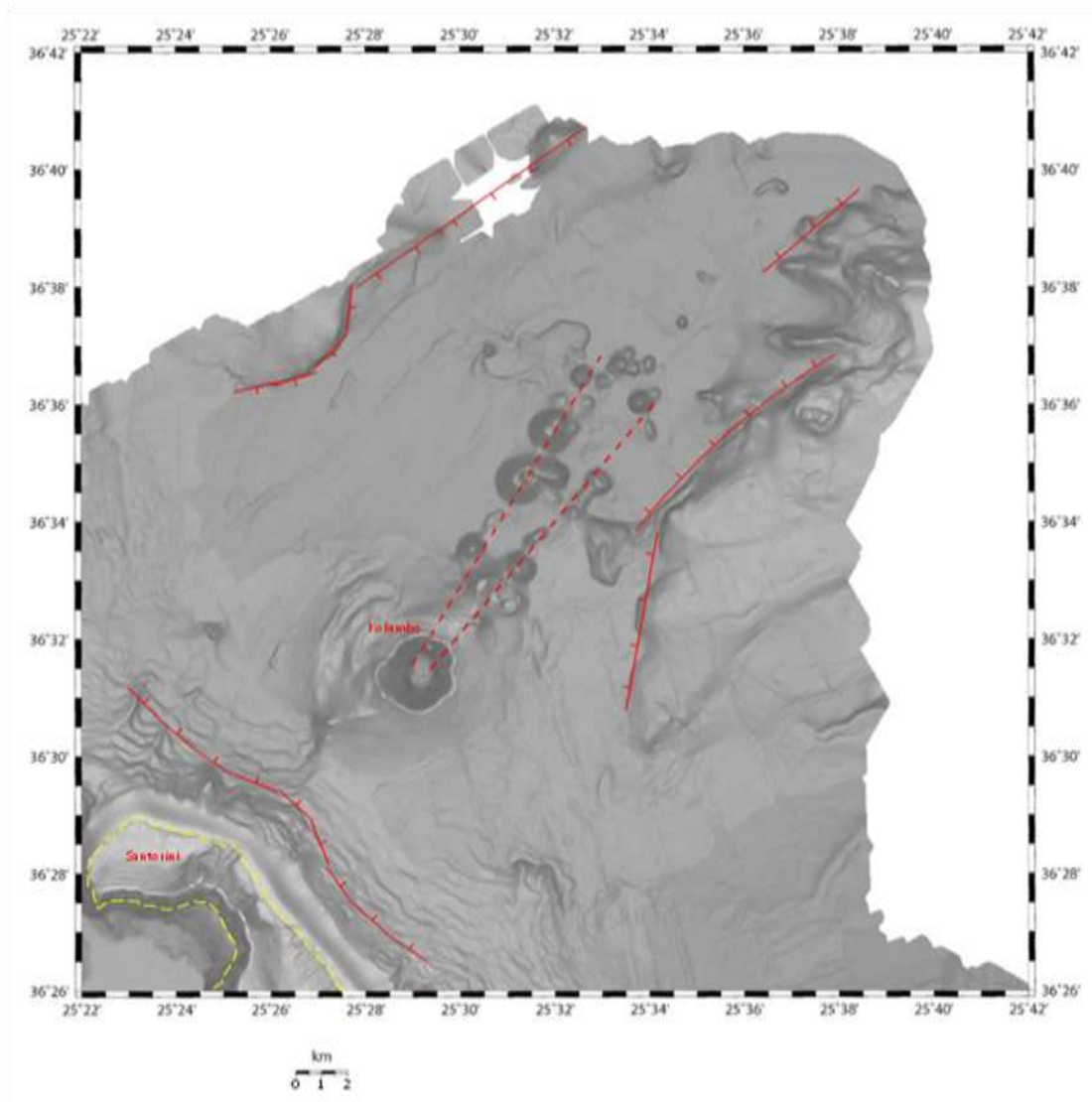


54. Histogram showing the distribution of morphological slopes in the studied area.

The lowest slope magnitudes (0-6%), which mostly occupy the submarine area between Anhydros and Santorini, are observed mainly around the depth of 400 – 450m. These areas represent the basinal space. The latter is bordered by areas of high morphological slope values (24-60%) which are distributed in a rather linear arrangement, trending NE-SW to the northeastern part of the basin and NW-SE to the southwestern. This linear configuration most probably corresponds to active marginal faults that have formed the basin. Intermediate slope values are almost absent at these areas except for the western part of the basin, where the slope is well developed and the slope values diminish gradually towards the basin. The highest slope values (40-60%) are also observed within the Kolumbo crater and around the external flanks of the minor volcanic cones towards the NE. This kind of distribution within Kolumbo crater can be attributed to a collapse of the central part of a former volcanic cone. The external slopes are gradually diminished from 40-60% to 0-6% morphological slope magnitude towards the deepest parts of the basin, whereas the volcanic cones VC11 and VC12 show abrupt change of slope from 40-60% to 0-6%.

The area of the Santorini caldera walls is distinct on the map with slope magnitudes 40-60%. The external submarine slopes of Santorini is also a region of high morphological slope aligned in a NW-SE orientation.

According to the morphological slope analysis a few first interpretations can be made for the morphotectonic structure of Anhydros basin, illustrated in Fig. 55. The linear zones of abrupt change of slope should correspond to the marginal faults of the basin, whereas the areas where the abrupt change of slope is distributed in a circular way correspond to the volcanic cones and specifically to their inner or external slopes.



55. Simplified tectonic sketch of the study area based on morphological slope analysis.

## **5. ROV Exploration**

ROV exploration during the Nautilus missions 2010 and 2011 was focused on Kolumbo volcanic chain. The main observations of this survey are presented in this paper through photographic material.

The flanks of Kolumbo are covered by a layer of lapilli size pumice with common outsized boulders of large pumice. During explosive submarine eruptions, large pumices that are ejected above the sea surface can float for significant periods of time but eventually become water-logged and sink. Smaller pumices tend to sink rapidly because they become saturated with water much more quickly (Carey, 2000). This model can explain the distribution of pumice on the flanks of Kolumbo, as a result of the 1650 AD eruption.



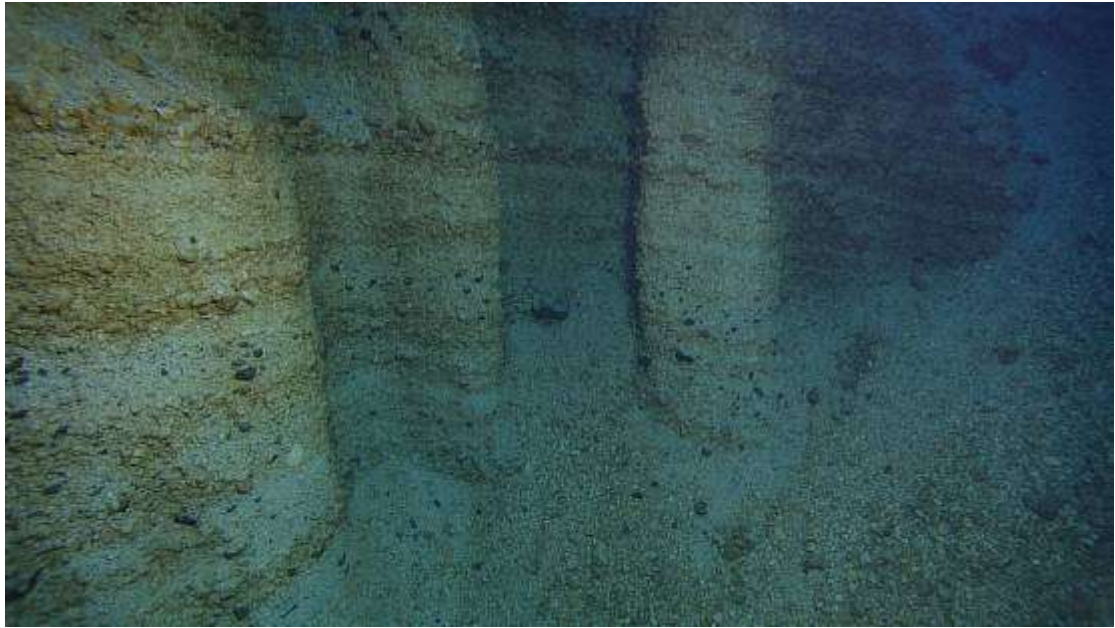
56. Large rhyolite pumices scattered on the seafloor around Kolumbo submarine volcano resulting from the sinking of material from pumice rafts.

The crater walls are steep and display a scalloped and terraced morphology. At specific points undulating cliff faces were revealed that have been formed as a result of mass wasting of unconsolidated pyroclastic deposits (fig. 56).

A variety of volcanic lithologies, including thick pumice fall/flow accumulations, dikes, intrusions, breccias and mass wasting deposits, constitutes the crater walls. ROV exploration revealed a thick (~200 m) sequence of pumiceous pyroclastic deposits that is the likely product of the 1650 AD eruption (Fig. 57, 58, 59). Two main lithologic units were recognized throughout the stratified pumice deposits; thick bedded pumice block breccia and thin interbedded block breccia and pumice lapilli (Cartner et al, 2010).



57. At the western wall there are also bedded pumices which can be observed on an almost vertical part of the crater walls.



58. Undulating cliff faces carved by mass wasting of pyroclastic deposits.



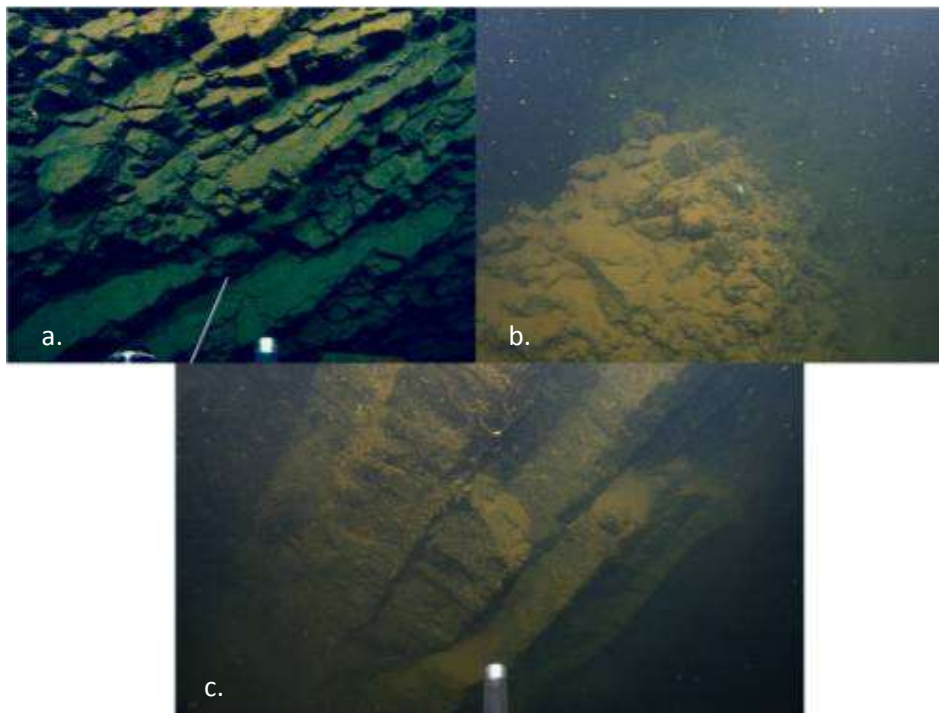
59. Stratified pyroclastic deposits of the crater walls.

Another morphologic feature within the crater is the presence of several prominent ridges that extent from the walls and reach the crater floor (fig. 60).



60. Ridge formed within the crater.

Finally, at the lower parts of the crater walls outcrops of massive lava flows, dikes (fig. 61) and intrusions were discovered that were emplaced prior to the 1650 AD eruption. Bacterial mat partially covered these outcrops.



61. a. Layered lavas, b. Lava flow, c. Dyke

Kolumbo crater floor is generally flat at an average depth of 500 m. The surface is covered by a thin orange layer of bacterial mat and at the lower NE slopes some white streams of bacteria were also discovered (fig. 62). At the NE part of the crater floor, the hydrothermal vent field deranges the smooth surface and creates the most spectacular features on the seafloor. The morphology of the vents varies from place to place. Some are small mounds on the seafloor, others are constituted by several spires a few high and some may reach several

meters in height (fig. 63). Some vents display vigorous release of gas and fluids while others don't. These features have been formed as a result of water circulation beneath the seafloor. More precisely, water seeps through cracks in the seafloor and is heated by molten rock deep below the ocean crust to as high as 400°C. The hot fluid rises to the surface and gushes out of the vent openings. This hydrothermal fluid carries with it dissolved metals and other chemicals from deep beneath the ocean floor the deposition of which is responsible for the construction of the chimneys.



62. Bacterial mat that covers the crater floor and the lower parts of the crater walls



63. Three different types of hydrothermal chimneys.



64. Perspective of the area

The rest of the Kolumbo volcanic chain was also investigated during the Nautilus mission in 2010. During the ROV survey, the scientific team focused on the most important volcanic cones, from the perspectives of the morphology, the texture of the deposits, and the structure as they have been revealed from captures and video footage. The cones belonging to the two distinct trends are mainly described in this paper. For the sake of brevity we have given each volcanic cone a distinctive name, as displayed on the map of fig. 48.

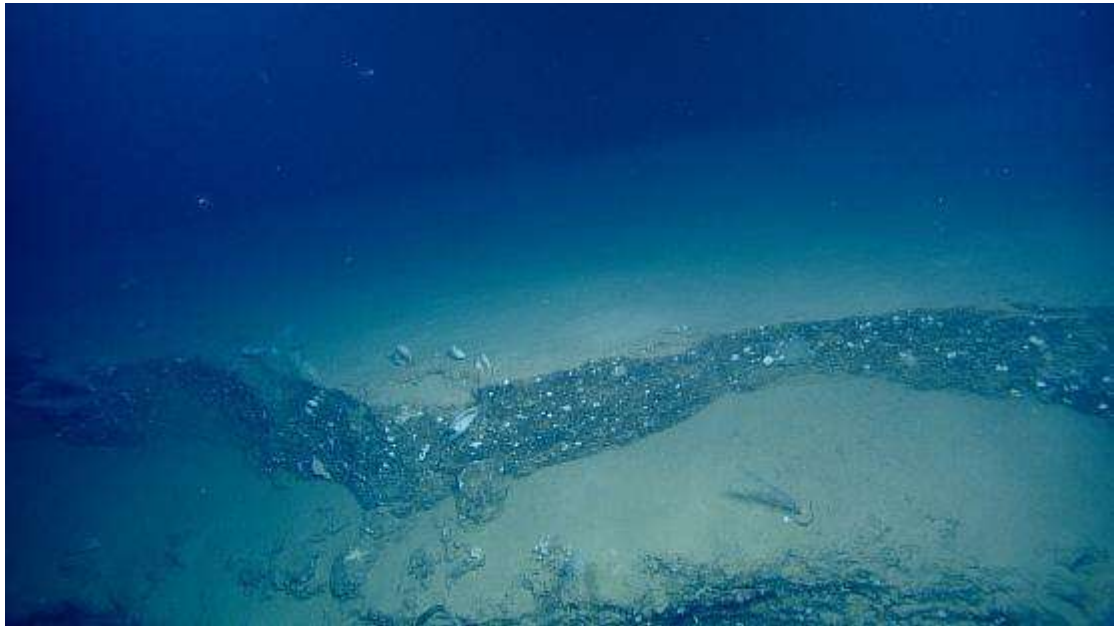
In general, tuffaceous deposits that biologically encrusted constitute the slopes of the volcanic cones (fig. 65). Towards their upper the slopes become steeper. Their lower parts and their flat summits are covered with fine grained sediment with occasional blocks of pumice (fig. 66). Linear scarps observed were interpreted as the surface expression of tectonic features (fig. 67).



65. Sample just retrieved from an outcrop of biologically encrusted tuffaceous deposits VC 3.

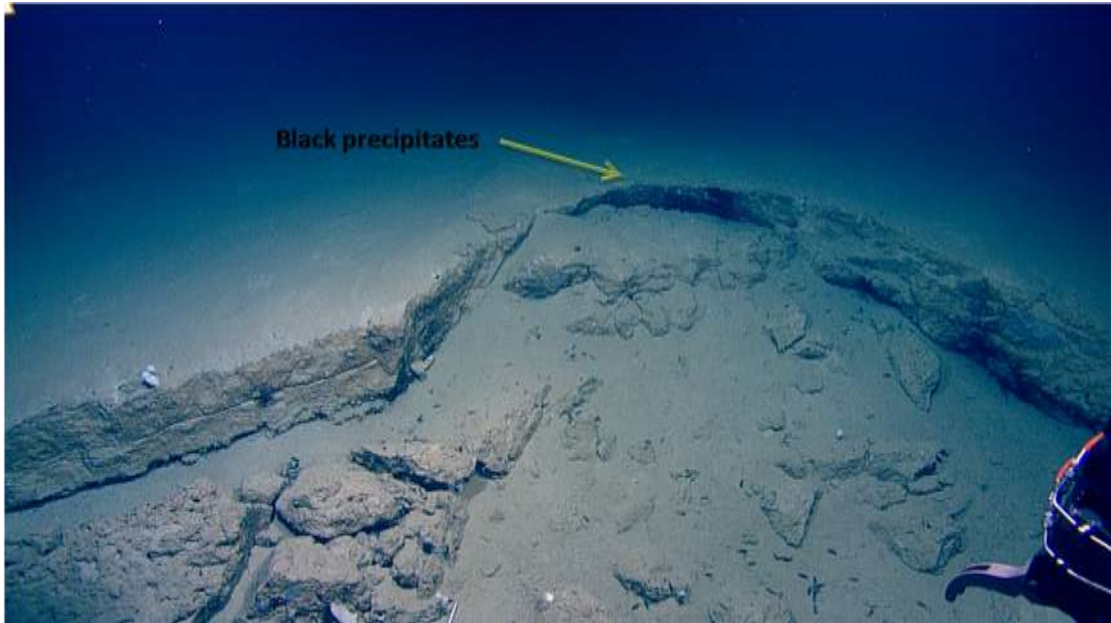


66. Angular block of lava on flat sediment surface VC 11.

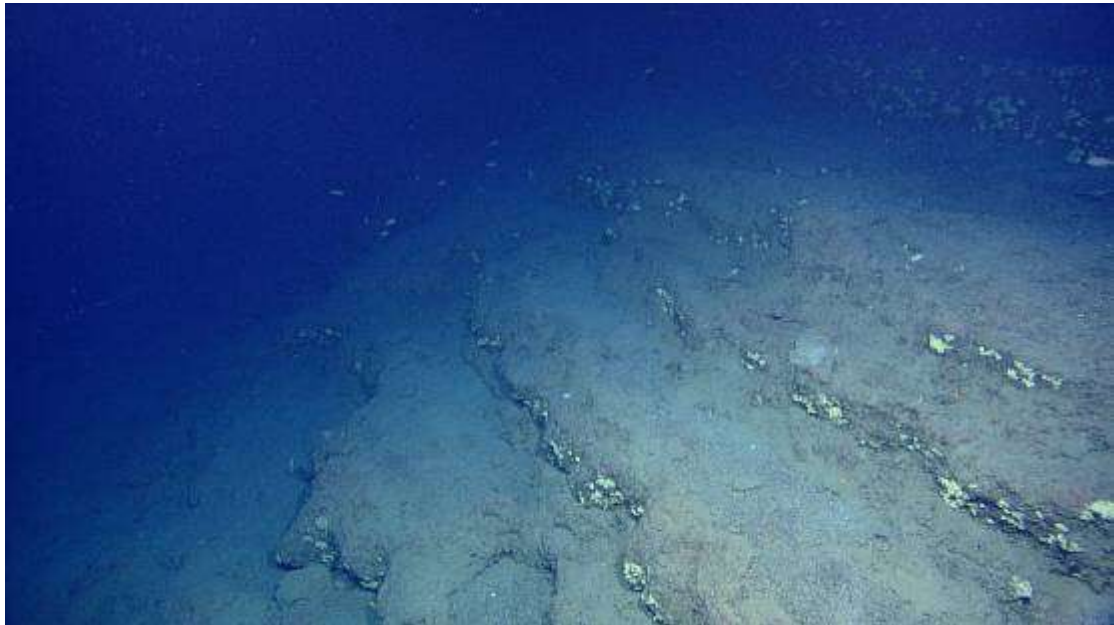


67. Linear steps in E-W direction –VC 9.

Some unique features were distinguished in some of the cones that generated further questions for the creation and evolution of Kolumbo volcanic chain. In VC7, between the two summits, a fragmented, slab like outcrop was observed. Some dark coloured precipitates at the base of a scarp suggest possible hydrothermal activity (fig. 68). The slopes of VC12 are characterized by a step-like morphology at their upper parts(fig. 69). At summit area of cone VC14 small, circular depressions form an irregular landscape. They are less than a meter in diameter and a few tens of centimeters in depth. (fig. 70). Some linear depressions were also discovered filled with black manganese precipitates, indicative of possible hydrothermal activity (fig. 71).



68. Fragmented outcrop with dark precipitates at the base of the scarp VC 7.



69. Step like morphology at the slopes of VC12.



70. Circular depressions in the summit area of cone VC14. Each depression is less 0.5 meter in diameter and several tens of centimeters in depth.

The black sediment was sampled in one of the depressions and found to consist of frambroidally precipitated manganese oxide that was growing on a variety of sedimentary particles (Nomikou et al. 2012a).

The abundance of manganese precipitates associated with fractures in outcrops and along downslope channels clearly indicates that low temperature hydrothermal venting is very active on cone 14 (e.g. Frank et al., 2006). The only other cone in the NE field that showed indication of this type of venting was cone 7 and the occurrence there appeared to be very much less abundant.



71. Linear depressions filled with black manganese precipitates in the summit area of cone VC 14.

## 6. Seismic Profiles

In order to have a better view of the tectonic configuration of Anhydros basin, we analyzed the seismic profiles obtained during the “THERA” oceanographic mission in 2006. The map that follows shows the tracks of the single channel seismic profiles (fig. ). They have been grouped in:

- a. Seismic profiles that cross-cut Kolumbo submarine volcano
- b. Seismic profiles that crosscut the external flanks of Kolumbo submarine volcano
- c. Seismic profiles that crosscut the Anhydros basin
- d. Seismic profiles parallel to the long axis of Anhydros basin

The seismic facies recognized on the profiles have also been grouped in the following table.

Letter designation	Seismic Facies	Description	Estimated Origin
<b>A</b>	Reflection free/Acoustically transparent	Highest unit that thins as distance from Kolumbo increases	Kolumbo 1650 AD pyroclastic deposits
<b>B</b>	Intense, continuous, parallel internal reflectors, slightly undulated	Layered unit that thins as distance from Santorini increases	Santorini pyroclastic deposits
<b>C</b>	Chaotic	Wedge-shaped unit that thins as distance from Kolumbo increases	Possibly pyroclastic deposit associated with a pre – 1650 AD eruptive event
<b>D</b>	Parallel reflectors with good continuity	Deformed by blind faults and domes or cryptodomes	Marine deposits Plio - Quaternary
<b>Domes</b>	Acoustically transparent ending with hyperbolic reflections on the surface of the seafloor	Crosscut and deform the sedimentary layering	Conduits of ascending magmatic fluids. Associated with the existing ruptures, indicating that the latter are preferred weak zone for the magmatic fluid flow.

<b>Cryptodomes</b>	Acoustically transparent ending with hyperbolic reflections, but die out before reaching the surface	Crosscut and deform the sedimentary layering.	Conduits of ascending magmatic fluids. Associated with the existing ruptures, indicating that the latter are preferred weak zones for the magmatic fluid flow.
--------------------	--	---	--

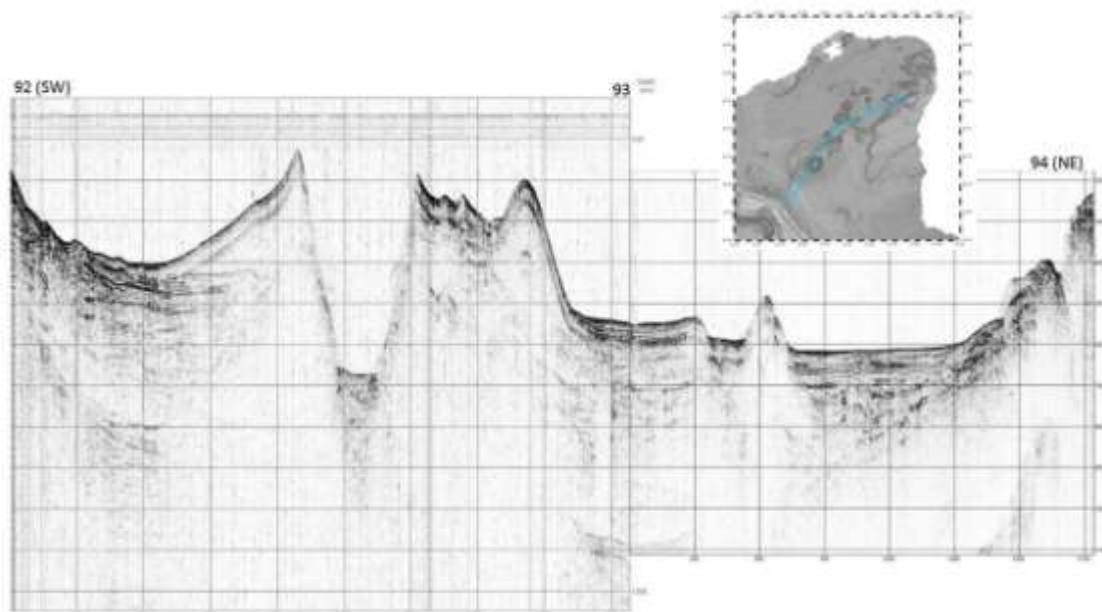
Table 1. Seismic facies that were recognized on the profiles

### **6.1 Seismic profiles that cross-cut Kolumbo submarine volcano**

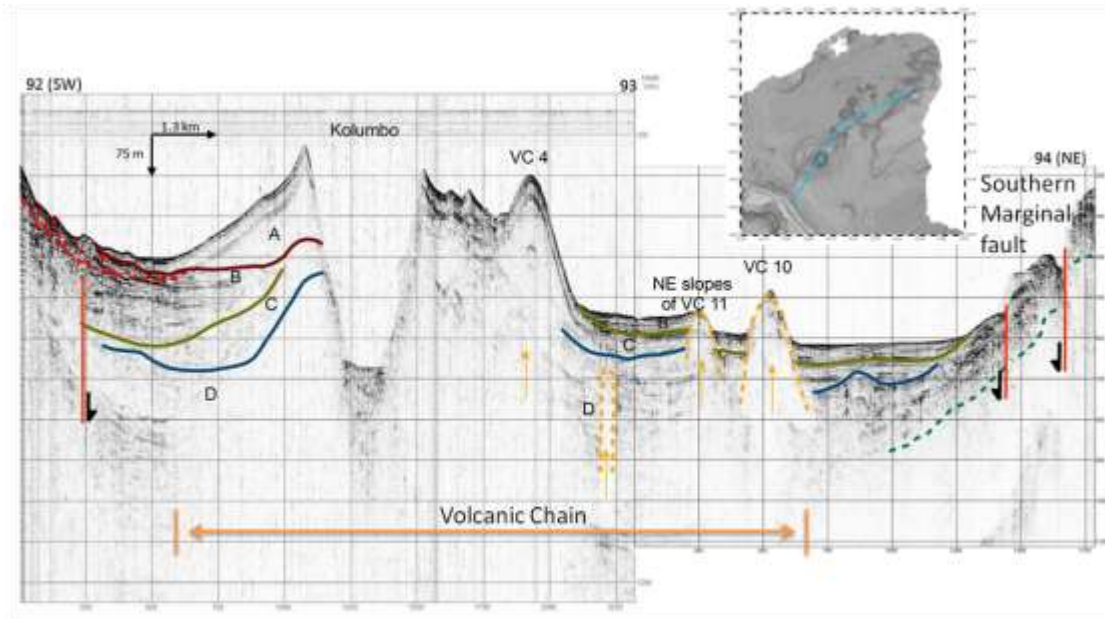
This profile is the junction of two separate seismic sections (92-93 and 93-94). The first part starts from the NE submarine slopes of Santorini, crosscuts Kolumbo and reaches the southern part of the smaller volcanic cones, whereas the second part has a different orientation, crosscuts part of the volcanic chain and reaches the southern marginal fault of Anhydros basin.

Starting from the slopes of Santorini, once again we observe the listric plane and the blocks that have slipped on it in a way that gives the seafloor a step like morphology. Further on, the volcanic edifice of Kolumbo is clearly shown in this section, with its almost vertical crater walls as well as the three smaller volcanic domes belonging to the Kolumbo Volcanic Chain. What is especially interesting, is that although layer A is present at the SW part, and in fact reaches 150 m in thickness at the slopes of Kolumbo, it is completely absent at the NE part. This indicates that the products of the 1650 AD eruption must have spread towards another direction.

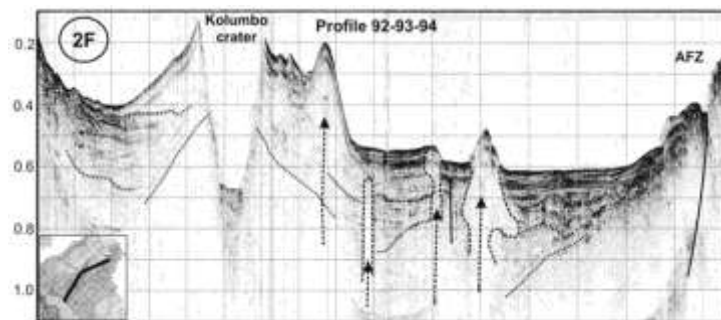
Beneath the listric plane, a normal fault disrupts the continuity of the different horizons. Finally, two normal faults form the southern boundary of Anhydros basin. The green line indicates an unconformity beneath which we have a transparent sequence.



72. Seismic profile 92-93-94 uninterpreted.



73. Seismic profile 92-93-94 interpreted



74. Seismic profile 92-93-94. Interpretation by Sakellariou et al. 2010.

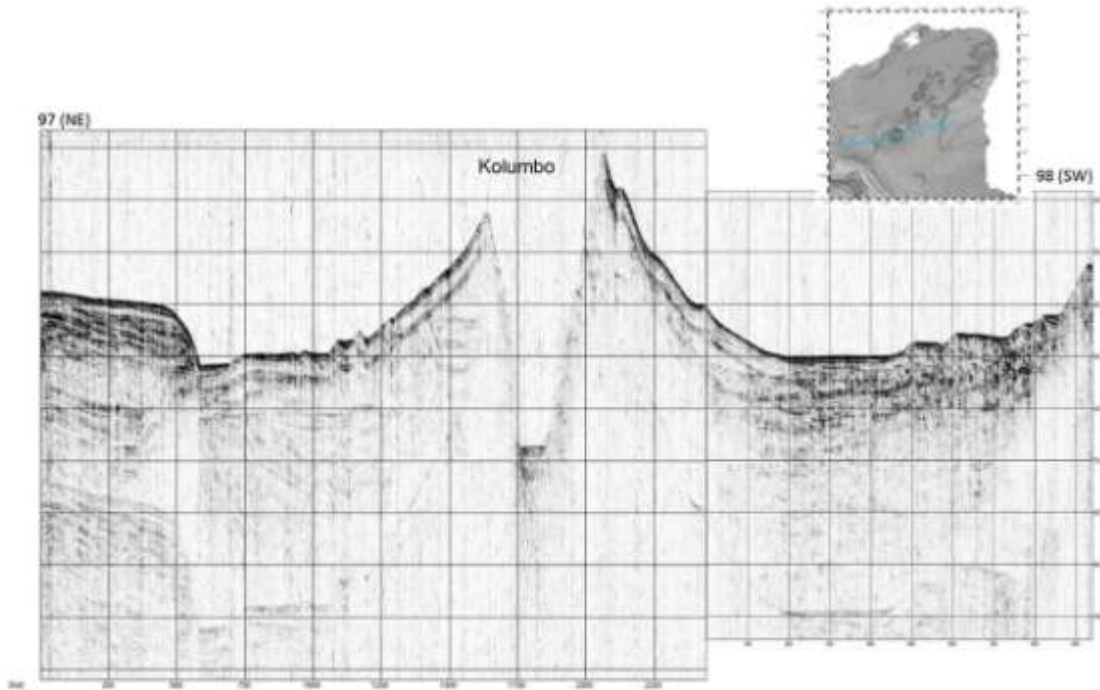
The seismic profile 97-98 starts from the Anhydros ridge, crosscuts Kolumbo and ends north of Santorini. It is approximately 15 km long.

The striking feature of this section is the volcanic edifice of Kolumbo volcano. Either side of the volcano we can distinguish the distribution of the pyroclastic products of 1650 AD eruption. As we can see these products are much less spread east of Kolumbo. The listric plane is also present towards Santorini.

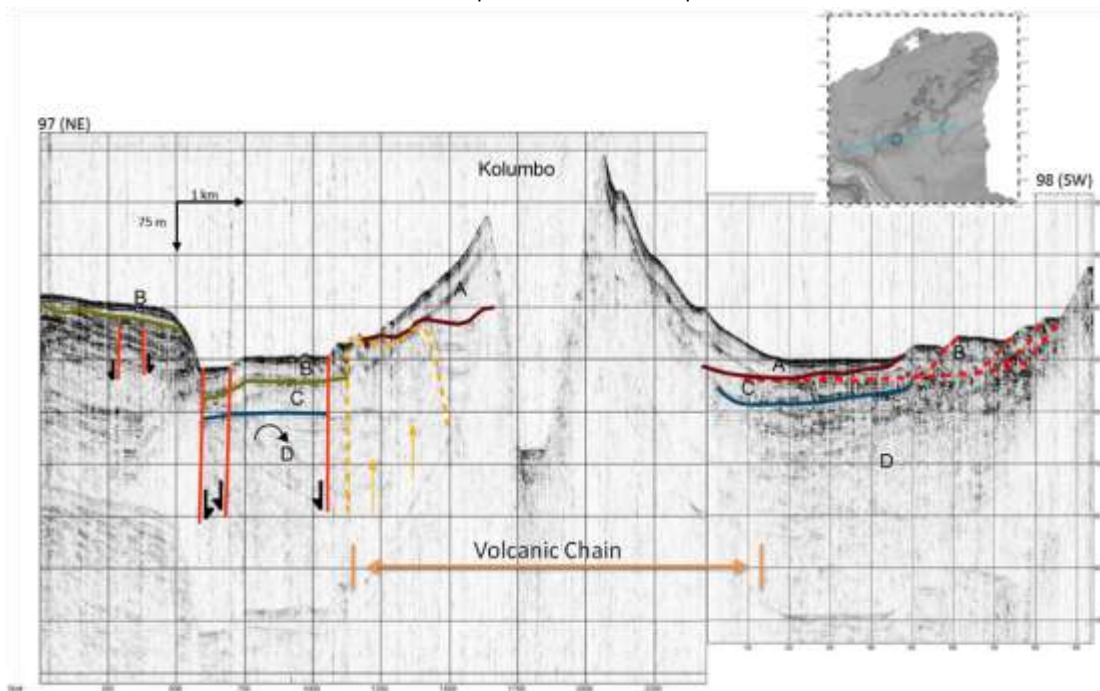
At the NE side we can see the Anhydros horst is constituted by marine sediments which have been deformed by inactive normal faults and covered by a layer of pyroclastic sediments associated to Santorini.

We can also distinguish the southern marginal normal fault of Anhydros basin and its antithetic. A tilted block is also observed due to the difference in the slip rates of the two active normal fault that form it.

Finally, it seems that at the east side of the external flanks of Kolumbo we have an ascending magmatic fluid flow that does not reach the surface.



75. Seismic profile 97-98 uninterpreted.



76. Seismic profile 97-98 interpreted.

## **6.2 Seismic profiles that crosscut the external flanks of Kolumbo submarine volcano**

The seismic profile 5-6-7 runs NE-SW, starts from 6km west of Anydhros island to the NE and ends near the eastern coast of Santorini island. It crosscuts the western trend of the smaller volcanic cones at the center of the basin, which have an acoustically transparent character. They crosscut the depositional sequences of the basin and disrupt the continuity of a previously flat seafloor.

The upper package recognized in this profile, with no apparent internal reflectors, corresponds to the pyroclastic flows emplaced during the 1650 volcanic activity. The thickness of this layer at the SW part reaches up to 80 m(100 milliseconds twtt) and becomes thinner as distance from Kolumbo increases. Gravity flows produced from the 1650 eruption spread around the volcanic center of Kolumbo, especially towards Santorini.

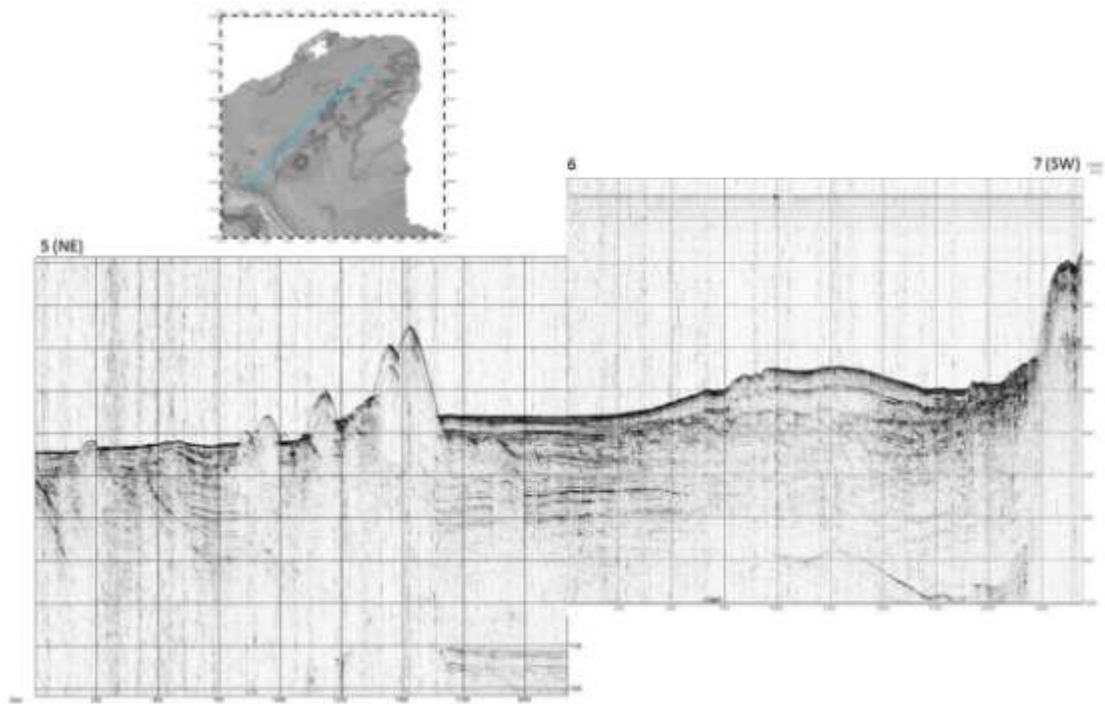
Beneath package A, a layer with continuous, sub-parallel, slightly undulating internal reflectors has been emplaced. This probably corresponds to Santorini volcanoclastic deposits. Its thickness is higher towards SW, closer to Santorini, while at the NE part it gradually diminishes.

The wedge-shaped, chaotic package C is probably the result of a former eruptive event at the area of Kolumbo.

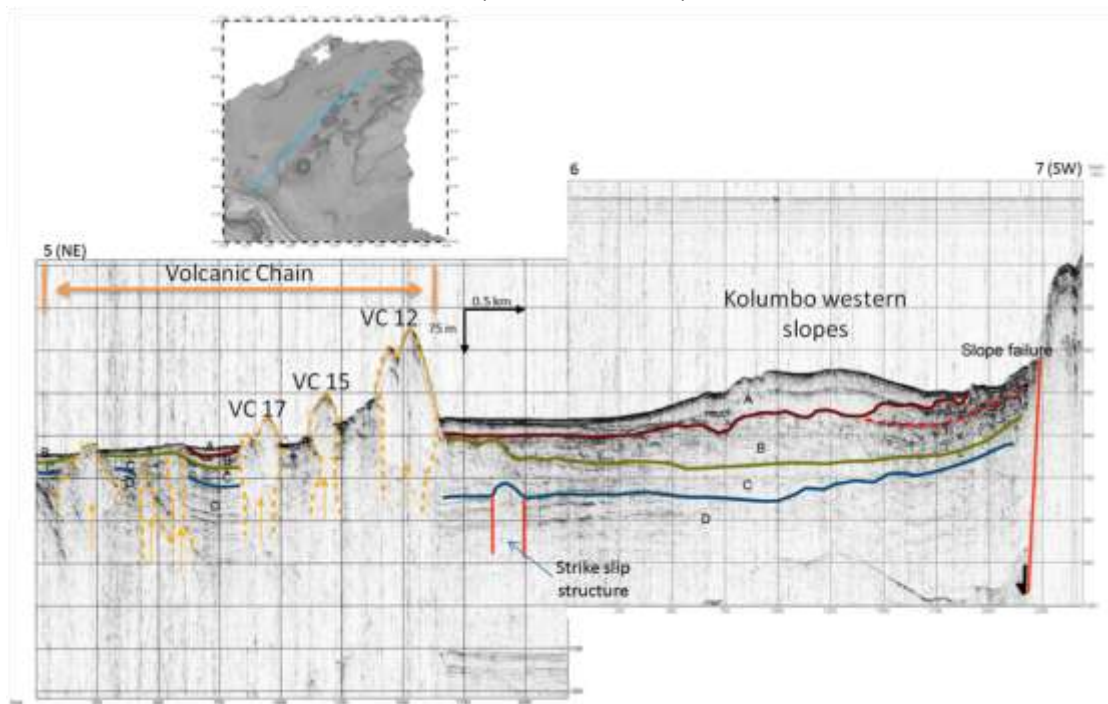
The lowest sequence is characterized by intense parallel reflectors and represents the Plio-Quaternary marine infill of the basin. Its continuity within the basin has been disrupted by the volcanic domes, which probably correspond to preexisting tectonic features that have served as conduits for magma ascend, and by some blind faults as indicated at the central part of the profile. The occurrence of the anticlinal fold between these tectonic features represents a positive flower structure, indicative of a strike slip character of the deformation at this area. Near the NW external flanks of Kolumbo, the lowest sequence has parallel internal reflectors which are undulated.

Towards the southwestern part of the profile we can observe a chaotic mass which seems to have slipped in the basinal area on a listric plane, indicated with a red, dashed line in the profile.

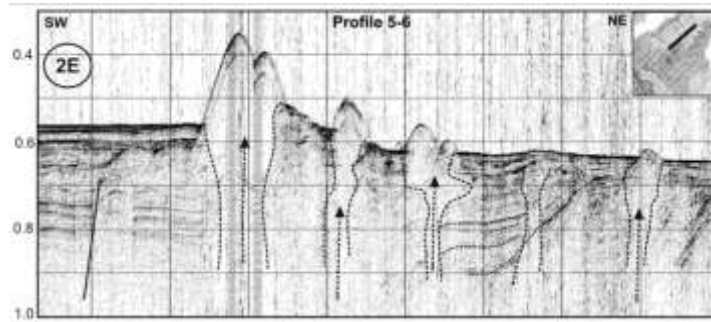
The stratigraphy changes radically, at the SW part of the profile, where A normal fault separates the basinal area from Santorini NE submarine slopes.



77. Seismic profile 5-6-7 uninterpreted.



78. Seismic profile 5-6-7 interpreted.



79. Seismic profile 5-6. Interpretation by Sakellariou et al. 2010

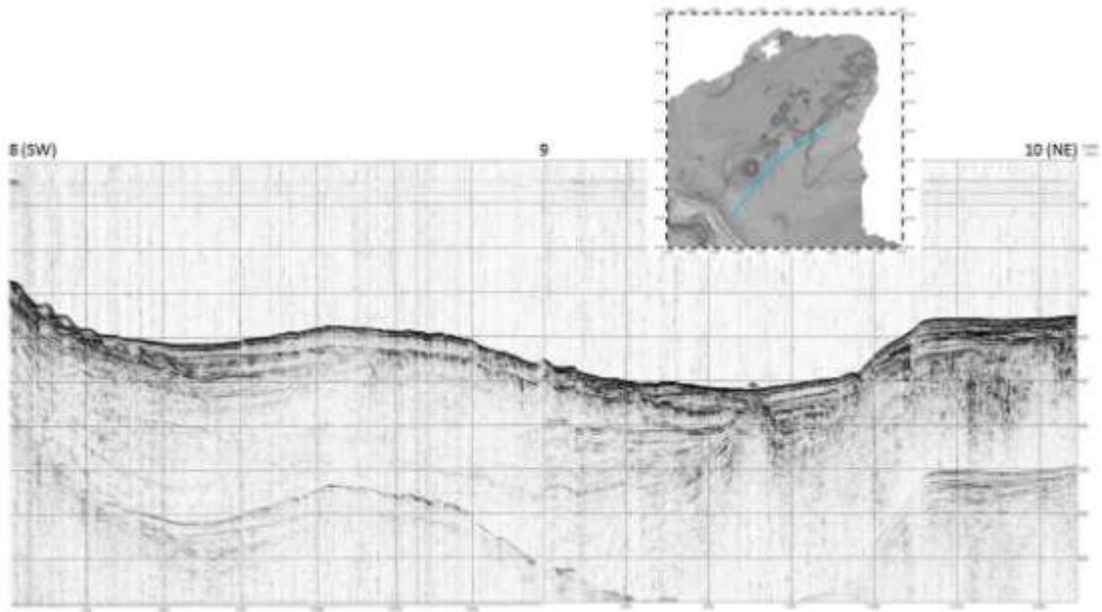
The seismic profile 8-9-10 starts from the eastern part of Santorini, runs parallel to the southeastern slopes of Kolumbo volcano and ends about 3km southwest of Anhydros island. Starting from the SW edge of the section, the first thing that is observed is a listric plane which has probably served as slipping surface for several blocks that belong to the NE volcanic slopes of Santorini. The slipping of these masses is responsible for the step like morphology of the seafloor at this area.

The upper sequence (layer A) of this profile is transparent with no internal reflectors. It corresponds to the pyroclastic flows of the 1650 AD event. The thickness of the upper unit decreases as distance from the volcanic center increases. In fact, towards the NE part, the Kolumbo pyroclastic flows are absent.

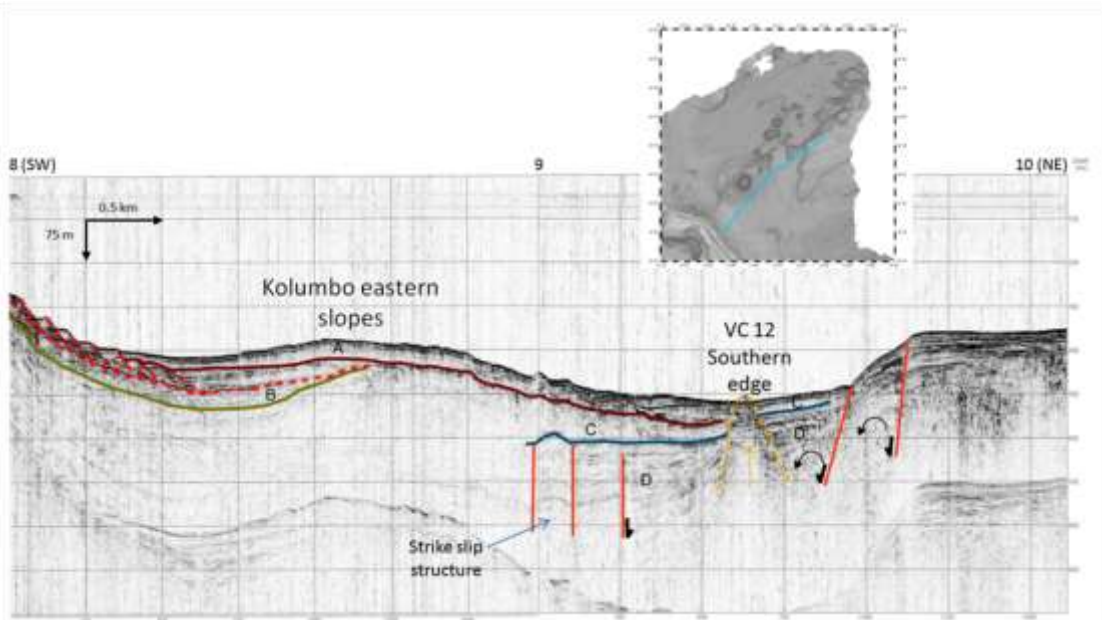
The underlying layer B is layered with sub-continuous, sub-parallel, slightly undulating internal reflectors. It can be interpreted as pyroclastic flows emplaced an eruptive phase of Santorini. At the NE part of the profile, the apparent layer C is associated with a pre-1650 AD eruptive event.

The lowest sequence has parallel internal reflectors which are undulated. This represents the Plio-Quaternary marine deposits of the basin.

Finally, towards the NE the stratigraphy is totally different. Two normal faults define three different blocks. The southwestern belongs to the basinal area. The middle one is a tilted block due to the higher slip rate of the western fault, and the third one consists of horizontal, parallel layers of marine deposits which overlay an acoustic basement.



80. Seismic profile 8-9-10 uninterpreted.



81. Seismic profile 8-9-10 uninterpreted.

### **6.3 Seismic profiles that crosscut the Anhydros basin**

The seismic profile 60-61 passes through the basinal area. It starts 6 km SE of the southwest point of Ios island to the SW and ends 10 km south of Anhydros. It is approximately 20 km long.

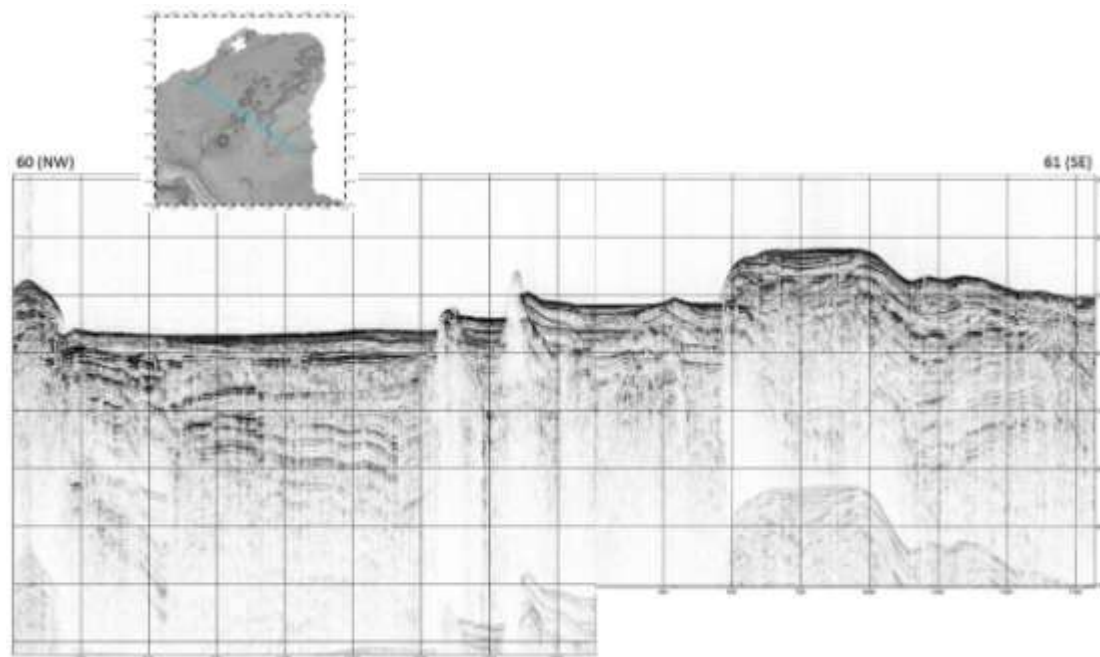
As shown in the profile, the basinal area has been formed as a result of the activity of marginal normal faults. The SE margin of the basin has been formed by a normal fault. About 1 km to the NW, its antithetic fault has been created.

Towards the SE, we can see the eastern edge of Anhydros ridge separated from the deeper eastern area by a normal fault. Both Anhydros horst and the deeper area are constituted by marine sediments which have been deformed by inactive normal faults and active normal faults respectively. At the SE edge of the section a positive flower structure indicates strike slip component at the area.

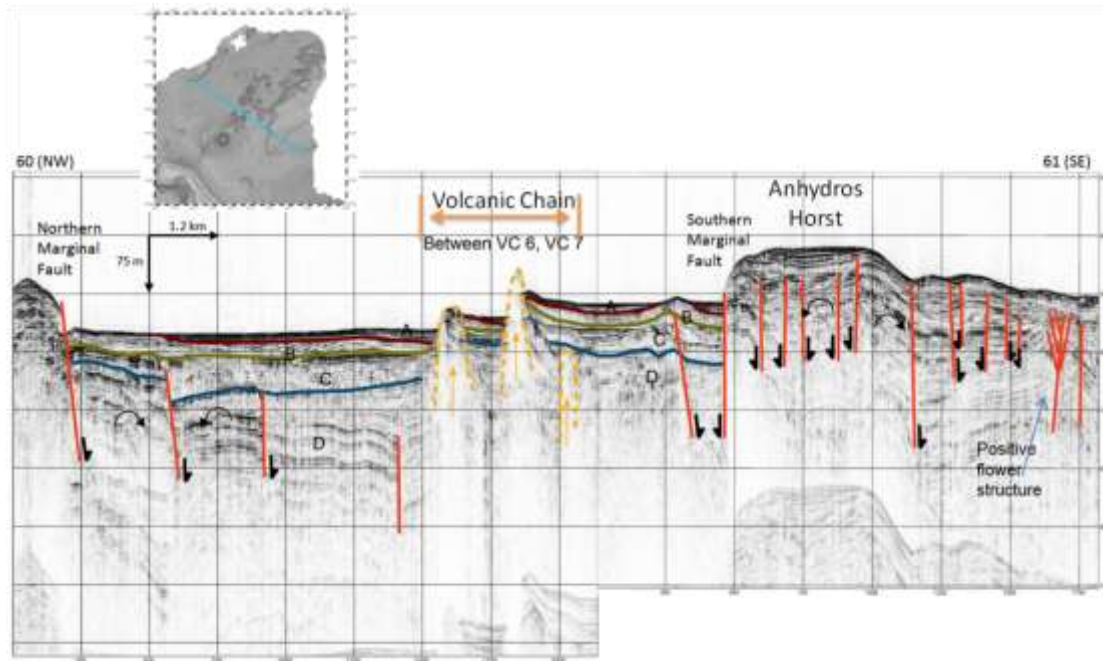
Within the Anhydros basin, the top unit, which has an insignificant thickness, corresponds to the pyroclastic flows of 1650 AD Kolumbo eruption. Unit B shows some parallel internal reflectors and probably corresponds to products of an eruptive event on Santorini. The chaotic unit overlaid by unit B, has probably been formed as a result of a former eruption of Kolumbo volcano.

At the center of this section there are three distinct areas of magma ascend belonging to the Kolumbo volcanic chain, two of which have reached the surface. These are most likely related to preexisting ruptures at the area that have served as conduits of ascending magmatic fluids.

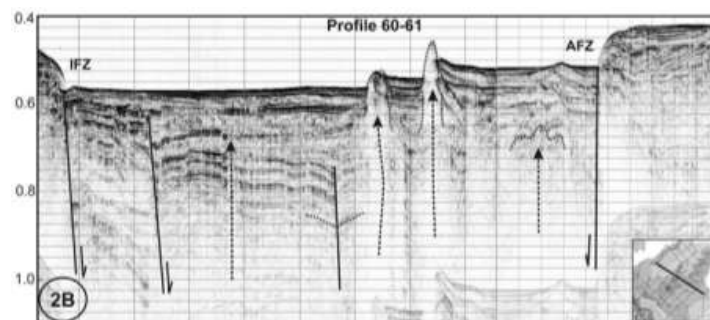
More to the N, three normal synsedimentary faults of different age can be distinguished. Starting from the SW, the first one deforms the lower part of the marine sedimentary sequence. The second one has reached the top of unit D whereas the third one has deformed layer C as well. The three different blocks between them have been tilted due to the different slip rates of the faults bordering them



82. Seismic profile 60-61 uninterpreted.



83. Seismic profile 60-61 interpreted.



84. Seismic profile 60-61. Interpretation by Sakellariou et al. 2010

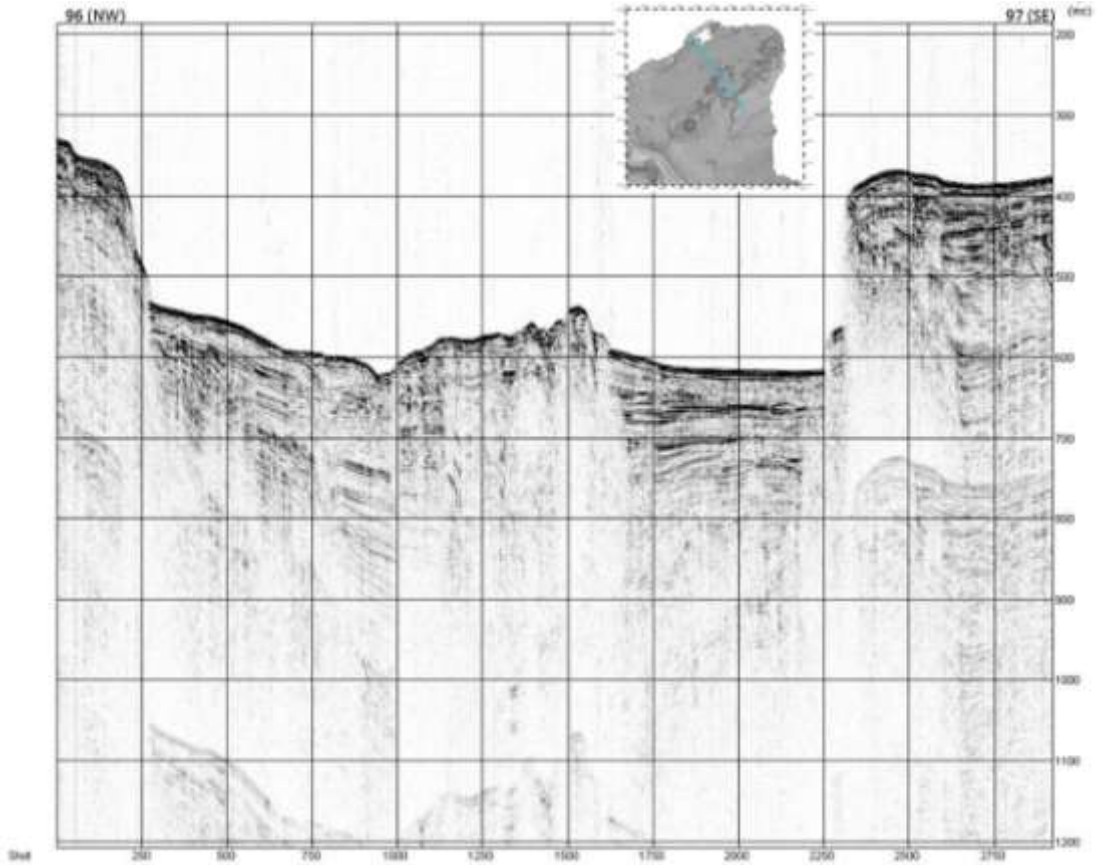
Profile 96-97 is also perpendicular to the long axis of Anhydros basin and approximately 16 km long. Here we can also attest the tectonic structure of the basin, which is a tectonic graben bordered by active normal faults.

In the middle of the basinal area we can recognize the volcanic relief formed by the development of the smaller volcanic craters belonging to the Kolumbo Volcanic Chain. The formation of these craters has been facilitated by preexisting ruptures that allowed magmatic fluid flow and resulted in an intra-graben tectonic horst.

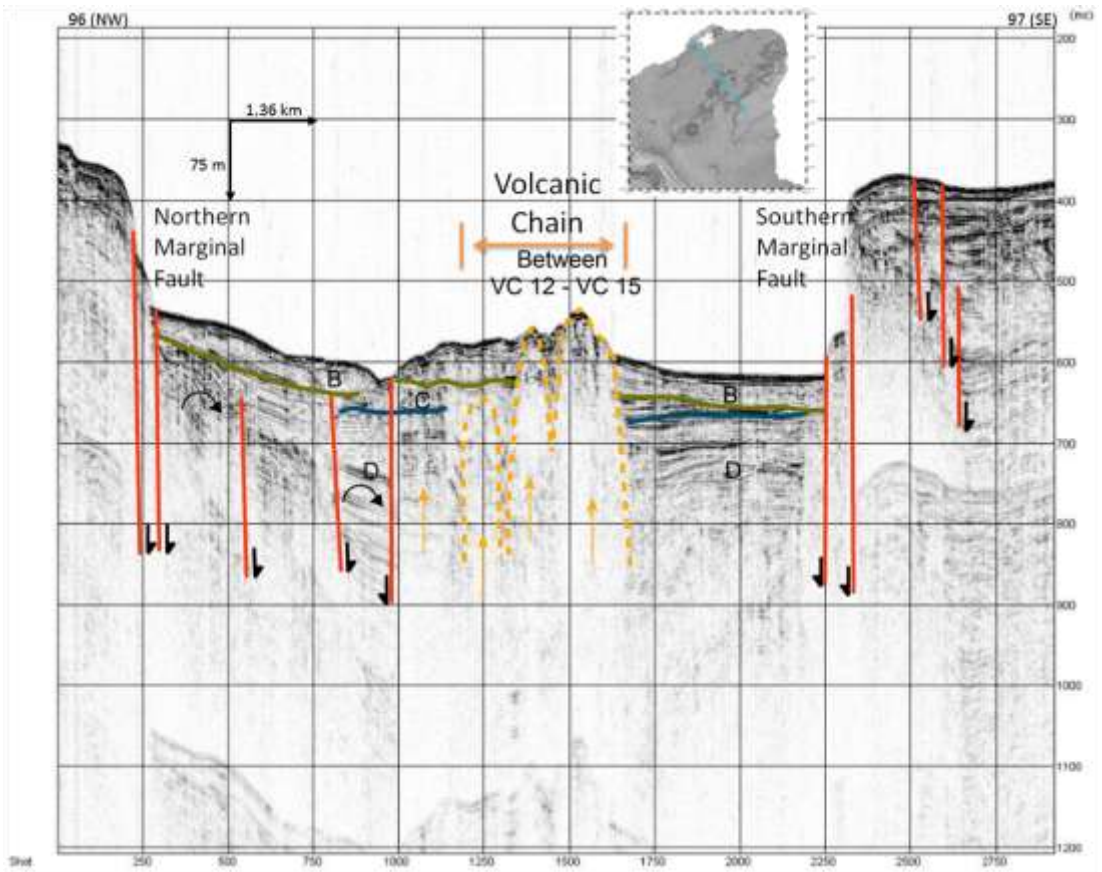
The products of Kolumbo 1650 AD eruption did not reach the area but layers B and C can still be distinguished here.

Some normal inactive faults have deformed the marine sedimentary sequence of the basin and the difference in their slip rates has caused tilting of the blocks they border.

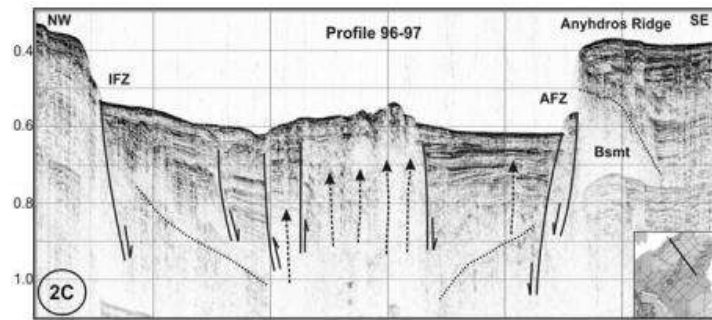
We can also observe the presence of an active normal fault within the basin which has a surface expression.



85. Seismic profile 96-97 uninterpreted.



86. Seismic profile 96-97 interpreted.

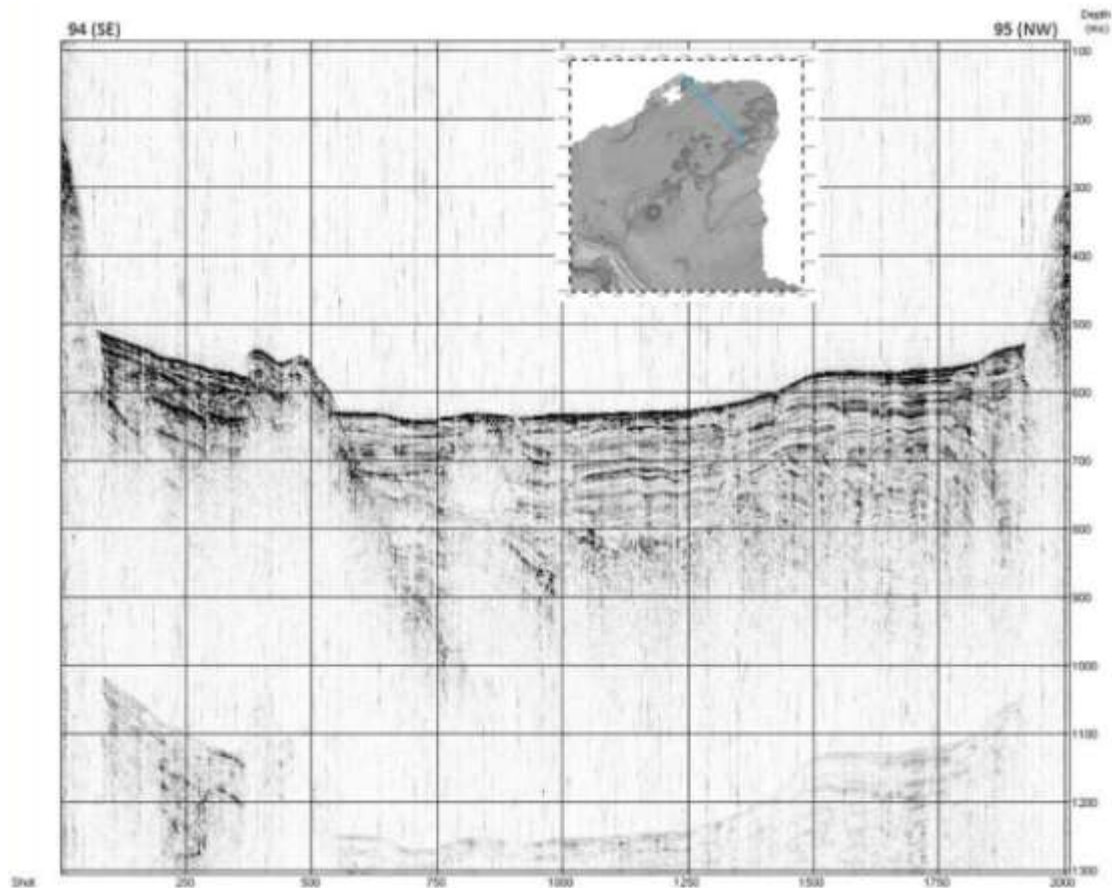


87. Seismic profile 96-97. Interpretation by Sakellariou et al. 2010

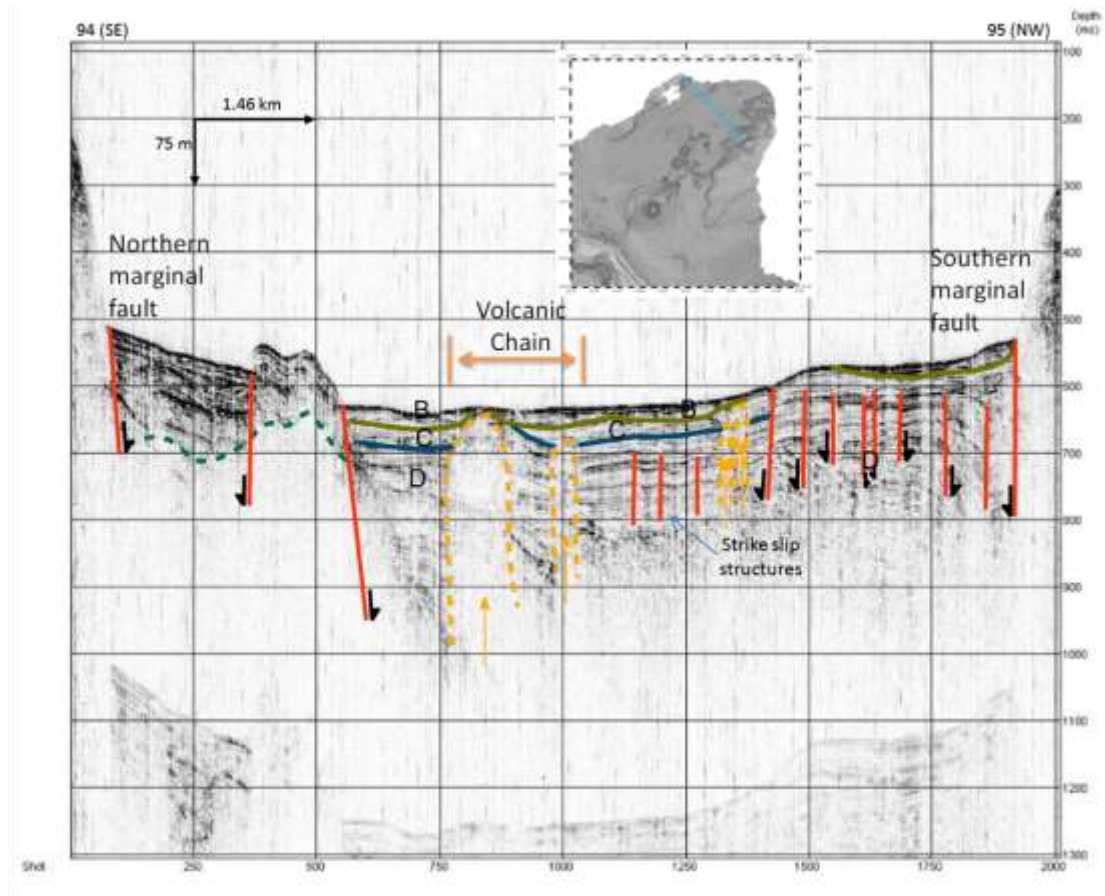
This profile crosscuts the long axis of Anhydros basin and clearly illustrates its tectonic structure. It is located at the NE part of the basin and is about 12 km long.

As shown in this section, Anhydros basin is a tectonic graben bordered by two normal marginal faults. In the middle of the basinal area we have conduits of magmatic ascend that have not reached the surface and can be included in the Kolumbo Volcanic Chain.

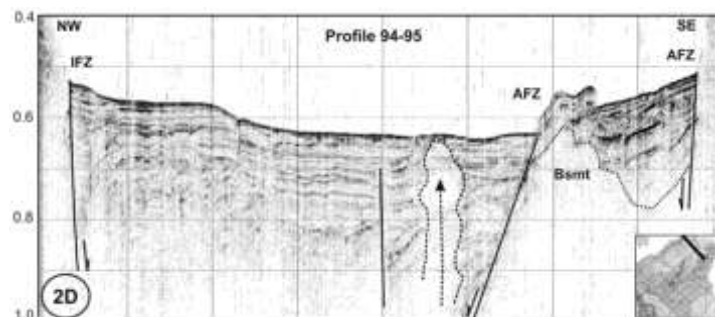
At the SE part, a ridge is formed and bordered by two active normal faults. More to the NW, we observe that layer A is absent, indicating that the products of the 1650 AD eruption did not reach at this point. Layers B and C, corresponding to Santorini volcanic products and a former Kolumbo eruption respectively, are present with approximately 20 m thickness each. Several inactive faults have deformed the marine depositional sequence of the basin, having a normal or strike slip character. An active normal fault within the basinal area has formed a step in the morphology.



88. Seismic profile 94-95 uninterpreted.



89. Seismic profile 94-95 interpreted.



90. Seismic profile 94-95. Interpretation by Sakellariou et al. 2010

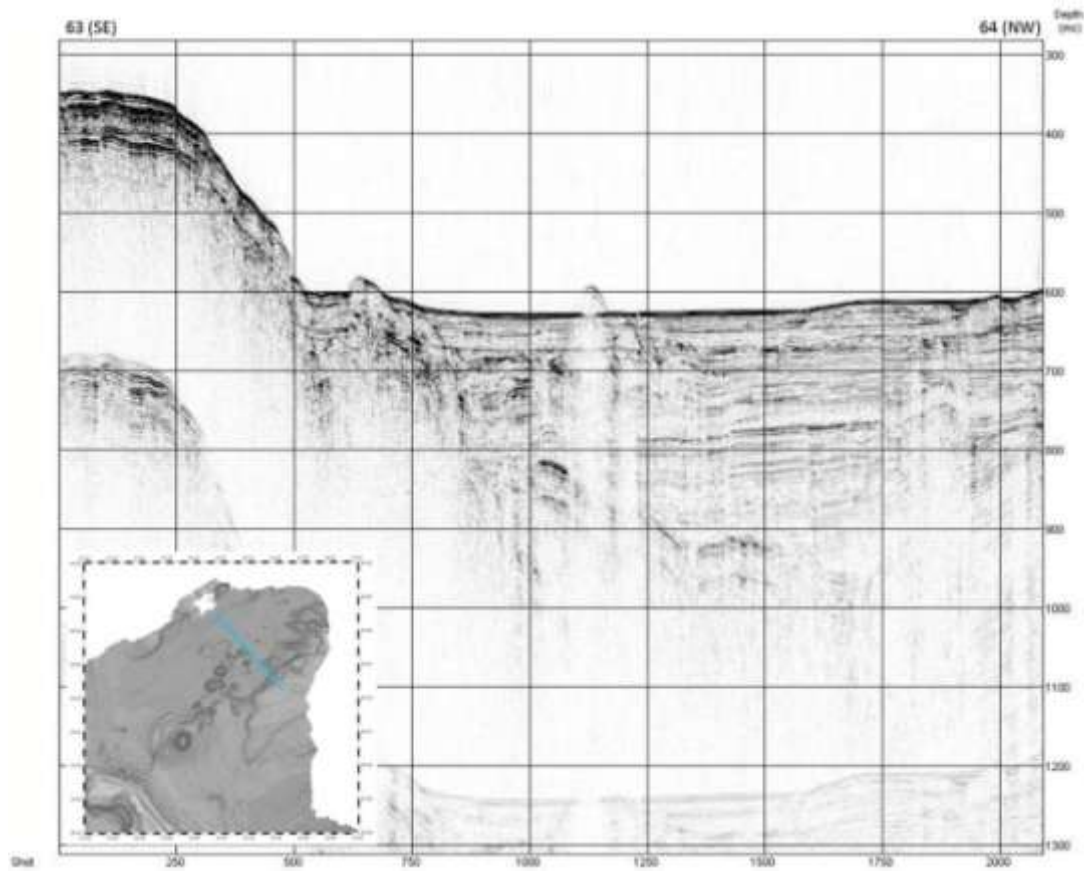
The seismic profile 63-64 starts from the Anhydros ridge to the SE and ends about 10 km to the NW, within Anhydros basin. It is about 11km long.

The SE part seems to belong to the Anhydros tectonic horst. The marginal fault seen at this area has uplifted the SE part and formed the horst, and subsided the NW part where the sedimentary basin was created.

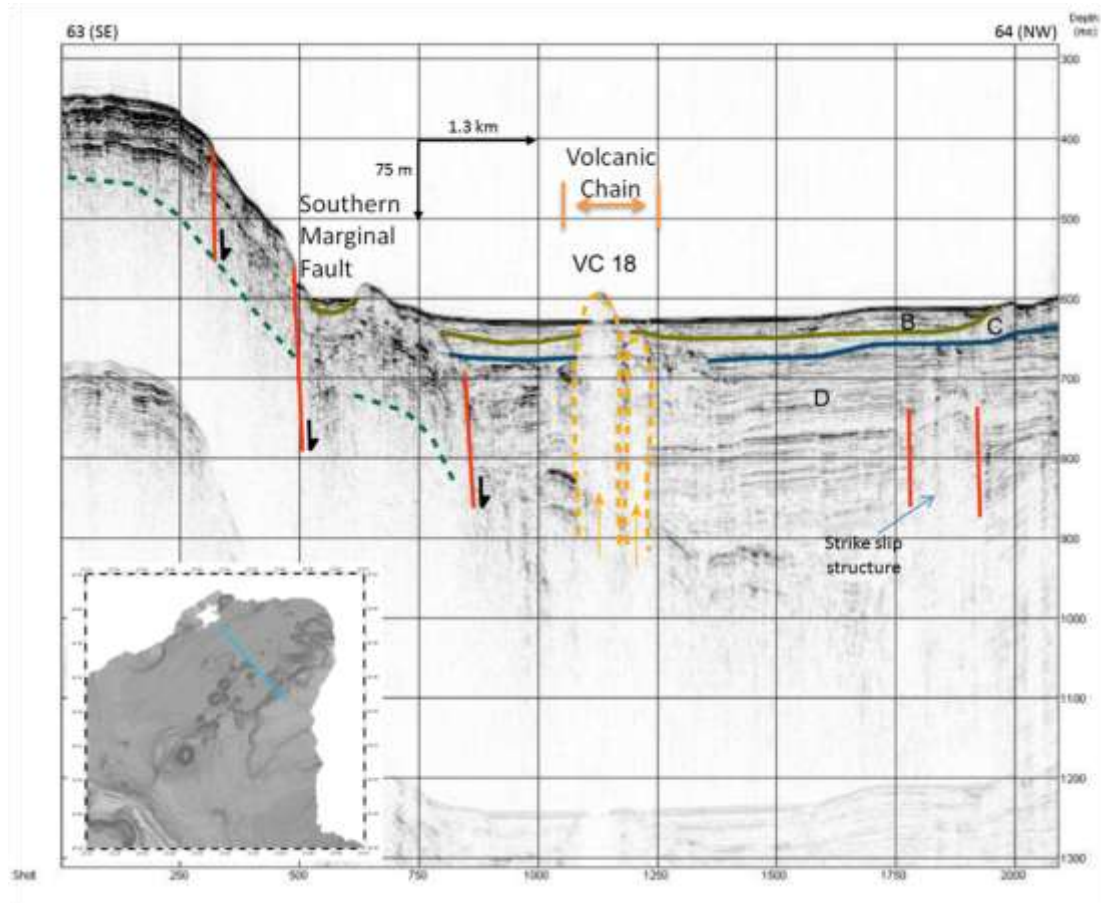
Kolumbo pyroclastic material are completely absent at this profile. Unit B, with the internal parallel reflectors, resembles the Santorini layered products seen before in other seismic sections. Layer C is also present here, with a chaotic seismic character, representing older volcanic products that probably are related to Kolumbo.

The continuity of the sedimentary infill of the basin (unit D) has been disrupted by the development of volcanic domes related to regional ruptures created at the center of the section.

Beneath the sedimentary sequence there is an evident unconformity that separates two totally different environments. This line probably corresponds to a preexisting relief and borders the transparent basement from the sedimentary sequence. A strike slip feature that has folded the stratigraphy of the lower parts of sequence D is also present at the NW part of the section.



91. Seismic profile 63-64 uninterpreted.

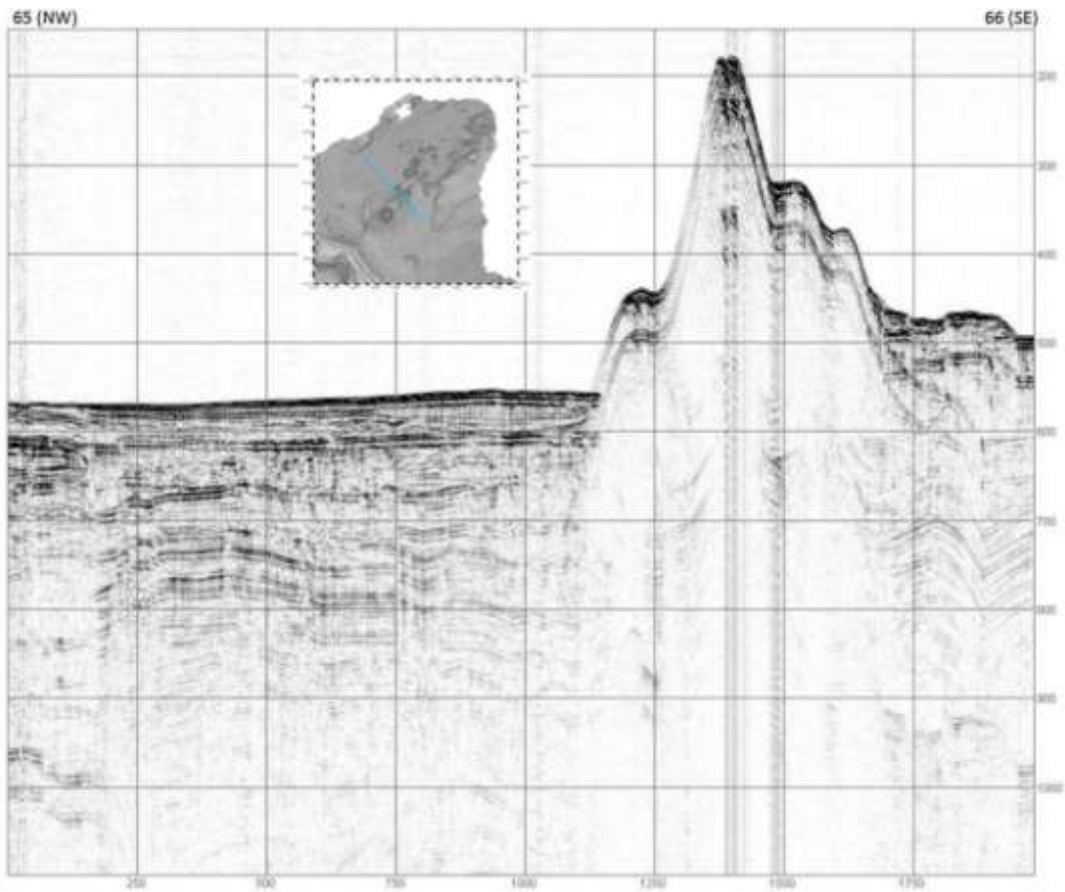


92. Seismic profile 63-64 interpreted.

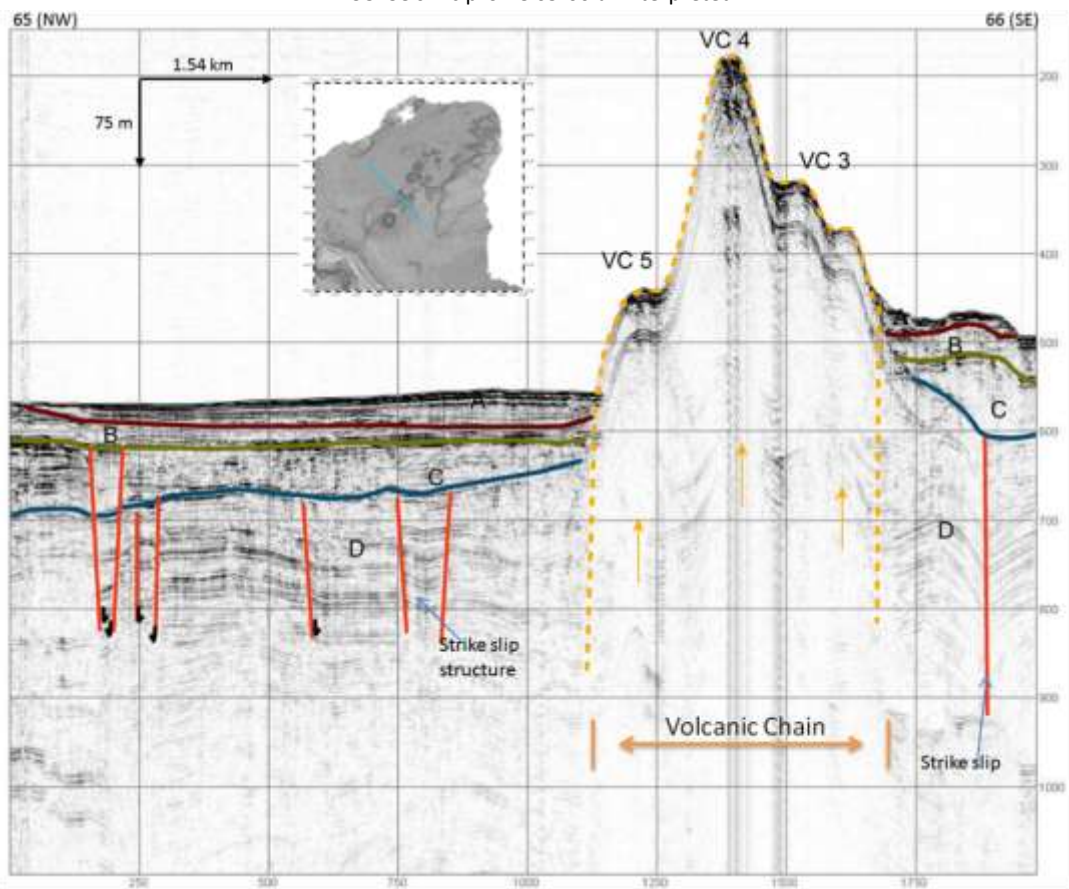
Section 65 – 66 is perpendicular to the long axis of the basin (NW-SE) and is approximately 12 km long.

The striking feature of this area is the abrupt alteration of the topography of the seafloor due to the occurrence of three volcanic cones. These are located at the lower parts of the NE external flanks of Kolumbo.

The upper seismic units (A and B) correspond to Kolumbo 1650 AD event and to an older Santorini eruptive event. Layer C is thicker here than other areas much further from Kolumbo, indicating the possibility of being the product of a pre-1650 AD event. At the NW part of the section its continuity has been disrupted by two antithetic normal faults. The marine sedimentary infill of the basin is deformed by several faults of normal and strike slip character.

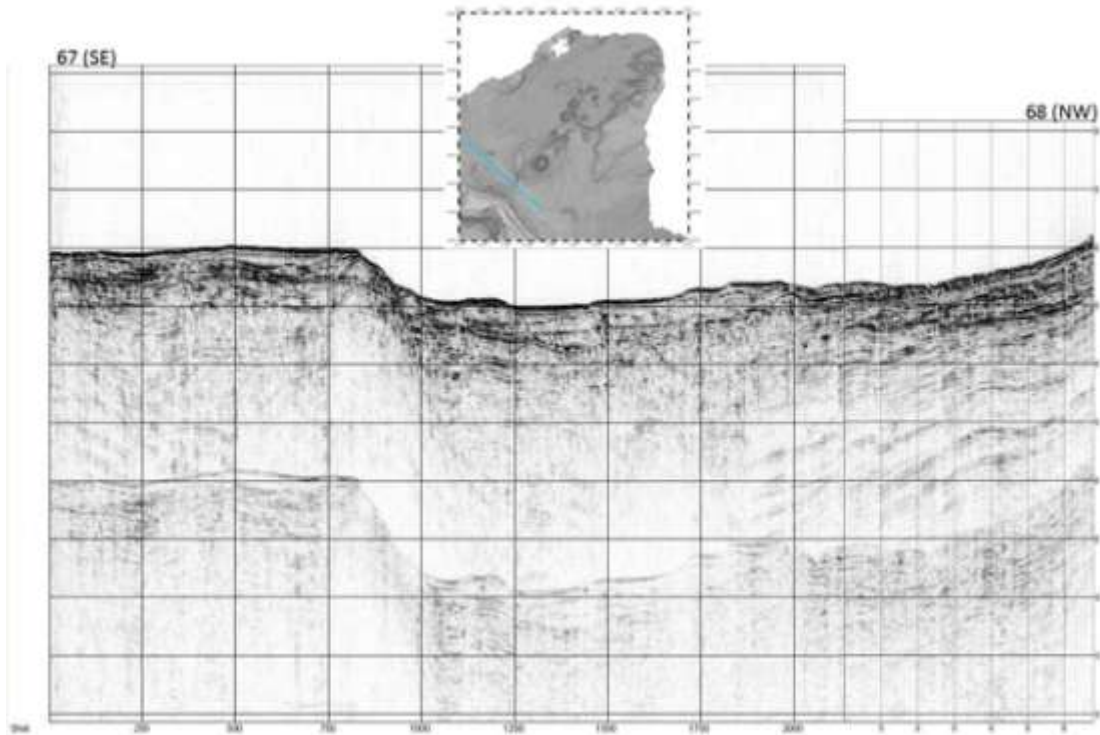


93. Seismic profile 65-66 uninterpreted.

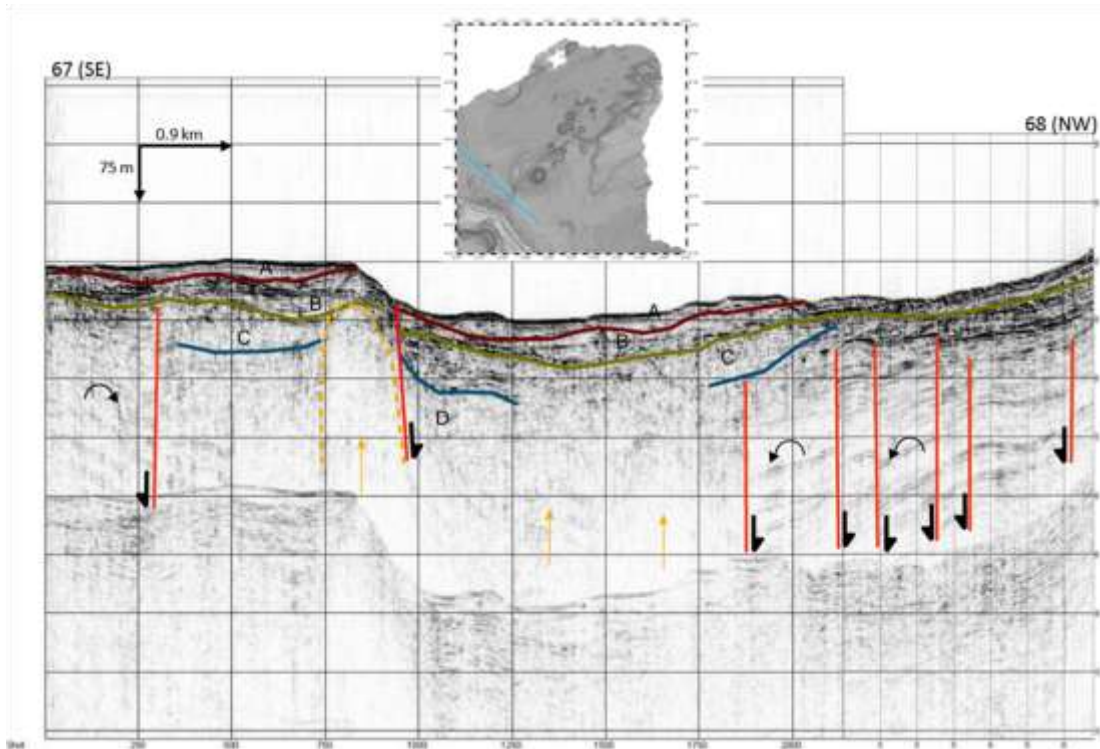


94. Seismic profile 65-66 interpreted.

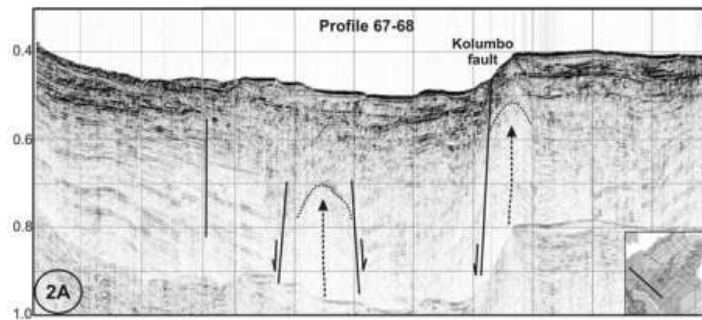
The seismic profile 67-68 runs parallel to the NE coast of Santorini and is about 12 km long. The SE part is an uplifted area due to the activity of an active normal fault. Just next to this fault we observe a conduit of magmatic fluid ascend, probably associated to the existing weak zone. Several inactive normal faults have deformed the marine sedimentary sequence and caused tilting of the intermediate blocks.



95. Seismic profile 67-68 uninterpreted.



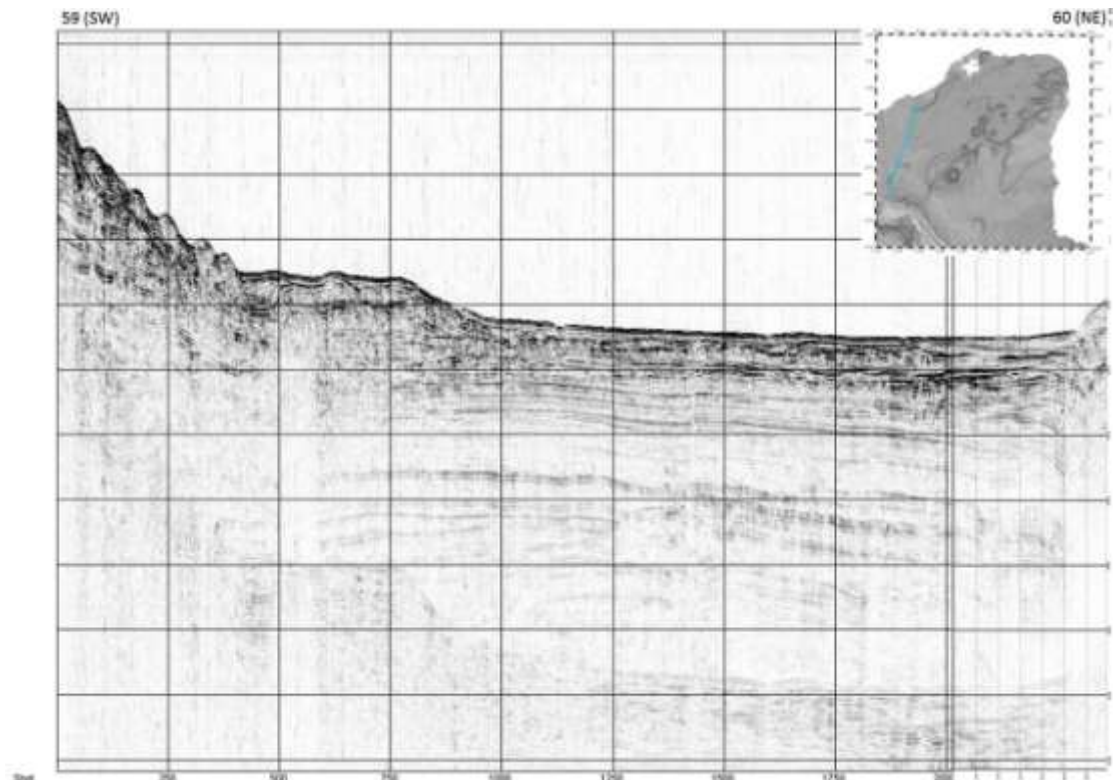
96. Seismic profile 67-68 interpreted.



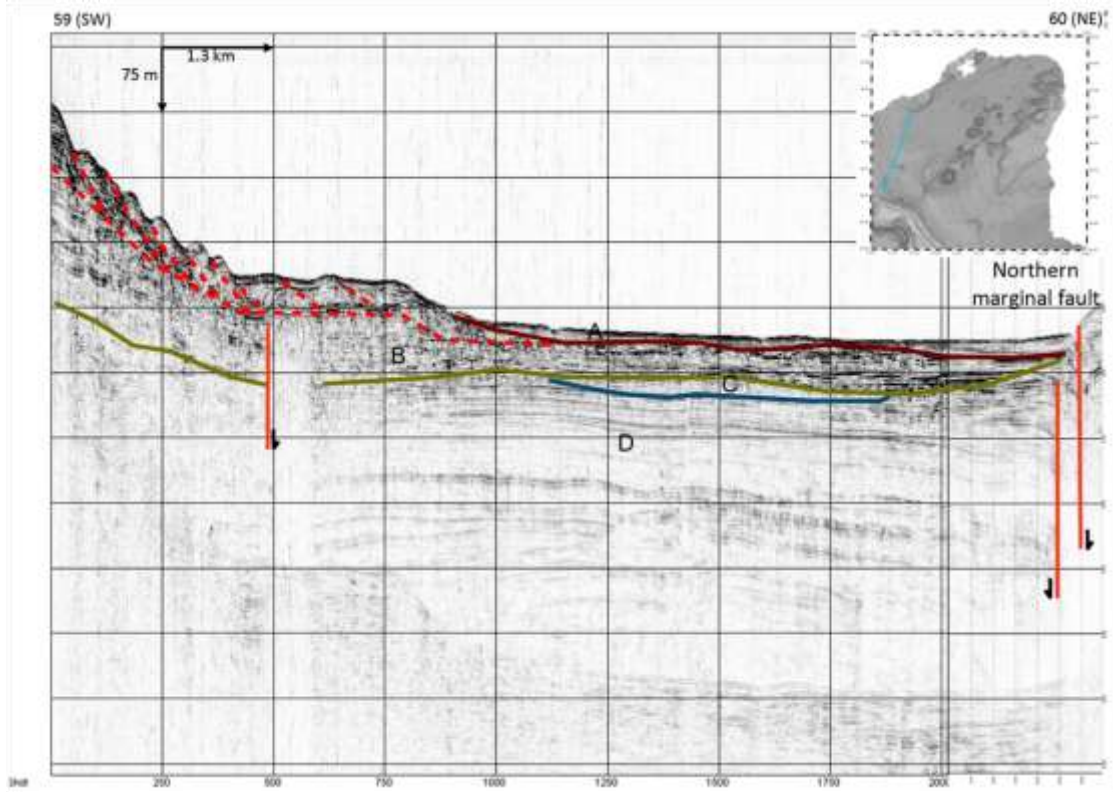
97. Seismic profile 67-68. Interpretation by Sakellariou et al. 2010

Profile 59-60 starts from the northern submarine slopes of Santorini and reaches the northern margin of the Anhydros basin. Its length is approximately 13 km. Water depth gradually diminishes from SW to NE, towards the basinal area where the morphology is smooth for several km. At the NE edge of the profile a couple of normal faults borders the basinal area.

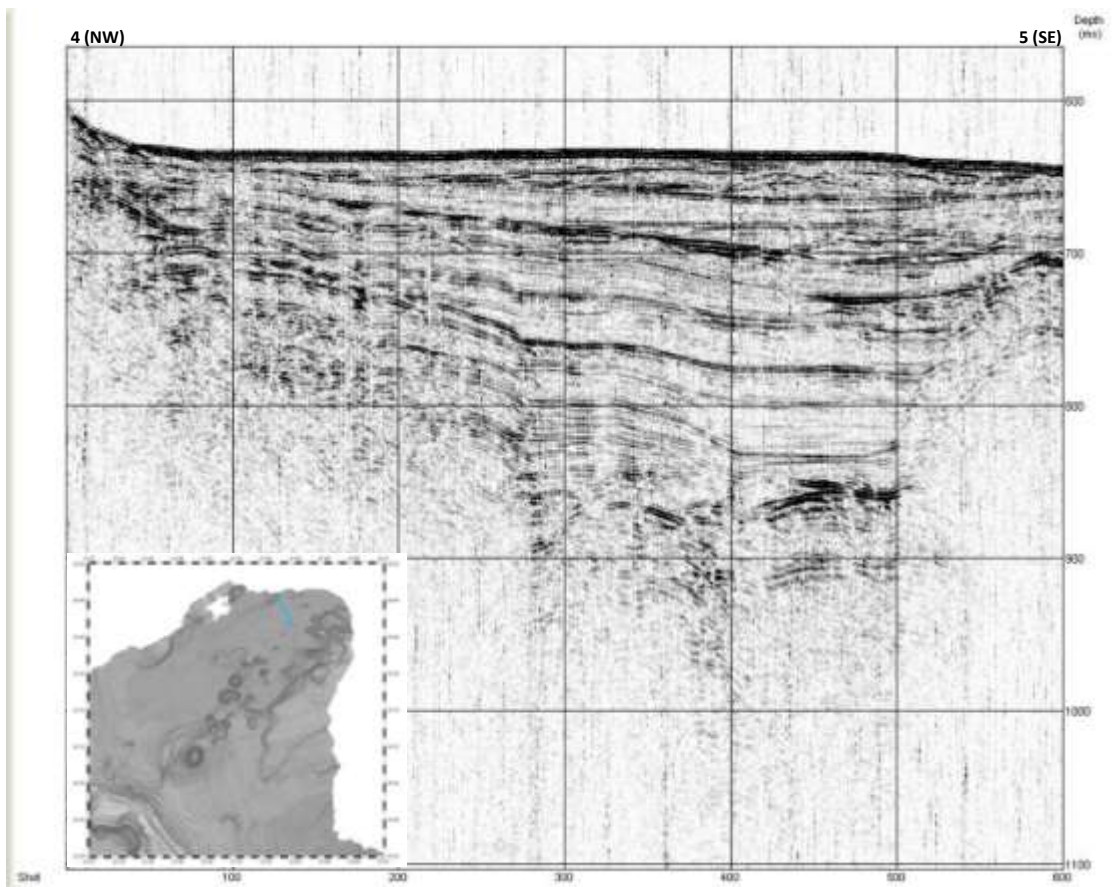
Starting from the SW edge of the section, the listric plane is present again with several blocks that have slipped on it. The NE edge of this feature is covered by the transparent layer A belonging to the Kolumbo 1650 AD eruption. The underlying seismic sequence (layer B) most likely represents layered Santorini pyroclastic deposits. And is characterized by undulated, parallel reflectors. Beneath the listric plane, a normal fault deforms layers B and D, the latter of which represents the sedimentary infill of the basin.



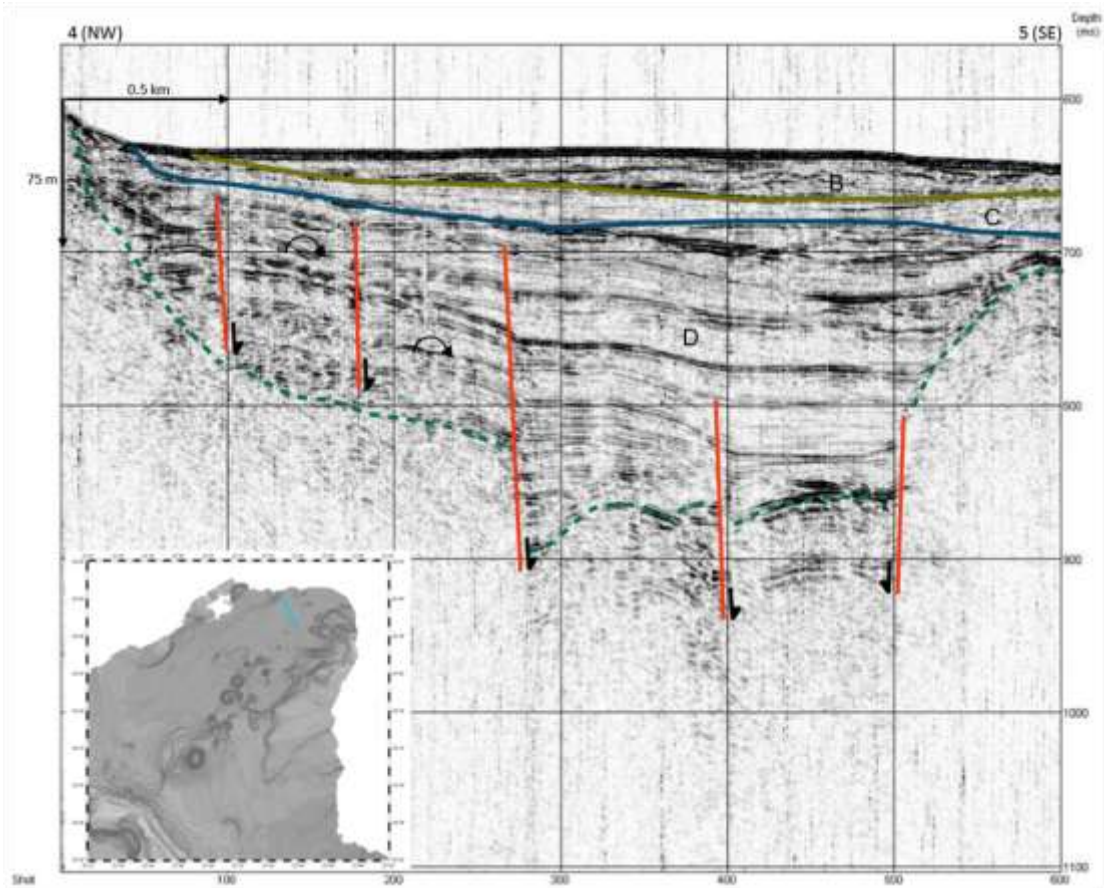
98. Seismic profile 59-60 uninterpreted.



99. Seismic profile 59-60 interpreted.



100. Seismic profile 4-5 uninterpreted.



101. Seismic profile 4-5 interpreted.

This seismic profile displays the central, smooth part of the Anydhros basin where we have the highest accumulation of marine deposits. These have been deformed by synsedimentary faults that are currently inactive. They are covered by a layer of pyroclastic deposits (layer B), which probably corresponds to Santorini pyroclastics. The products of the 1650 AD eruption of Kolumbo are not present at this area. The green line represents a an unconformity. Beneath it we can observe a rather transparent acoustic basement.

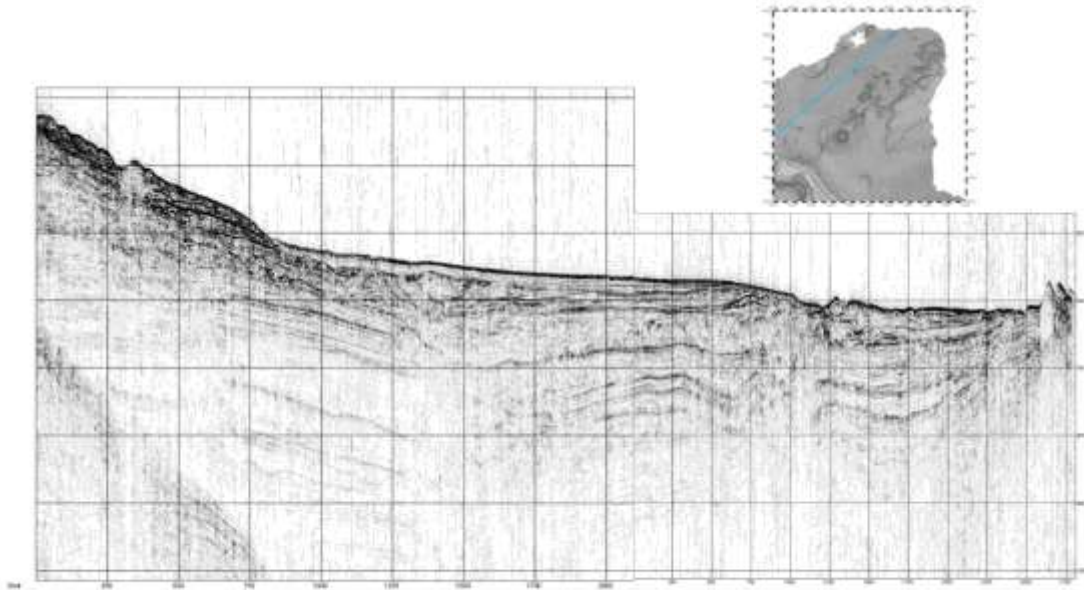
#### **6.4 Seismic profiles parallel to the long axis of Anhydros basin**

The profile 3-4 is a seismic section which traverses the center of Anhydros basin and is oriented parallel to its long axis (NE-SW). Its length is approximately 25km and a number of tectonic and morphologic features can be recognized along it and several seismic facies as well. Water depth gradually increases from SW to NE, towards the basinal area where the morphology is smooth for several km. At the NE edge of the profile there is a dome shaped feature, probably formed by the emission of fluids.

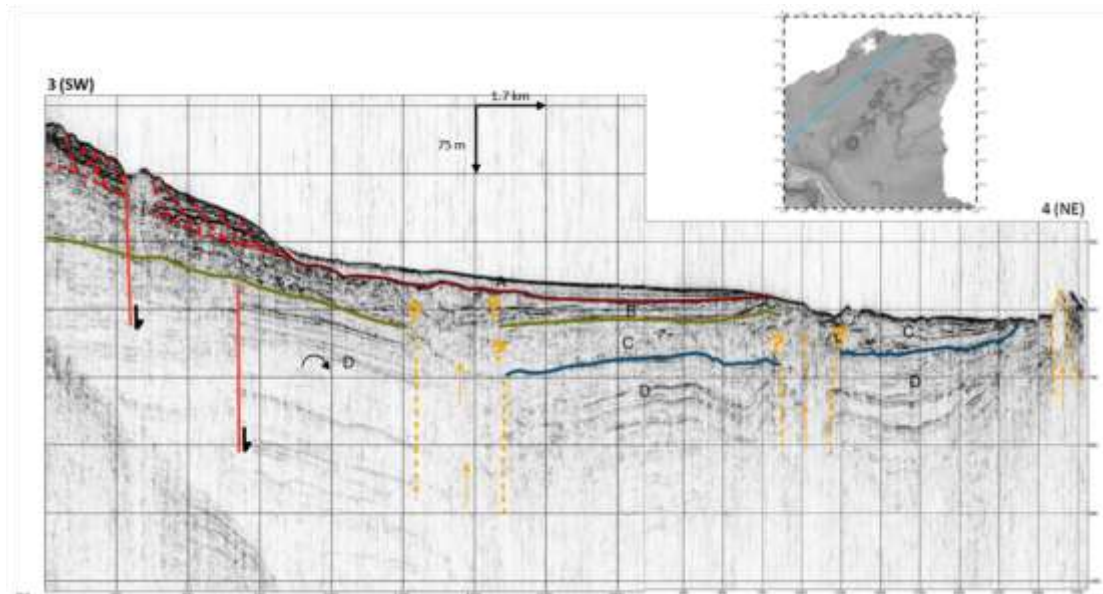
Starting from the SW edge of the section, the first thing that is observed is a listric plane which has probably served as slipping surface for several blocks that belong to the NE volcanic slopes of Santorini. The slipping of these masses is responsible for the step like morphology of the seafloor at this area. The continuity of the listric plane is intermitted by a younger normal fault that reaches and deforms the seafloor. The throw of this fault is about 25-30m. The underlying seismic sequence (layer B) most likely represents layered Santorini pyroclastic deposits. Another characteristic of this sequence is the undulated, parallel reflectors at the SW part of the seismic section. The younger seismic sequence observed is A which most likely corresponds to the Kolumbo 1650 AD eruption. It's an acoustically transparent layer consisting of pyroclastic deposits.

In general, 3 zones that cause perturbation of the stratigraphy can be traced. These zones mostly affect the continuity of the marine deposits (layer D), which have filled the Anydhros basin, in a way that 4 different blocks are formed. In some cases, as shown in the profile, these zones have served as a conduit for magma ascend, as indicated by the diffuse or transparent character crosscutting the sedimentary layering. In this profile, the conduits have laterally supplied with magma the upper part of the sedimentary sequence (layer C) causing some disturbance to the upper layers.

The lower seismic sequence (layer D) is characterized by parallel reflectors representing marine sediments that have been deposited at the area of Anydhros basin. A normal fault has deformed this sequence at the SW part of the section. The faulted block towards the west side of the fault is characterized by parallel, horizontal seismic reflectors. The eastern block is also characterized by parallel reflectors that dip towards NE, indicating a dextral tilt of the whole block. This probably happens because the diffusion zone coincides with a tectonic feature with a slip rate higher than the one of the previously mentioned blind fault.

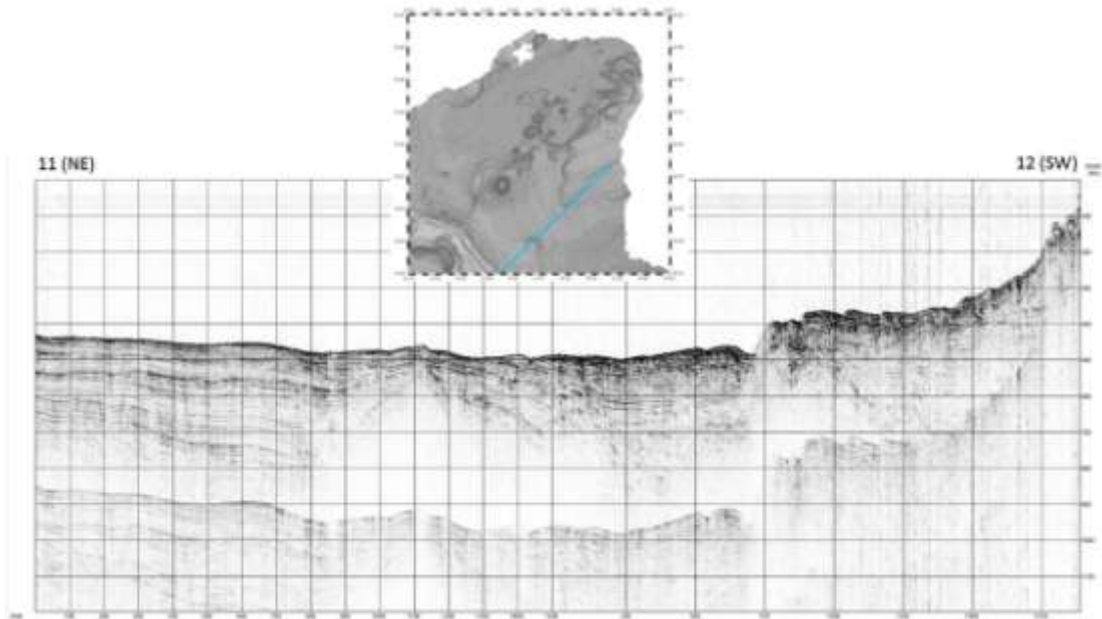


102. Seismic profile 3-4 uninterpreted.

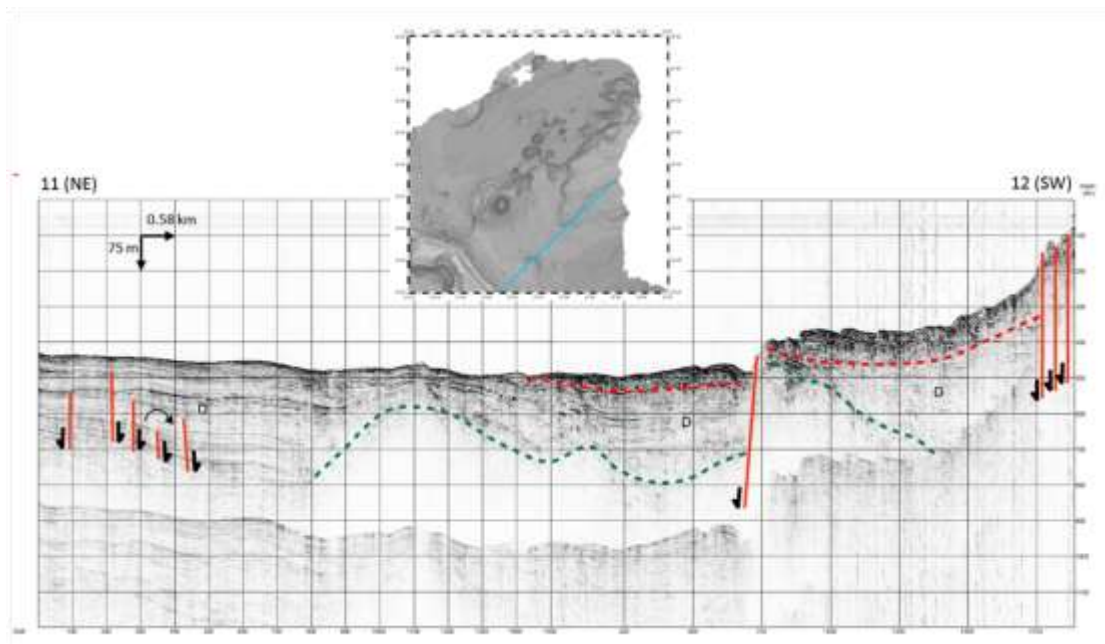


103. Seismic profile 3-4 interpreted.

Profile 11-12 is approximately 17,5 km long. It starts from the eastern submarine slopes of Santorini to the SW and reaches the southern edge of the Anhydros ridge. At the southwestern part of the profile we can clearly distinguish the listric plane, previously mentioned in other sections, the continuity of which seems to be interrupted by normal faults. Beneath it, a sequence characterized by parallel internal reflectors is present. This corresponds to the sedimentary sequence of the basin and towards the NE it seems to have been deformed by syndepositional normal faults. The unconformity, illustrated with a green line, separates the depositional sequence from a highly transparent basement.



104. Seismic profile 11-12 uninterpreted.

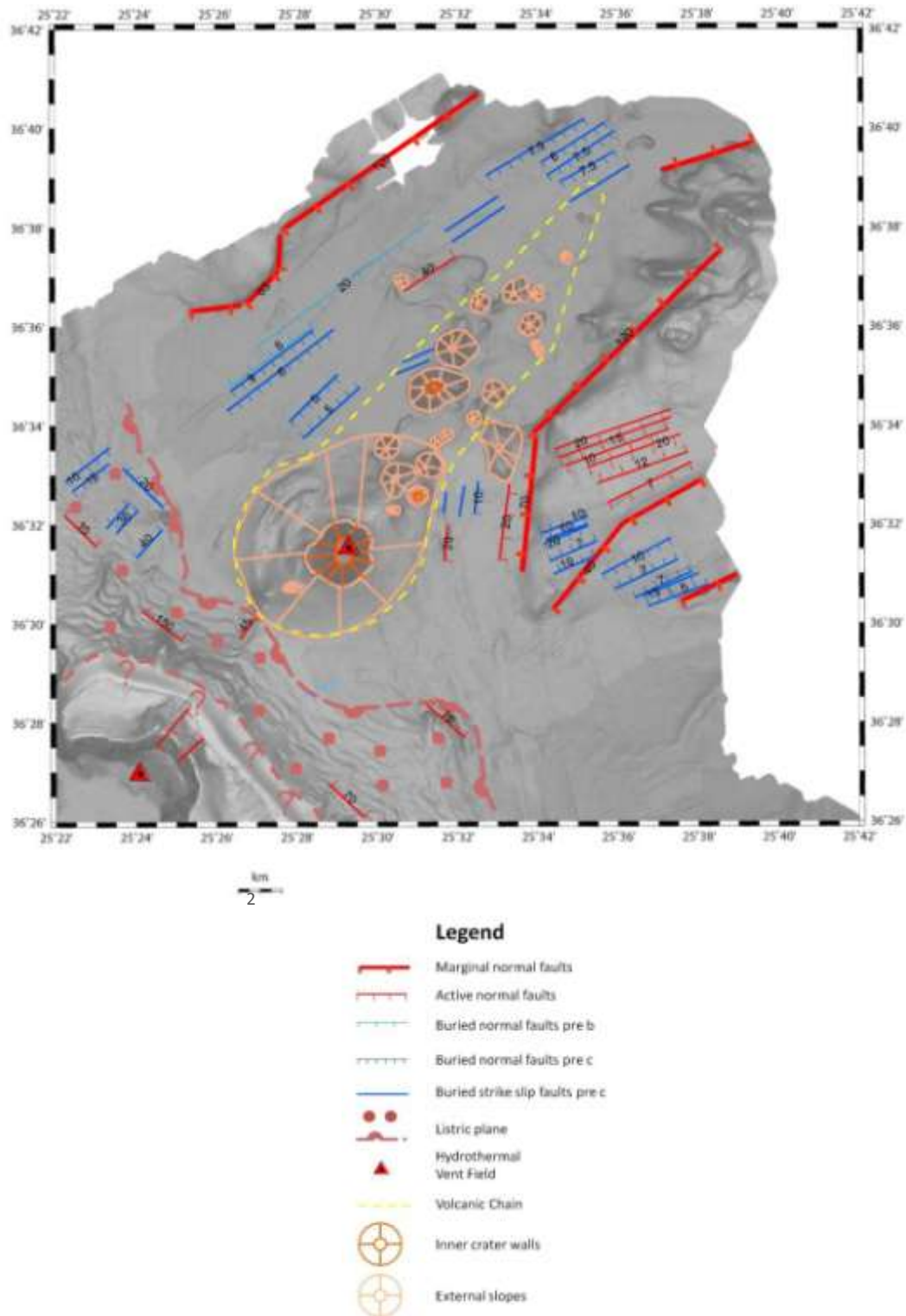


105. Seismic profile 11-12 uninterpreted.

## 7. Results

### 7.1 Tectonic Analysis

Based on the analysis of the bathymetry and the interpretation of the lithoseismic profiles, we attempted to distinguish the morphotectonic structure of the Anhydros basin (fig. 106 ).



106. Morphotectonic map of Anhydros basin. Numbers on the fault lines represent the throw measurements.

Within the basin there are no apparent major faults, but approximately in the middle of the basin volcanism has created an intragaben horst. The occurrence of volcanic centers within the basin is most probably associated to tectonic processes. Magmatic fluids ascend has been facilitated through the faulting of the crust. Thus, volcanic cones developed wherever the magmatic fluids have reached the surface of the seafloor. These are aligned along two linear trends ((N 29°E and N42° E), reinforcing the suggestion of their tectonic origin.

The overall Kolumbo Volcanic Chain has a NE-SW orientation following Kolumbo fault line at the NE part of Santorini.

The tectonic graben structure of Anhydros basin is apparent on the seismic sections that are perpendicular to its long axis.

The northern border of the basin is separated in two different marginal normal faults. The northern one has a N55°E direction and about 11 km long. The SW part is curved. The throw measured is 120 m for the NE part and 65 m for the SW.

The southern border of the basin is composed by three marginal normal faults. The one to the north has a N70°E orientation. More to the south, another normal fault (N45°E) forms the southern border of the basin. It is about 12 km long and the measured throw is 120 m. The orientation of the southern border changes to N05°E. The marginal fault that forms it, is about 6 km long and its measured throw is 70m. Within the basinal area there are several secondary faults the majority of which is inactive. North of Kolumbo Volcanic Chain their orientation follows the direction of the basin, whereas east of Kolumbo th direction changes to NNE-SSW. The older ones are synsedimentary and have deformed the Plio-Quaternary marine infill of the basin. Some of them are strike slip structures judging by the anticlinal and synclinal folds created. The latter correspond to positive and negative flower structures. On the other hand, blocks bordered by normal faults of the same age, are usually tilted due to difference in the slip rates.

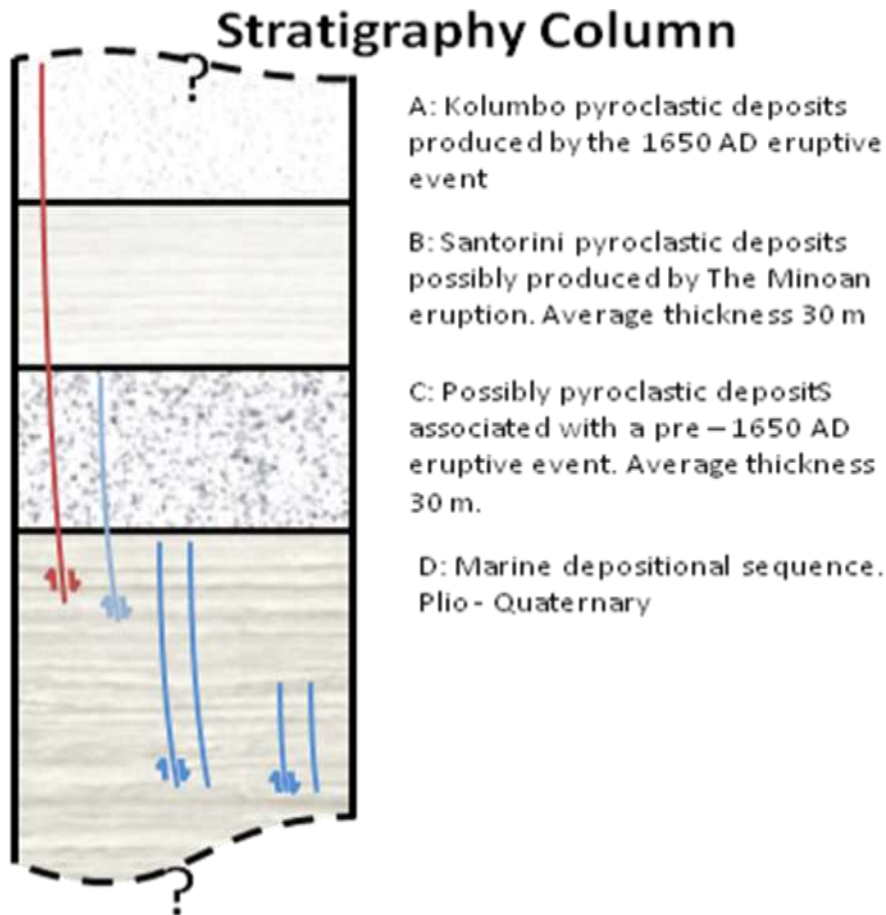
Inactive normal faults, younger than the previous ones, are observed north of Kolumbo following the orientation of the basin. These have deformed the marine sedimentary sequence and the volcanic unit C , probably corresponding to a former eruption of Kolumbo.

Two active faults are also present within the basin, one north of the volcanic chain and one just east of Kolumbo with a NE-SW and NNE-SSW orientation respectively.

Southeast of Anhydros tectonic graben we have the Anhydros horst which is deformed by normal faults which have a N65°E orientation.

At the western slopes of the basin, the listric plane has given an irregular step like morphology, since several blocks seem to have slipped on it. This forms the SW boundary of Anhydros basin and separates Santorini from Kolumbo submarine volcano. Some active faults disrupt its continuity, whereas blind faults have deformed the marine sedimentary sequence beneath it.

The following stratigraphic column (fig. 107) summarizes the evolution of Anhydros basin and has been designed based on 30cm/yr according to the analysis of the boxcores collected during the Nautilus mission 2010 (Prof. Carey personal communication).

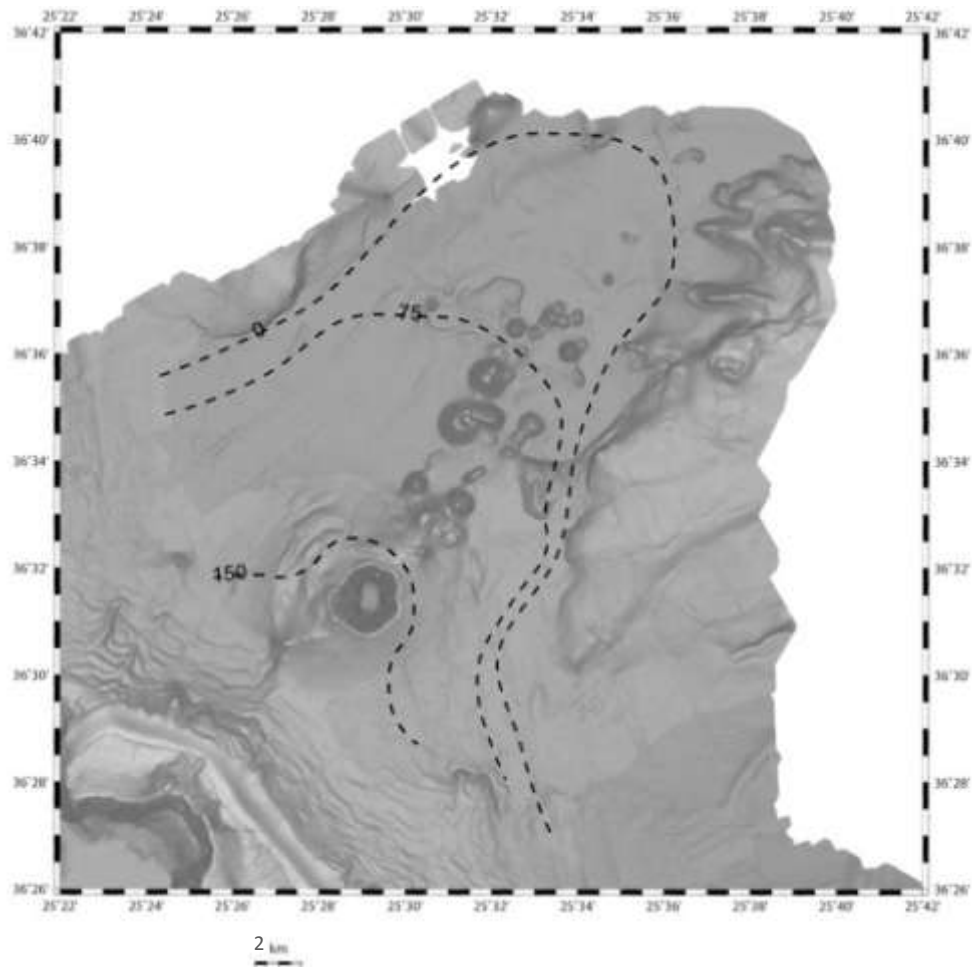


107. Stratigraphy column of Anhydros basin.

### 7.2 Paleogeographic Synthesis

Based on the seismic sections, the following map was designed illustrating the distribution and thickness of the volcanic sequences within the basinal area.

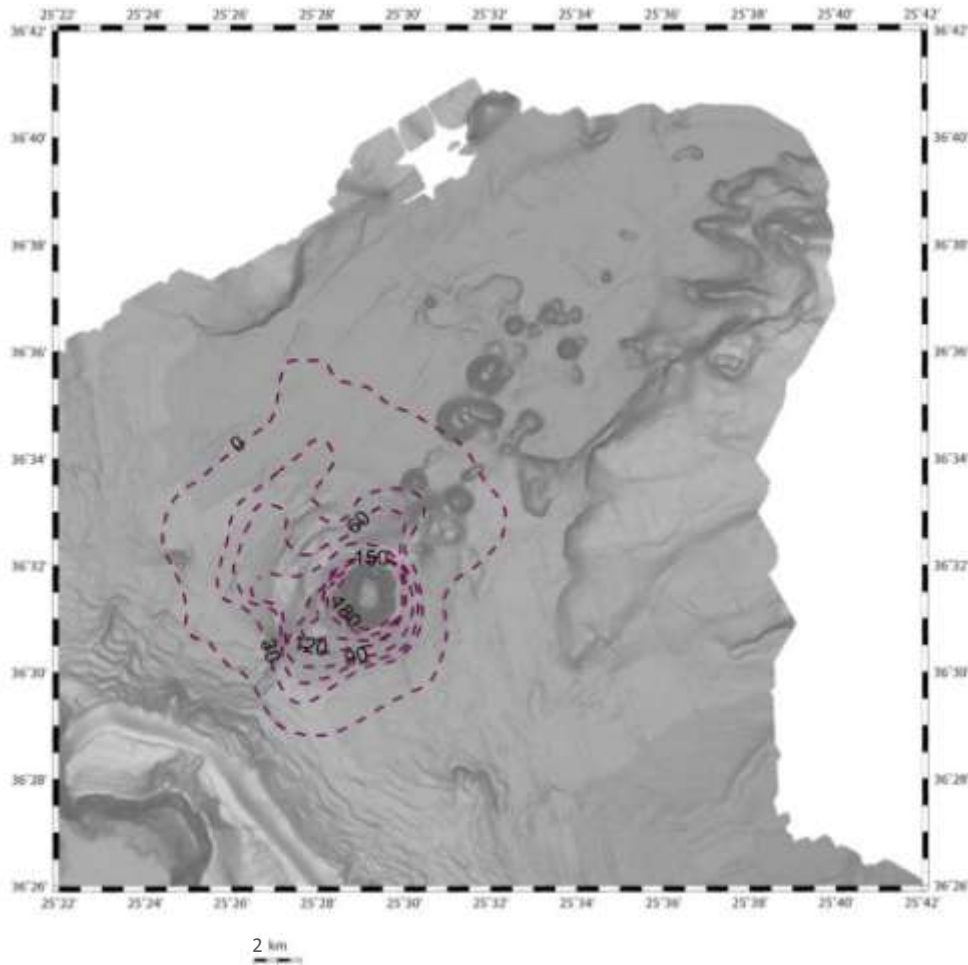
This map shows that the pyroclastic products of a previous eruptive phase of Santorini (layer B) and of a pre 1650 AD Kolumbo eruption (layer C) have been widely distributed within Anhydros basin and covered the marine sediments. Maximum concentration of all the three volcanic sequences is observed around Kolumbo volcano and reaches up to 250m.



108. Map showing the distribution of all the volcanic sequences (A, B and C) deposited within the basinal area. Black contours indicate how deep beneath the seafloor the base of the volcanic sequences is.

The correlation of all the seismic profiles around Kolumbo volcano resulted in a thickness map (fig. 109) which shows the distribution of the pyroclastic deposits of the 1650 AD eruption. The maximum thickness of these deposits is approximately 180 m at the western part of the crater and they cover an area of about 97.4 km<sup>2</sup>.

This map permits us to better comprehend the paleogeographic configuration of the basin, before the deposition of the volcanic sequences.



109. Map showing the distribution of the pyroclastic deposits from the 1650 AD eruption in the Anydhros basin. The thickness of the upper sequence is shown with 30-meter-spaced contours.

### **7.3 Tsunami generation mechanisms**

Tsunamis from the 1650 AD were likely generated by a variety of mechanisms including shallow submarine explosions, discharge of pyroclastic flows into the sea, and edifice collapse as a result of magma withdrawal from a shallow crustal magma chamber. Of these mechanisms, discharge of pyroclastic flows into the sea may have played a dominant role, but our data precludes us from making a quantitative assessment of the relative role of each mechanism. It is worthy to note, however, that the eruptive behavior of Kolumbo clearly presents numerous ways for generating tsunamis in close proximity to Santorini.

There are several lines of evidence which suggest that Kolumbo could pose significant risk to inhabitants of Santorini and neighboring islands from future eruptive activity. First, recent seismic studies indicate that the most frequently occurring zone of earthquakes in the Santorini volcano field is located beneath Kolumbo (Bohnhoff et al. 2006). Furthermore, tomographic studies have suggested the existence of an active crustal magma chamber at depth of about 5 km beneath the volcano (Dimitriadis et al., 2010). This is the same depth as the pre-eruption pressure/temperature conditions inferred for the 1650 AD rhyolite magma (Cantner et al., 2012). In addition, a widespread hydrothermal vent field was discovered on the northern part of the Kolumbo crater floor during ROV dives in 2006 (Sigurdsson et al.,

2006). A Kuroko-style massive sulfide deposit is currently forming there with fluid venting temperatures in excess of 200° C.

It is difficult to predict the exact nature of a future eruption of Kolumbo volcano given that a detailed history of the volcano has yet to be determined. ROV explorations of the crater indicate that dacite and rhyolite are the most common products of the volcano with little evidence of more mafic compositions. In addition, the inner crater wall consists dominantly of bedded pyroclastic and dike injections. There has yet to be any evidence of extensive dome-building episodes in the evolution of the volcano. If renewed activity taps a volatile-rich rhyolite magma from the current chamber at 5 km depth then eruptive scenarios similar to the 1650 AD sequence could be anticipated. In this case the east of coast of Santorini and neighboring island could experience tsunamis of similar magnitude to those generated during the last eruption. According to historical accounts, it has been possible to assess that the 1650 AD tsunamis had a maximum intensity of VI degrees in the six grade modified Ambraseys–Sieberg tsunami intensity scale (Ambraseys, 1962; Papadopoulos and Chalkis, 1984). This is in contrast to more recent studies (Dominey-Howes et al., 2000) which suggest that the magnitude of the 1650 AD tsunami has probably been overestimated since palaeontological and lithological studies along the eastern coast of Thera has shown no bio- or lithostratigraphic evidence for the deposition of marine- (tsunami) deposited sediments. In light of the recognition of the potential tsunami-generating mechanisms at Kolumbo volcano, a useful next step would be to carry out computer simulations of possible tsunami magnitudes using geologically constrained parameters determined from new knowledge about the scale of the 1650 AD eruption. This modeling could include wave generation from pyroclastic flow discharge into the sea and small-scale caldera collapse to investigate the plausible ranges of coastal impacts in the Santorini area. Such modeling could help the local authorities in their efforts towards hazard evaluation, emergency planning and disaster management.

## **8. Conclusions**

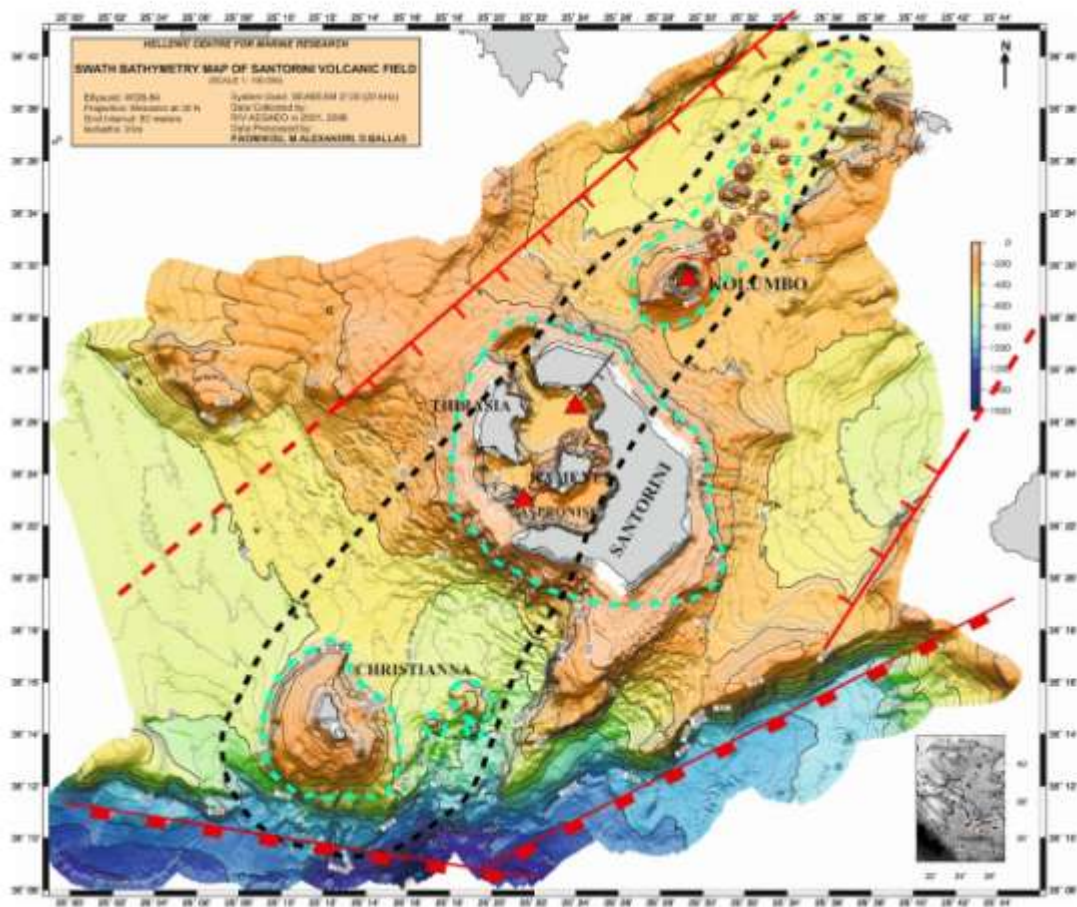
Numerous oceanographic surveys have been conducted in Santorini Volcanic Group (South Aegean Sea) since 2001, revealing the spectacular morphology of the seafloor (multibeam data) and the sub-seafloor stratigraphic horizons (seismic profiles). Technological advancements in seafloor exploration such as ROVs and a submersible, enabled us to observe products of submarine volcanism that were previously inaccessible. In addition, gravity and box coring, geological and biological samples have been collected from selected areas for further analysis.

The offshore geophysical survey in Santorini shows that recent volcanism occurred along a NE-SW tectonic zone named as Christianna-Santorini-Kolumbo (CSK) line. Christiana islets and three newly discovered submarine volcanic domes, with small colonies of yellow, presumably sulfur-reducing hydrothermal bacteria, occur in the southwestern part of the line. The presently active intra caldera volcanic domes of Palea and Nea Kameni islands and the low temperature (17-24 C) vent mounds covered by yellowish bacterial mat occupy the middle part of the line. The Santorini vent field is linked with the Kolumbo normal fault onshore which is likely controlling the pathways of hydrothermal circulation within the caldera. The most prominent feature at the NE part of this zone, is Kolumbo submarine

volcanic chain which is extended 20Km with several volcanic domes aligned along this direction. The Kolumbo volcano had an explosive eruption in 1650 that killed 70 people on Santorini. The hydrothermal vent field in the crater floor of Kolumbo consists dominantly of active and inactive sulfide-sulfate structures in the form of vertical spires and pinnacles, mounds and flanges along a NE-SW trend, with temperatures up to 220 C and vigorous CO<sub>2</sub> gas emission.

For several years, the highest frequency of earthquakes was concentrated mainly in the vicinity of Kolumbo volcano. However, during 2011-2012 both seismic and geodetic unrest began abruptly inside Santorini caldera related to a shallow magmatic intrusion indicated by inflation. Recently, several earthquakes occurred in the region south of Christianna at the SW edge of the CSK line.

This CSK line has possibly fed the post-caldera eruptions and is the main path for fluid circulation. In conclusion, the CSK tectonic line displays a special character in terms of morphology, volcanism, hydrothermal activity, seismicity and tectonic structure. It may cause important geohazards to the highly touristic Santorini island. Further seafloor investigations along this active line can provide insights into the overall geodynamic activity and aid the archipelago's hazard preparedness.



110. Morphotectonic sketch map of the Santorini Volcanic Field.

The analysis and correlation of both bathymetric data and seismic profiles has shown that Anhydros basin is a NE-SW oriented tectonic graben formed by normal marginal faults during Pliocene. The major morphotectonic structure observed within the basinal area is the Kolumbo Volcanic Chain which forms an intra-caldera tectonic horst. Secondary tectonic features of normal or strike slip character, active or inactive were observed within the basinal area. KVC is under tectonic control and is in line with Kolumbo Fault line onshore at the NE part of Santorini, the hydrothermal field at the NE part of Santorini caldera and the dykes that occur at the northern Santorini caldera walls and the southern tip of Therasia. It is also in correspondence with the overall configuration of Santorini Volcanic Field that includes Christiana as well, since the distribution of all the volcanic features of the area has a NE-SW orientation (fig. 110).

Thus, we propose that KVC is part of a wider NE-SW volcanotectonic zone developed within a tectonic graben bordered by Ios fault zone to the north and Anafi fault zone to the southeast.

What was discovered through the seismic profiles was the listric plane at the NE submarine slopes of Santorini. It has served as a slipping surface for several blocks and attributed a step like morphology to the SW border of Anhydros basin. Further seismic surveys should be conducted at the area in order to better understand how this structure may be responsible for any differentiations between Santorini and KVC and have a clearer view of spatial distribution.

Further on, additional surveys are needed to be done in order to have a more comprehensive and multidisciplinary study on Anhydros basin which is a very active region both from the perspective of seismicity and volcanic activity.

## **9. Acknowledgments**

This study was supported by Hellenic Centre for Marine Research (HCMR), Institute for Exploration (IFE-USA) and the collaborative project "New Frontiers in the Ocean Exploration" between the Graduate School of Oceanography at the University of Rhode Island (URI-USA) and the Dept. of Geology & Geoenvironment of University of Athens (NKUA-GREECE). The officers and the crew of the E/V NAUTILUS are gratefully acknowledged for their important and effective contribution to the field work and sampling. I am very grateful to Dr. Dimitris Sakellariou, Research Director of Structural/Marine Geology and Marine Geoarchaeology at the Institute of Oceanography of HCMR for sharing the seismic profiles of the study area. Finally, I would like to thank Prof. Dimitris Papanikolaou and Dr. Nomikou Paraskevi for their valuable support and guidance throughout the writing of my master thesis.

## **10. References**

1. Alexandri, M., Papanikolaou D. & Nomikou, P. 2003. Santorini volcanic field - new insights based on swath bathymetry. Abstracts IUGG, 30 June-11 July 2003, Sapporo, Japan.
2. Bohnhoff, M., M. Rische, T. Meier, D. Becker, G. Stavrakakis, and H.-P. Harjes 2006. Microseismic activity in the Hellenic Volcanic Arc, Greece, with emphasis on the seismotectonic setting in the Santorini- Amorgos zone. *Tectonophysics*, 423 p.17–33.

3. Cantner, K., Carey, S., Sigurdsson, H., Vougioukalakis, G., Nomikou, P., Roman, C., Bell, K., Alexandri, M. 2010. Pre-eruption pressure, temperature and volatile content of rhyolite magma from the 1650 AD eruption of Kolumbo submarine volcano, Greece. 2010 Fall Meeting, AGU, San Francisco, Calif., 13-17 Dec. 2010.
4. Carey, S.N., 2000. Volcaniclastic sedimentation around island arcs. In: Sigurdsson, H., Houghton, B., McNutt, S.R., Rymer, H., Stix, J. (Eds.), *Encyclopedia of Volcanoes*. Academic Press, San Diego, pp. 627–642.
5. Carey S., Bell K. L. C., Nomikou, P., Vougioukalakis, G., Roman, C., Cantner, K., Bejelou, K., Bourboulis, M., Martin Fero J. 2011. Exploration of the Kolumbo Volcanic Rift Zone. *Oceanography*, Vol.24, No. 1, Supplement, “New Frontiers in Ocean Exploration” The E/V Nautilus 2010 Field Season. March 2011, p. 24-25.
6. Dimitriadis, I., Karagianni, E., Panagiotopoulos, D., Papazachos, C., Hatzidimitriou, P., Bohnhoff, M., Rische, and M., Meier, T., 2009. Seismicity and active tectonics at Kolumbo Reef (Aegean Sea, Greece): Monitoring an active volcano at Santorini Volcanic Center using a temporary seismic network. *Tectonophysics* 465, 136-149.
7. Dimitriadis, I., Papazachos, C., Panagiotopoulos, D., Hatzidimitriou, P., Bohnhoff, M., Rische, M., and Meier, T., 2010. P and S velocity structures of the Santorini- Kolumbo volcanic system (Aegean Sea, Greece) obtained by non-linear inversion of travel times and its tectonic implications. *Journal of Volcanology and Geothermal Research* 195, 13-30.
8. Druitt, T.H., Mellors R.A, Pyle D.M., Sparks R.S.J 1989. Explosive volcanism on Santorini, Greece. *Geological Magazine*, 126, vol. 2:95-126.
9. Druitt, T.H. et al. (1999). Santorini Volcano. *Geological Society Memoir no. 19*. The Geological Society of London.
10. Frank, M., Marbler, H., Koschinsky, A., van de Fliedert, T., Klemm, V., Gutjahr, M., Halliday, A., Kubik, P., and Halbach, P., 2006. Submarine hydrothermal venting related to volcanism in the Lesser Antilles: Evidence from ferromanganese precipitates. *Geochem., Geophys Geosys*, vol. 7, Q04010, doi:10.1029/2005GC001140.
11. Fytikas, M, Guliani, O, Innocenti, F, Marinelli, G, Mazzuoli, R 1976. Geochronological data on recent magmatism of the Aegean sea. *Tectonophysics* 31, 29–34.
12. Fytikas M, Innocenti F, Manetti P, Mazuoli R, Peccerilo A, Villari L 1984. Tertiary to Quaternary evolution of the volcanism in the Aegean Region. In: Dixon JE, Robertson AHF (ed) *The Geological Evolution of the Eastern Mediterranean*. Geol Soc London Spec Pub. 17: 687–699.
13. Francalanci, L., Vougioukalakis, G., Perini, G., Manetti, P., 2005. A West–East Traverse along the magmatism of the south Aegean volcanic arc in the light of volcanological, chemical and isotope data. *The South Aegean Active Volcanic Arc: Present Knowledge and Future Perspectives: Developments in Volcanology*, vol. 7, pp. 65–111.
14. Friedrich, W., 2000. *Fire in the Sea, The Santorini Volcano: Natural History and the Legend of Atlantis*. Cambridge University Press, Cambridge,.
15. Friedrich, W.L. (1994) *Feuer im Meer*. Spektrum Akademischer Verlag, Heidelberg, Berlin Oxford, 256 p.
16. Fouque, F. 1879. *Santorin et ses Iruptions*, Masson et Cie, Paris.
17. Stephanos P. Kiliadis, Paraskevi Nomikou, Dimitrios Papanikolaou, Paraskevi N. Polymenakou, Athanasios Godelitsas, Ariadne Argyraki, Steven Carey, Platon

- Gamaletsos, Theo J. Mertzimekis, Eleni Stathopoulou, Joerg Goettlicher, Ralph Steininger, Konstantina Betzelou, Isidoros Livanos, Christos Christakis, Bell Croff Catherine, Michael Scoullou, 2013 (in review) New insights into hydrothermal vent processes in the unique shallow-submarine arc-volcano Kolumbo, Santorini, Nature Scientific Reports.
18. Kreemer C. and Chamot-Rooke N. 2004. Contemporary kinematics of the southern Aegean and the Mediterranean Ridge. *Geophysical Journal International*, 157:1377–1392.
  19. Nomikou, P. 2003. Santorini and Nisyros: Similarities and differences between the two calderas of the modern Aegean Volcanic Arc. CIESM Workshop on “Human records of recent geological evolution in the Mediterranean Basin-historical and archaeological evidence” Santorini 22-25 October 2003, Greece. CIESM Workshop Monographs n24, p.103-108.
  20. Nomikou, P., Papanikolaou, D. & Alexandri, M. 2003. Varying modes of submarine volcanism within the Kos-Nisyros volcanic field. Abstracts IUGG, 30 June-11 July 2003, Sapporo, Japan. V05 in *Volcanic Flows: Observation, Experiment and Theory*.
  21. Nomikou P., Carey S., Papanikolaou D., Croff Bell K., Sakellariou D., Alexandri M., Bejelou K. 2012a. Submarine Volcanoes of the Kolumbo volcanic zone NE of Santorini Caldera, Greece. *Global and Planetary Change* 90-91 (2012) 135-151. doi:10.1016/j.gloplacha.2012.01.001.
  22. Nomikou P., Papanikolaou D., Alexandri M., Sakellariou D., Rousakis G. 2012b. Submarine Volcanoes along the Aegean Volcanic Arc. In Special Issue of *Tectonophysics*: «The Aegean: a natural laboratory for tectonics» (in press).
  23. Nomikou P., Carey S., Croff Bell K., Papanikolaou D., Bejelou K., Cantner K., Sakellariou D., Perros I. 2012c. Tsunami Hazard Risk of a future volcanic eruption of Kolumbo submarine volcano, NE of Santorini Caldera, Greece: *Natural Hazards*, doi: 10.1007/s11069-012-0405-0.
  24. Nomikou P., Carey S., Bell K.L.C., Papanikolaou D., Bejelou K., Alexandri M., Cantner K., Fero Martin J. 2013 (in press). Morphological Analysis and related volcanic features of the Kolumbo Submarine Volcanic Chain (NE of Santorini Island, Aegean Volcanic Arc). *Geomorphology*
  25. Papanikolaou, D. 1993. Geotectonic evolution of the Aegean. *Bull. Geol. Soc. Greece*, XXVII, 33-48.
  26. Papanikolaou, D, Nomikou, P. 2001. Tectonic structure and volcanic centres at the eastern edge of the Aegean volcanic arc around Nisyros Island. *Bull. Geol. Soc. Greece* 34 (1), 289–296.
  27. Papastamatiou, I. 1958. The age of Crystalline Limestones of Thira. *Bull. Geol. Soc. Greece* 3 (1), 104-113.
  28. Pavlakis, P, Lykoussis, V, Papanikolaou, D, Chronis, G. 1990. Discovery of a new submarine volcano in the western Saronic Gulf: The Paphsanias Volcano. *Bulletin of the Geological Society of Greece* 24, 59–70.
  29. Percival, J. B., and D. E. Ames 1993. Clay mineralogy of active hydrothermal chimneys and an associated mound, middle valley, northern Juan-de-Fuca Ridge, *Can. Mineral.*, 31, 957–971.

30. Pyle D.M., 1990. New estimates for the volume of the Minoan eruption. Pp. 113-121. In: Hardy D.A et al. (eds), Thera and the Aegean World III vol.2 (Earth Sciences), The Thera Foundation, London.
31. Roman N., Inglis G., Vaughn I., Williams S., Pizarro O., Friedman A., Steinberg D. 2011. Development of High-Resolution Underwater Mapping Techniques Oceanography, Vol.24, No. 1, Supplement, "New Frontiers in Ocean Exploration" The E/V Nautilus 2010 Field Season. March 2011, p.12-13.
32. Sakellariou D., Sigurdsson H., Alexandri M., Carey S., Rousakis G., Nomikou P., Georgiou P. and Ballas D. 2010. Active tectonics in the Hellenic Volcanic Arc: the Kolumbo submarine volcanic zone. Bull. Geol. Soc. of Greece, Vol. XLIII/2, 1056-1063.
33. Skarpelis, N. et al. (1992). Occurance and  $40\text{Ar}/39\text{Ar}$  dating of a granite in Thera
34. (Santorini, Greece). Geologishe Rundschau 81, 3, 729-735.
35. Sigurdsson, H., S. Carey, M. Alexandri, G. Vougioukalakis, K. L. Croff, C. Roman, D. Sakellariou, C. Anagnostou, G. Rousakis, C. Ioakim, A. Gogou, D. Ballas, T. Misaridis, and P. Nomikou 2006. Marine investigations of Greece's Santorini volcanic field. EOS, 87(34):337, 342.
36. Tataris, A. 1965. The Metamorphic basement (Hocene) of Thira. Bull. Geol. Soc. Greece 6, 232-238.
37. Usui, A., T. A. Mellin, M. Nohara, and M. Yuasa 1988. Structural stability of marine  $10\text{A}^\circ$  manganates from the Ogasawara (Bonin) Arc: Implication for low temperature hydrothermal activity, Mar. Geol., 86, 41-56.
38. Varnavas, S.P., Cronan, D.S., 2005. Submarine hydrothermal activity off Santorini and Milos in the Central Hellenic Volcanic Arc: A synthesis. Chemical Geology 224 (1-3), 40-54.